Aus der Chirurgischen Klinik, Campus Charité Mitte | Campus Virchow-Klinikum

der Medizinischen Fakultät Charité - Universitätsmedizin Berlin

Dissertation

Optimierung der Ratten- und Schweineleber-Dezellularisierung durch Anwendung von oszillierenden Umgebungsdruckschwankungen und Analyse der Morphologie und Funktion von parenchymatös rebesiedelten Rattenlebern

zur Erlangung des akademischen Grades
Doctor medicinae (Dr. med.)

vorgelegt der Medizinischen Fakultät
Charité – Universitätsmedizin Berlin

von
Antje Butter

aus Bergen auf Rügen

Datum der Promotion: 23.06.2019

Inhalt

1. Abstrakt

Die Dezellularisierung ist eine Technik aus dem Bereich des *Tissue Engineering*, mit welcher durch Perfusion von Detergenzien Zellen von soliden Organen gelöst und entfernt werden. Die zurückbleibende Extrazellulärmatrix ist weniger immunogen und kann als natürliches Gerüst für die Wiederansiedelung von Zellen anderen Ursprungs genutzt werden. Zielsetzung dieser Arbeit war eine Verbesserung der bestehenden Dezellularisierungstechnik der Leber durch die Nutzung des arteriellen Gefäßzuganges sowie die Anwendung oszillierender Umgebungsdruck-schwankungen. Anschließend sollten diese Extrazellulärmatrices im Rattenmodell mit primären Ratten-Hepatozyten rezellularisiert und deren Funktion sowie Morphologie über einen Zeitraum von 7 Tagen untersucht werden.

Die arterielle Perfusion sowie die Anwendung oszillierender Umgebungsdruckschwankungen führte in den hier beschriebenen Versuchen zu einer Verbesserung der Dezellularisierungs-Technik. Rezellularisierte Ratten-Hepatozyten adhärierten an der Extrazellulärmatrix und bildeten clusterartige Formationen im Leberparenchym.

1.2. Abstract in English

The decellularization is a technique, that removes all cells from a solid organ, using organ perfusion with detergents. The remaining extracellular matrix is less immunogenic and can be used as a natural scaffold for recellularization with cells from a different origin. The aim of the underlying work was to improve the existing technique of liver-decellularization by using the hepatic artery for detergent perfusion while applying oscillating pressure conditions. Then, rat extracellular matrices were repopulated with primary rat hepatocytes to examine their function and morphology over a time period of about 7 days.

In this experimental setting the perfusion via the hepatic artery and the application of oscillating pressure conditions led to an improvement of the existing decellularization technique. Recellularized primary rat hepatocytes adhered on the extracellular matrix and formed cell cluster formations in the liver parenchyma.

2. Einführung

Häufig ist die Transplantation einer Spender-Leber die einzige kurative Therapie für Patienten mit fortgeschrittenen Lebererkrankungen. Aktuell befinden sich mehr

Patienten auf der Leber-Empfänger-Warteliste als transplantable Organe gespendet und durch Eurotransplant vermittelt werden können [1]. Eine Möglichkeit diesem Organmangel zu begegnen könnte die Schaffung von Organunterstützungsverfahren oder aber die Schaffung zu transplantierender Organe sein.

Im Rahmen der Dezellularisierung von Lebergewebe – im klinischen Umfeld langfristig beispielsweise einer porcinen Leber – werden die Zellen eines Organs von der Extrazellulärmatrix (ECM) gelöst und entfernt, sodass die weniger immunogene Matrix als Gerüst für die Rebesiedelung (Rezellularisierung) mit Zellen anderen Ursprungs – z.B. humane Zellen – genutzt werden kann. Die bisher gängigste Technik zur Leberdezellularisierung ist die Perfusion mit Detergenzien über die Portalvene.

Im Rahmen dieser Arbeit wurde die arterielle mit der existierenden portalvenösen Perfusions-Technik zur Dezellularisierung von Ratten- sowie Schweinlebern verglichen. Für die Dezellularisierung wurden die Detergenzien Triton X-100 und SDS in einer Konzentration von 1 % verwendet. Zudem evaluierten wir die Anwendung oszillierender Umgebungsdruckschwankungen während der Organperfusion, mit dem Ziel die Mikroperfusion innerhalb des Leberparenchyms zu verbessern.

Die verbesserte Mikroperfusion sollte eine vollständige und einheitliche Dezellularisierung bis in die Peripherie der Lebersegmente gewährleisten, sodass keine potentiell immunogen wirkenden Zellbestandteile auf der ECM zurückbleiben.

Die dezellularisierten Ratten-Matrices wurden anschließend über den arteriellen Gefäßzugang mit primären Hepatozyten rebesiedelt und für bis zu 7 Tage in einem Bioreaktor kultiviert, wobei zu vorher definierten Zeitpunkten Gewebe und Medium-Proben entnommen wurden und die rebesiedelten Konstrukte histologisch aufgearbeitet wurden.

Die Dezellularisierung der Leber mittels arterieller Perfusion ist der portalvenösen Perfusion überlegen. Oszillierende Umgebungsdruckschwankungen, die intermittierend auf das Organ angewendet werden, können die Mikroperfusion verbessern. Durch eine homogene Perfusion können die Detergenzien gleichmäßiger Zellbestandteile lösen und die Perfusionszeit reduziert werden.

Die dreidimensionale dezellularisierte Matrix ist aufgrund der vorhandenen Matrix-Proteine, Fragmenten von Wachstumsfaktoren sowie des intrahepatischen Gefäßgerüstes und der Dreidimensionalität geeigneter zur Kultur von primären Hepatozyten, als die zweidimensionale Zellkultur in Zellkulturschalen.

Zielsetzung der vorliegenden Arbeit war die Optimierung der Leberdezellularisierung durch die Nutzung des arteriellen Gefäßzuganges sowie durch die Anwendung oszillierender Umgebungsdruckschwankungen.

Zudem sollte die Morphologie und Funktionalität von rebesiedelten Rattenlebern über die definierte Zeitspanne von 7 Tagen in einem Bioreaktor untersucht werden.

3. Methodik

3.1. Versuchsaufbau

3.1.1 Versuchstiere

Ratten

Lewis Ratten wurden innerhalb der Tierexperimentellen Einheit (FEM, Charité – Universitätsmedizin Berlin, Deutschland) in Einhaltung der geltenden Landesgesetze und Regularien des Landesamtes für Gesundheit und Soziales (LaGeSo Berlin, Deutschland, Reg. Nr. O 365/11) gehalten und operiert. Die weiblichen Lewis Ratten (n=24 für die reine Dezellularisierung, weitere n=21 für die anschließende Rezellularisierung) wogen zwischen 200 – 300 g und dienten als Organspender für die Leberentnahme und anschließende Dezellularisierung. Männliche Lewis Ratten mit einem Gewicht von 300 – 400 g (n=21) wurden zur Organentnahme für die Hepatozyten-Isolation zur anschließenden Rezellularisierung genutzt [2,4].

Das Organentnahmeprotokoll wurde durch die Tierexperimentelle Einrichtung festgelegt und angepasst. Die Rattenlebern wurden über einen Aortenpatch des Truncus coeliacus (18 G Kanüle, Braun, Melsungen, Deutschland) sowie über die Portalvene (24 G Kanüle, Braun, Melsungen, Deutschland) kanüliert, sodass die Leber mit ca. 500 ml PBS (*phosphat buffer saline*, eigene Herstellung) gespült werden konnte [2,4].

Schweine

Schweinelebern mit einem Gewicht von 600 – 1500 g wurden von weiblichen sowie männlichen Hausschweinen mit einem Lebendgewicht von 20 - 60 kg entnommen (n=19). Alle Tiere wurden innerhalb der Tierexperimentellen Einheit (FEM, Charité, Berlin, Deutschland) in Einhaltung der geltenden Landesgesetze und Regularien des Landesamtes für Gesundheit und Soziales (LaGeSo Berlin, Deutschland, Reg. Nr. G 0116/14) gehalten und operiert.

Während der Organentnahme wurde die Pfortader präpariert, inzidiert und ein Spülkatheter (100 % Silikon, 6,7 mm; Rüsch, Teleflex Medical GmbH, Kernen,

Deutschland) eingelegt und fixiert. Die Pfortader wurde sofort mit 2 l heparinisierter Elektrolytlösung (5000 IE Einheiten Heparin, Jonosteril; Fresenius SE & Co. KGaA, Bad Homburg, Deutschland) perfundiert. Nach der Explantation der Leber und vor Beginn der Dezellularisierung wurden die die A. hepatica und der supra- sowie infra-hepatische Teil der Vena Cava kanüliert (Portalvene, Vena Cava: Spülkatheter 100 % Silikon, 6.7 mm; Rüsch, Teleflex Medical GmbH; A. hepatica: Metall-Verbinder 3.0 mm; Carl Roth GmbH & Co. KG, Karlsruhe, Germany) [3].

3.1.2 Perfusionskammern und Bioreaktor

Für die Dezellularisierung der Ratten- und Schweinelebern wurde jeweils eine Perfusionskammer entworfen und gebaut. Für die Rezellularisierungs-Versuche im Rattenmodell wurde ein Bioreaktor konzipiert, dessen Herzstück ebenfalls eine Perfusionskammer war. Diese Perfusionskammern waren flüssigkeitsdicht und enthielten multiple Gefäßanschlüssen, sodass eine selektive und simultane Perfusion über verschiedene Gefäße (z. B. die A. hepatica und die Pfortader) möglich war. Zusätzlich verfügten die Kammern über Anschlüsse, über die oszillierende Schwankungen des Umgebungsdruckes auf die perfundierten Lebern ausgeübt werden konnten, um die intraabdominellen Verhältnisse während der Atmung zu imitieren und so die Perfusion im Organ zu optimieren (siehe [2,3,4]).

3.2 Dezellularisierung

Rattenmodell

Nach Befestigung der explantierten und kanülierten Leber in der Perfusionskammer, an den arteriellen sowie portalvenösen Gefäßanschlüssen, begann die fluss-gesteuerte Organperfusion:

Es wurden insgesamt 4 experimentelle Gruppen untersucht (je n=6) [4]:

- arterielle Perfusion mit Ausübung oszillierender Umgebungsdruckschwankungen **(A+P)**
- arterielle Perfusion ohne die Ausübung oszillierender Umgebungsdruckschwankungen **(A-P)**
- portalvenöse Perfusion mit Ausübung oszillierender Umgebungsdruckruckschwankungen **(P+V)**

- portalvenöse Perfusion ohne die Ausübung oszillierender Umgebungsdruckschwankungen **(P-V)**

Gruppe	**PV-P**	**PV+P**	**A-P**	**A+P**
Perfusionsweg	Pfortader	Pfortader	A. hepatica	A. hepatica
1. Triton X-100 1 %	90 min	90 min	90 min	90 min
2. SDS 1 %	90 min	90 min	90 min	90 min
Anwendung osz Umgebungsdruckschw.	nein	ja	nein	ja

Schweinemodell

Die explantierten Schweinelebern wurden mithilfe einer modifizierten Herz-Lungen-Maschine (SIII; Sorin Group, Milan, Italien) in einer proprietär entwickelten Perfusionskammer über die arteriellen sowie portalvenösen Gefäßanschlüsse perfundiert:

Es wurden zwei experimentelle Gruppen untersucht (je n=6) [3]:

- druckgesteuerte arterielle und portalvenöse Perfusion mit Ausübung oszillierender Umgebungsdruckschwankungen **(P+)**
- druckgesteuerte arterielle und portalvenöse Perfusion ohne die Ausübung oszillierender Umgebungsdruckschwankungen **(P-)**

Gruppe	**P-**	**P+**
Perfusion	portalven. + art. Perf.	portalven. + art. Perf.
1. Triton x-100 1 %	180 min *	180 min *
2. SDS 1 %	180 min *	180 min *
Anwendung osz. Umgebungsdruckschw.	nein	ja

* Nach jeweils 90 min wurde die Leber manuell um 180 ° gedreht und die Perfusion anschließend fortgesetzt.

3.3 Zellisolation im Rattenmodell

Die Isolation primärer Ratten-Hepatozyten erfolgte streng nach einem bereits publizierten Protokoll [5]. Danach wurden die isolierten Ratten-Hepatozyten mit einem

Percoll-Gradienten aufgereinigt (Easycoll Separating Solution; Biochrom GmbH) und erreichten eine reproduzierbare Viabilität von mindestens 80 % [2].

3.4 Statische Zellkultur im Rattenmodell

Nach erfolgreicher Zellisolation wurden primäre Ratten-Hepatozyten in einer statischen Zellkultur (37° C, 95 % O2, 5 % CO2), in 6-Well-Platten (Falcon Tissue Culture Plates; Corning Inc, New York, NY, USA) mit jeweils 1 Mio. viablen Hepatozyten und 3 ml DMEM (ThermoFisher Scientific, Waltham, Massachusetts, USA) kultiviert. Aus dem Medium wurden – analog zu den Versuchen im Bioreaktor – nach 1 h, 6 h, 12 h, 1 d, 2 d, 3 d, 4 d, 5 d, 6 d und 7 d Proben entnommen und asserviert. Ein vollständiger Mediumwechsel erfolgte nach jeweils 24 h [2].

3.5 Rezellularisierung im Rattenmodell

Der zuvor sterilisierte Bioreaktor befand sich während der Rezellularisierung und der anschließenden Kultivierung in einem Brutschrank bei 37 °C. Vor der ersten Hepatozyten-Infusion begann die Leberperfusion mit oxygeniertem (95 % O_2, 5 % CO_2) DMEM bei 37 °C über die Portalvene, sodass sich die Matrix ausreichend entfalten konnte. Die zuvor isolierten Ratten-Hepatozyten wurden in einer Multistep-Technik über die A. hepatica infundiert (150 Mio. viable Hepatozyten / 40 ml DMEM). Die Zellgabe erfolgte kontrolliert über ein Perfusionssystem (Braun, Melsungen, Deutschland) mit einer Laufrate von 1 ml/min über eine Zeitspanne von 10 min. Anschließend stoppte die Perfusion für 10 min, um die Zelladhärenz zu unterstützen. Während der Zellgabe erfolgte parallel die Organperfusion über die Portalvene mit 2 ml/min. Diese Schritte wurden wiederholt bis insgesamt 150 Mio. Zellen infundiert waren. Nach einer weiteren 30-minütigen Ruhephase wurde die A. hepatica ligiert und die Organperfusion über die Pfortader mit 5 ml/min gestartet. Das Medium wurde 24 h über den Antrieb einer Rollerpumpe über einen Oxygenator und eine Blasenfalle rezirkuliert. Ein Mediumwechsel erfolgte täglich nach jeweils 24 h. Die rezellularisierten Leber wurden für bis zu 7 d perfundiert. Die Entnahme von Medium- und Gewebe-Proben aus dem Bioreaktor erfolgte nach den zuvor festgelegten Zeitpunkten (1 h, 6 h, 12 h, 1 d, 2 d, 3 d, 4 d, 5 d, 6 d, 7 d) [2].

3.6. Probenanalyse

3.6.1 Asservieren der Gewebeproben im Ratten- und im Schweinemodell

Für die histologische Analyse wurden sämtliche Proben in Formalin (4 %) für mindestens 24 h konserviert und anschließend in Paraffin eingebettet. Von den Paraffin-Blöcken wurden mittels Mikrotom 5 µm dicke Schnitte angefertigt. Weitere Gewebeproben dezellularisierter Lebern wurden homogenisiert in PBS (Ultra-Turax T25; IKA Werke GmbH & Co. KG, Staufen, Deutschland) aliquotiert und gefriergetrocknet [2, 3, 4].

3.6.2 Histologische Analyse

Dezellularisierung im Ratten- sowie Schweinemodell

Hämatoxylin und Eosin (H&E, AppliChem, Darmstadt, Deutschland) gefärbte histologische Schnitte wurden verblindet durch eine erfahrene Oberärztin der Klinik für Pathologie (Charité Campus Mitte, Berlin, Deutschland) befundet. Dazu wurde der prozentuale Anteil des dezellularisierten Gewebes im histologischem Schnitt bestimmt. Weiterhin wurden Sirius Red (Sigma-Aldrich Inc., St Louis, MO, USA), Alcian Blue/PAS (Morphisto, Frankfurt am Main, Deutschland) sowie Van Gieson (Morphisto GmbH, Frankfurt am Main, Deutschland) Färbungen nach Standardprotokoll angefertigt. Immunhistochemische Färbungen von Collagen IV, Laminin und Fibronectin wurden ebenfalls nach Standardprotokoll durchgeführt (Abcam Cambridge, Großbritannien) [3,4].

Rezellularisierung im Rattenmodell

Es wurden zunächst ebenfalls die o.g. Färbungen durchgeführt. Zusätzlich wurde ein TUNEL Assay (TdT-mediated-dUTP-biotin-nick-end -labelling; R&D systems, Minneapolis, MN, USA) durchgeführt zur Visualisierung von apoptotischen Hepatozyten. Eine PCNA (proliferating cell nuclear antigen; Dako, Glostrup, Denmark) Färbung diente dem Nachweis der Zellreplikation. Diese Färbungen erfolgten ebenfalls nach Standardprotokoll [2].

3.6.3 Biochemische Analyse

Dezellularisierung im Rattenmodell

In gefriergetrockneten Gewebeproben wurde die Quantität residualer DNA bestimmt (QiAmp DNA FFPE tissue kit, Qiagen, Hilden, Deutschland; Nanodrop ND-1000, Peq-Lab, Biotechnologie, Erlangen Germany). Zudem wurden dezellularisierte Proben mittels Papain-Assay (Papain, Farndale et al., 1986) verdaut und der Glykosaminoglykan-Gehalt photometrisch (FLUOSTAR, Optima, BMG Labtech, Ortenberg Deutschland) gemessen. Der HGF-Gehalt (hepatocyte growth factor) der Matrix wurde mittels HGF-ELISA bestimmt (Ref.-No. K2002-1, B-Bridge International, Inc., Cupertino, CA, USA; Biomol; FLUOSTAR Optima, BMG Labtech, Ortenberg, Deutschland) [4].

Dezellularisierung im Schweinemodell

Zusätzlich zu den o. g. Methoden wurde mittels Collagen Assay (Quickzyme Biosciences, Leiden, Niederlande) im Schweinemodell der Kollagen-Gehalt der ECM nach Dezellularisierung bestimmt [3].

3.6.4 Mediumanalyse der Rezellularisierung im Rattenmodell

Die Mediumproben wurden mittels Blutgasanalysegerät (ABL800 FL; Radiometer GmbH, Willich, Deutschland) untersucht und hinsichtlich des aktuellen Glukose-, Kalium- und pH-Wertes analysiert. Weiterhin wurden photometrisch die Transaminasen (AST, ALT) sowie die Laktatdehydrogenase (LDH, Flui Kit Analyticon, Lichtenfels, Deutschland; FLUOSTAR, Optima, BMG Labtech, Ortenberg Deutschland) als Parameter für Zellschäden bestimmt. Ratten-Albumin wurde mittels ELISA und anschließender Photometrie gemessen (Biomol; FLUOSTAR Optima, BMG Labtech, Ortenberg, Deutschland) [2].

3.6.5 Statistische Analyse

Die statistische Analyse erfolgte mit Prism 6.0b für Mac OSX (GraphPadSoftware, Inc., La Jolla, CA, USA) [2,3,4].

Dezellularisierung

Die erhobenen Daten wurden als Mittelwerte ± Standartabweichung des Mittelwertes aufgeführt. Graphisch wurden die Daten als Box und Whisker Plots dargestellt. Aufgrund der begrenzten experimentellen Fallzahl (je n=6) wurden die Gruppen mittels

parameterfreien Kruskal-Wallis Test verglichen, gefolgt vom Dunn's Test. Gemessene Differenzen wurden ab einem $p < 0,05$ als signifikant gewertet [3,4].

Rezellularisierung

Die erhobenen Daten wurden beschrieben als Mittelwerte ± Standardabweichung bzw. als Standardfehler. Zur Testung der Standard-Normalverteilung wurde ein D'Agostino-Pearson Omnibus Test durchgeführt. Eine zweifache Varianzanalyse (two-way ANOVA) wurde durchgeführt um zu untersuchen, ob die beiden unabhängigen Variablen „experimentelle Gruppe" und „Zeitpunkt" den Verlauf der Produktion von Leberenzymen sowie des Albumins beeinflussten. Auf die zweifache Varianzanalyse folgten vergleichende „post hoc" Tests, mit welchen verschiedenen Zeitpunkten innerhalb einer experimentellen Gruppe (Turkey) oder verschiedene Gruppen an spezifischen Zeitpunkten (Sidak) verglichen werden sollten. Als signifikant wurden Differenzen mit $p > 0,05$ angesehen [2].

4. Ergebnisse

4.1. Makroskopische Beobachtungen

Dezellularisierung im Rattenmodell

Nach Beginn der Perfusion mit Triton X-100 1 % färbten sich die Rattenlebern zunächst weiß und anschließend von zentral nach peripher transparent. Die Fortsetzung des Perfusionsprotokolles mit SDS 1 % führte zu einem allmählichen Lösen der Zellen von der ECM, sodass diese nahezu vollständig transparent wurde. Die Dezellularisierung über die Portalvene führte zu einem inhomogenen Ergebnis und es blieben Inseln mit residualen Zellen zurück, die als bräunliche oder weiße punktförmige Areale sichtbar wurden. Die Dezellularisierung über die A. hepatica führte zu einer gleichmäßigen Entfärbung, sodass makroskopisch keine Zellrückstände sichtbar waren. Die zusätzliche Anwendung oszillierender Umgebungsdruckschwankungen beschleunigte eine homogene Perfusion zusätzlich [4].

Dezellularisierung im Schweinemodell

Unmittelbar nach Beginn der Perfusion mit Triton-X 100 1 % begann sich die Schweineleber zügig zu entfärben. Am Ende der Perfusion mit Triton-X 100 zeigten sich die Lebern weißlich, wenngleich nicht transparent. Die Fortsetzung der Perfusion der Organe mit SDS 1 % führte zu einer nahezu vollständigen Entfärbung. Nach

manueller Drehung des Organs (siehe Protokoll) kam es jeweils zu einer Zunahme der Viskosität des Perfusates. Eine makroskopisch homogenere Entfärbung der Leber konnte mit der Ausübung oszillierender Druckschwankungen erzielt werden [3].

Rezellularisierung im Rattenmodell

Hepatozyten, die in die anfangs noch transparente ECM infundiert wurden, verteilten sich über alle Leberlappen und waren sehr gut makroskopisch sichtbar. Während des primären Hepatozyten-Infusionsschrittes verblieben die Zellen im ehemaligen Gefäßsystem. In den darauffolgenden zweiten und dritten Infusionsschritten bildeten sich punktförmige bräunliche Zellanreicherungen im Parenchym, zunächst in den kleinen Leberlappen nahe der Insertion der A. hepatica. Im vierten und letzten Infusionsschritt konnten Hepatozyten auch in den peripheren Leberlappen beobachtet werden. Diese Anordnung der Zellen geschah vor allem um Gefäßstrukturen und konnte bis zum Abschluss der Perfusion über einen Zeitraum von maximal 7 Tagen makroskopisch beobachtet werden [2].

4.2. Auswertung der Histologie

Dezellularisierung im Rattenmodell

Die histopathologische Auswertung durch das Institut für Pathologie, Charité Campus Mitte, ergab keine mikroskopisch sichtbaren Zell-Residuen in den arteriell dezellularisierten Ratten-Lebern, ungeachtet ob mit oder ohne Anwendung oszillierender Umgebungsdruckschwankungen, d.h. der ermittelte Anteil dezellularisierten Gewebes lag hier bei 100 %. Die portalvenös perfundierten Ratten-Lebern enthielten Zellrückstände bzw. Anteile von Zell-Detritus. In den portalvenös dezellularisierten Lebern mit Anwendung oszillierender Umgebungsdruckschwankungen lag der Anteil des vollständig dezellularisierten Gewebes, je nach bewerteten Schnitt, bei 40-90 % (durchschnittlich 80 %). Ohne die Anwendung oszillierender Umgebungsdruckschwankungen lag der prozentuale Anteil des dezellularisierten Gewebes bei 50-90 % (durchschnittlich 60 %). Kollagen IV sowie Laminin konnte unabhängig der experimentellen Gruppe in allen bewerteten Schnitten nachgewiesen werden, wobei es einen vermehrten Nachweis um Zellresiduen portalvenös perfundierter Lebern gab [4].

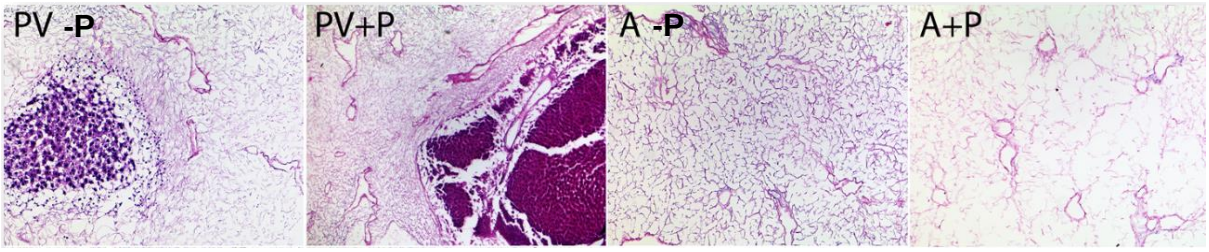

Abb. 1. H&E Färbung dezellularisierter Ratten-ECM: portalven. ohne Umgebungsdruckschw. (PV-P), portalven. mit Umgebungsdruckschw. (PV+P), arteriell ohne Umgebungsdruckschw. (A-P), arteriell mit Umgebungsdruckschw. (A+P)

Dezellularisierung im Schweinemodell

Mittels H&E Färbung konnte die ECM nach Dezellularisierung strukturell verbunden nachgewiesen werden, dies in beiden experimentellen Gruppen. Ohne die Anwendung der oszillierenden Umgebungsdrücke zeigte sich die ECM in der H&E sowie in der Van Gieson Färbung in ihrer Struktur aufgelockert und es konnten Zellrückstände sowie Zelldetritus auf der ECM nachgewiesen werden. In der Gruppe mit Anwendung oszillierender Umgebungsdrücke wurden keine Zellrückstände beobachtet und die ECM war strukturell unversehrter. Kollagen konnte in beiden Gruppen quantitativ einheitlich mittels Sirius Red sowie in der immunhistochemischen Färbung nachgewiesen werden. Laminin und Fibronectin wurden ebenfalls konstant in beiden Versuchs-Gruppen immunhistochemisch nachgewiesen. Mit Anwendung oszillierender Umgebungsdrücke waren die Laminin- sowie Fibronectin-Verteilungen vergleichbar mit Schnitten nativer Schweinelebern. Die Alcian-Blue-Färbung wies Glykosaminoglykane in beiden Gruppen ohne signifikanten Unterschiede nach [3].

Abb. 2. H&E Färbung einer nativen (Native) Schweineleber, einer dez. Schweineleber ohne (-P) und mit (+P) Anwendung oszillierender Umgebungsdruckschwankungen

Rezellularisierung im Rattenmodell

Die H&E Färbung bestätigte mikroskopisch die Cluster-artige Anordnung der Hepatozyten um das Gefäßsystem sowie im darum liegenden Parenchym. Teile der rezellularisierten Lebern zeigten sich nach abgeschlossener Hepatozyten-Infusion

zell-leer. Zell-Cluster-Formationen konnten hauptsächlich um die Gefäßäste herum beobachtet werden. Während sich die viablen Zellen zu Beginn der Rebesiedelung mehrheitlich noch im Gefäßsystem befanden, konnten nach > 24 h vermehrt viable Hepatozyten-Cluster im umliegenden Parenchym nachgewiesen werden. Ein TUNEL-Assay wurde zum Nachweis von apoptotischen Zellen durchgeführt. Dieser zeigte eine Zunahme der TUNEL-positiven Zellen zu späteren Zeitpunkten. Trotzdem konnten auch 7 Tage nach Beginn der Perfusion im Bioreaktor große Anteile TUNEL negativer Zellen nachgewiesen werden. Leberzellverbände, die sich in Clustern um die Gefäßäste gebildet hatten, zeigten nur in den Randzonen einen Saum aus apoptotischen Zellen. Solitäre oder im Gefäßsystem adhärierte Zellen waren zum Ende des Versuches, nach 7 Tagen, nahezu zu 100 % apoptotisch. Eine PCNA-Färbung wurde zur Darstellung der Zellreplikation durchgeführt. Es konnten zu allen Versuchszeitpunkten PCNA-positive Zellen nachgewiesen werden. Hepatozyten in Zell-Clustern waren vermehrt PCNA positiv. Die immunhistochemischen Färbungen der ECM-Proteine Kollagen IV, Fibronectin und Laminin zeigten eine ähnliche Intensität bei den dezellularisierten sowie bei den rezellularisierten Rattenlebern. Die spezifische Färbung für Glykosaminoglykane (Alcian Blue) sowie die Sirius Red Färbung zeigten ebenfalls ein konstantes Bild der dezellularisierten gegenüber den rezellularisierten Rattenlebern [2].

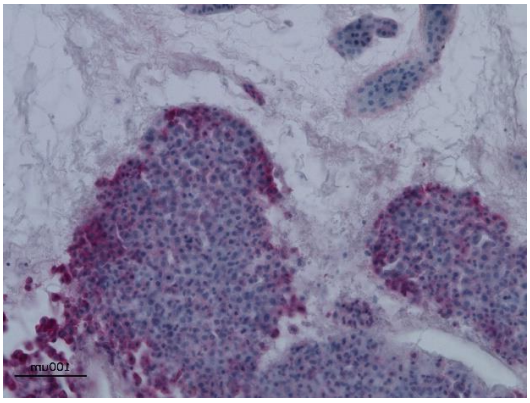

Abb. 3. H&E ECM 1 h nach Rezelluarisierung [2]

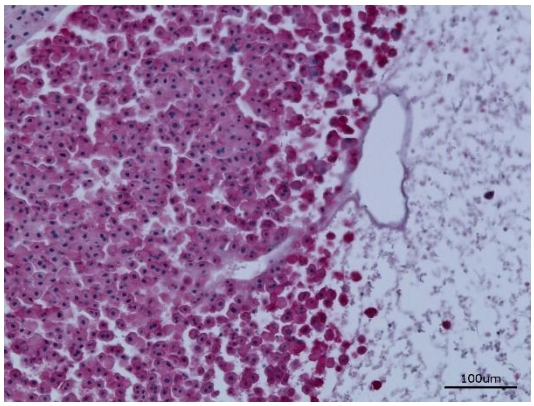

Abb. 4. H&E ECM 24 h nach Rezellularisierung [2]

4.3 Biochemische Analysen

Dezellularisierung im Rattenmodell

Nach Dezellularisierung sank der DNA-Gehalt der ECM im Vergleich mit Proben nativer Lebern (nativ vs. PV-P p=0,2408; nativ vs. PV+P p=0,0152; nativ vs. A-P p=0,0735; nativ vs. A+P, p<0,0001). Es zeigten sich quantitativ weniger DNA-Rückstände bei Lebern, auf die oszillierende Umgebungsdruckschwankungen

ausgeübt wurden, als bei Lebern die ohne oszillierende Umgebungsdruckschwankungen dezellularisiert wurden (PV-P: 3439 ± 1648 ng/mg; PV+P: 1576 ± 379 ng/mg; A-P: 2504 ± 1685 ng/mg; A+P: 723 ± 119 ng/mg). Die arterielle Perfusion mit Anwendung oszillierender Umgebungsdruckschwankungen zeigte die geringsten DNA-Rückstände [4].

Der GAG-Gehalt dezellularisierter Lebern war ebenfalls geringer als in Proben aus nativen Rattenlebern (nativ: 83,48 ± 26,61 mg/g; PV-P: 7,97 ± 3,00 mg/g; PV+P: 8,26 ± 7,95 mg/g; A-P: 1,85 ± 1,54 mg/g; A+P: 15,27 ± 4,52 mg/g). Ein vergleichsweise erhöhter Gehalt an GAG wurde in der Gruppe mit arterieller Perfusion und unter Ausübung oszillierender Umgebungsdruckschwankungen gemessen. Dabei konnte ein signifikanter Unterschied zwischen der arteriellen Perfusion mit oszillierenden Umgebungsdruckschwankungen gegenüber der arteriellen Perfusion ohne Anwendung der oszillierenden Druckschwankungen beobachtet werden (A-P vs. A+P, p=0,0229). Der HGF-Gehalt der dezellularisierten ECM war – berechnet auf das Trockengewicht – höher als bei Proben nativer Lebern (PV-P: 2,30 ± 1,03 pg/g; PV+P: 2,43 ± 1,01 pg/g; A-P: 1,24 ± 1,04 pg/g; A+P: 1,63 ± 0,70 pg/g; nativ: 0,41 ± 0,24 pg/g). Ein signifikanter Unterschied des HGF-Gehaltes konnte beim Vergleich zwischen nativen Rattenlebern und portalvenös dezellularisierten ECM nachgewiesen werden (PV-P vs. nativ: p= 0,0090; PV+P. vs. nativ: p = 0,0043) [4].

Dezellularisierung im Schweinemodell

Proben dezellularisierter Schweinelebern zeigten einen niedrigeren DNA-Gehalt der ECM als Proben nativer Schweinelebern (nativ: 4774 ± 3354 ng/mg; P-: 659 ± 744,7 ng/mg; P+: 400,9 ± 587,8 ng/mg). Lebern die zusätzlich oszillierenden Umgebungsdruckschwankungen ausgesetzt waren zeigten die geringste Menge an residualer DNA (nativ vs. P+, p< 0,0001). Der auf das Trockengewicht bezogene Kollagenanteil der dezellularisierten Lebern erhöhte sich in allen experimentellen Gruppen (nativ: 2,92 ± 0,40 µg/mg; P-: 35,44 ± 25,35 µg/mg; P+: 52,19 ± 11,18 µg/mg). Signifikante Unterschiede ergaben sich im Vergleich nativer gegenüber jenen dezellularisierten Lebern, die zusätzlich oszillierenden Druckschwankungen ausgesetzt waren (nativ vs. P+, p=0,0193) [3].

Es ergab sich kein signifikanter Unterschied des GAG-Gehaltes (nativ: 7,39 ± 2,33 µg/mg; P-: 5,62 ± 0,65 µg/mg; P+: 5,49 ± 0,39 µg/mg). Insgesamt sank der GAG-

Gehalt leicht nach Dezellularisierung gegenüber nativer Schweinelebern [3].

Mediumanalyse nach Rezellularisierung im Rattenmodell

Zu Beginn der Kultur der rezellularisierten Rattenlebern im Bioreaktor sowie der Rattenhepatozyten in der statischen Zellkultur zeigte sich ein deutlicher Anstieg der Transaminasen (AST, ALT) und der LDH. Die AST erreichte nach 1 h (Rezellularisierung: 23,75 ± 5,85 U/l) sowie 1 d (statische Zellkultur: 26,97 ± 3,35 U/l) das höchste Niveau. Nach Überwinden dieser Höchstwerte fiel die AST kontinuierlich bis zu einem Erreichen des jeweils niedrigsten Wertes nach 5 d (Rezellularisierung: 3,85 ± 1,89 U/l) und 2 d (statische Zellkultur: 2,44 ± 1,24 U/l). Die AST war im Perfusat des Bioreaktors – verglichen mit den Werten nach 2 d (p=0,0079) und 3 d (p=0,0210) – nach 1 h signifikant erhöht.

Die ALT zeigte mit einem maximalen Anstieg der Werte nach 1 h (Rezellularisierung 20,64 ± 3,52 U/l) sowie nach 6 h (Statische Zellkultur: 14,58 ± 0,29 U/l) und einem Minimum nach 7 d (Rezellularisierung: 1,91 ± 0,98 U/l) sowie 6 d (statische Zellkultur: 4,92 ± 1,21 U/l) eine ähnliche Dynamik. Die ALT im Medium des Bioreaktors war – verglichen mit den Werten nach 2 d (p=0,005) und 3 d (p=0,0033) und 5d (p=0,0054) und 7 d (p=0,0421) – nach 1 h signifikant erhöht (Abb. 5) [2].

Die LDH zeigte ein ähnliches Bild: nach 6 h (Rezellularisierung: 54,61 ± 30,57 U/l) bzw. 1 h (Statische Zellkultur: 39,81 ± 16,7 U/l) wurden Höchstwerte gemessen. Anschließend fiel die LDH in beiden Kulturen kontinuierlich ab. Die LDH war im Perfusat des Bioreaktors – verglichen mit den Werten nach 3 d (p=0,0153), 4 d (p=0,0074), 5 d (p=0,0051) sowie 6 d (p= 0,0431) – nach 1 h signifikant erhöht. Nach 1 d war die LDH gegenüber 5 d signifkant erhöht (p=0,0384) (Abb. 5) [2].

Die Analyse des Albumin-Gehalts im Perfusat des Bioreaktors ergab einen Höchstwert nach 1 d (Rezellularisierung: 22966 ± 4361 ng/ml). Nach diesem Peak fielen die Werte kontinuierlich bis zum Erreichen des Minimums nach 7 d (Rezellularisierung: 3934± 1501 ng/ml). Der Albumin-Gehalt im Perfusat war nach 1 d im Vergleich zu Analysen nach 6 d (p= 0,0321) und 7 d (p= 0,0176) Perfusion signifikant erhöht. Im Vergleich dazu zeigte sich der niedrigste Wert in der statischen Zellkultur nach 6 h (2390 ± 375,1 ng/ml) sowie der höchste Wert nach 4 d (14335 ± 2512 ng/ml) [2]. Nach 1 d war der Albumin-Gehalt des Mediums im Bioreaktor signifikant erhöht gegenüber 1 d der statischen Kultur (p=0,0088, Abb. 5) [2].

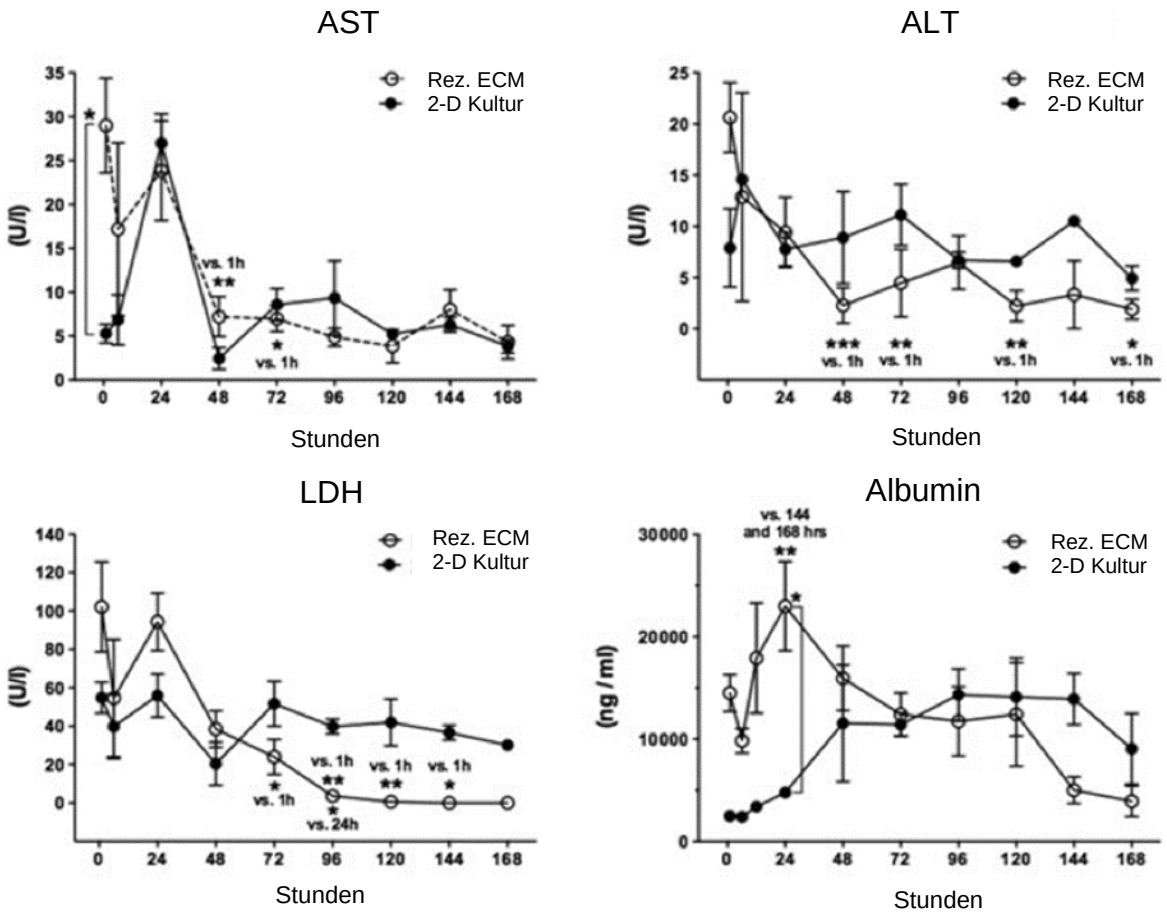

Abb. 5: Analyse der intrazellulären Enzyme Aspartataminotransferase (AST), Alaninaminotransferase (ALT), Laktatdehydrogenase (LDH) sowie Albumin in den entnommenen Mediumproben in Bioreaktor (Rez. ECM) sowie statischer 2-D Kultur [2].

Der Glukose-Gehalt des durch den Bioreaktor perfundierten Mediums zeigte sich während des gesamten Versuchs konstant (Nativprobe: 106 ± 5,74 ng/ml; 7 d: 105 ± 2,83 ng/ml). Nach erfolgter Rebesiedelung stieg der pH-Wert an (Nativ: 7,59 ± 0,13; 7 d: 7,70 ± 0,06). Der Kalium-Gehalt des Perfusats war zwischen den Zeitpunkten 1 h (5,53 ± 0,09 mmol/l) und 12 h (5,7 ± 0,17 mmol/l) konstant. Danach stieg der Wert bis zu einem Plateau von 4 d (6,1 ± 0,07mmol/l) bis 7 d (6,1 ± 0,01 mmol/l) an [2].

5. Diskussion

Die bis dato in Publikationen erwähnte Standard für die Dezellularisierung von Lebern war die Perfusion über die Portalvene mit enzymatischen Lösungen oder Detergenzien über deutlich variierende Zeitspannen und Flussraten [6-9]. Die Perfusion mit Detergenzien via A. hepatica wurde mit dieser Arbeit erstmals beschrieben. Wir etablierten ein arterielles Dezellularisierungsprotokoll und verglichen die Perfusion von Ratten-Lebern über den portalvenösen sowie den arteriellen Gefäßzugang unter der

Anwendung oszillierender Umgebungsdruckschwankungen. Dabei konnten wir eine homogenere Perfusion der Ratten-Lebern über die A. hepatica zeigen [4].

Die arterielle Dezellularisierung benötigte eine kürzere Perfusionszeit – makroskopisch kam es zu einer gleichmäßigeren und schnelleren Entfärbung der Ratten-Lebern. Die portalvenös perfundierten Lebern wurden im Vergleich deutlich langsamer von den Zellen befreit: sie waren nach Abschluss des Dezellularisierungs-vorgangs in der Peripherie makroskopisch nicht vollständig transparent und zeigten zudem in der histologischen Untersuchung Zellresiduen [4]. Die vollständige Dezellularisierung der portalvenös perfundierten Lebern konnte mit einer Verlängerung der Perfusionszeit oder mit einer Erhöhung der Perfusionsrate erreicht werden. Durch diese Maßnahmen und somit durch Erhöhung des Perfusionsdruckes kommt es in bereits dezellularisierten Arealen zu einer verlängerten Exposition der ECM gegenüber den Detergenzien. Dies kann zum Auswaschen der Matrix-Proteine [10] führen und hat potenziell negative Auswirkung auf eine spätere Repopularisierung der ECM. Die Gleichmäßigkeit der Perfusion steht in direktem Bezug zum Ausmaß des Erhalts der Matrix-Proteinstruktur. So zeigten die arteriell perfundierten ECM keine Zellrückstände und im Vergleich weniger DNA/mg ECM, hatten jedoch einen quantitativ höheren Anteil GAG/g ECM und HGF/g ECM [4].

Die Anwendung oszillierender Umgebungsdruckschwankungen unterstützte die Homogenität der Organperfusion zusätzlich. Neuhaus et. al. [13], entwickelte eine Organ-Perfusions-Kammer, mit welcher simultan zur Organperfusion oszillierende Umgebungsdruckschwankungen auf porcine Lebern ausgeübt werden konnten. Die oszillierenden Umgebungsdruckschwankungen sollten dabei die intraabdominellen Gegebenheiten während der Atmung imitieren: *in vivo* führt die Atemmechanik mit intermittierenden Kontraktionen des Zwerchfelles während der Inspiration sowie Entspannung während der Exspiration zu ganz natürlichen intraabdominalen oszillierenden Umgebungsdruckschwankungen, die auf die Leber einwirken.

Die von uns durchgeführten druckgesteuerten Dezellularisierungen von Schweinelebern nutzten eine modifizierte „Neuhaus-Perfusionskammer“. Hierbei zeigte sich eine wesentlich gleichmäßigere Perfusion der Schweinelebern unter der Anwendung oszillierender Umgebungsdruckschwankungen [3]. Zudem ergab die histologische Auswertung weniger DNA-Rückstände im Verhältnis zur ECM-Masse. Schweinelebern, die lediglich druckgesteuert perfundiert wurden, wiesen dagegen eine zerklüftete ECM mit Zell- sowie DNA-Rückständen auf [3].

Tatsächlich ist der Erfolg einer Dezellularisierung in der Literatur nicht einheitlich definiert: Es werden Kriterien herangezogen, die sich hauptsächlich auf die Abwesenheit der Zellen bzw. von DNA-Rückständen beziehen, da diese bei einer Implantation des dezellularisierten Grafts potentiell immunogen wirken könnten. Crapo et al. empfehlen den visuellen indirekten Nachweis durch die Färbung dezellularisierter Schnitte mit H&E oder DAPI. Zusätzlich sollte bei einer erfolgreichen Dezellularisierung die residuale dsDNA < 50 ng/mg Trockengewicht des Gewebes nicht übersteigen und die Fragmente nicht länger als 200 Basenpaare sein [8,9]. Eine allgemein akzeptierte Definition für die Unversehrtheit der ECM nach Dezellularisierung existiert aktuell nicht. Fest steht jedoch, dass eine Dezellularisierung durch die Perfusion mit Detergenzien immer eine ECM-Schädigung bedingt. So beschrieben bereits Badylack et al., dass die Anwendung von Triton X-100 stets eine Schädigung der Glykosaminoglykane zur Folge hat [14]. Dieser Effekt zeigte sich auch in unseren Versuchen: der GAG-Gehalt nach Dezellularisierung war im Vergleich mit nativen Lebern deutlich geringer [3, 4]. Es gilt daher, die Methode dahingehend anzupassen, dass die Schädigung der ECM möglichst geringgehalten wird. Das in unserem Versuchsaufbau effizienteste und im Hinblick auf den Erhalt bestimmter ECM-Proteine zugleich schonendste Dezellularisierungs-Protokoll basierte auf arterieller Perfusion unter Anwendung oszillierender Umgebungsdruckschwankungen [3,4]. Die durch die arterielle Perfusion dezellularisierten Rattenlebern wurden in weiterführenden Repopularisierungs-Versuchen mit primären Hepatozyten der Ratte rezellularisiert. Die Applikation der Hepatozytensuspension über die A. hepatica geschah in vier Teilschritten mit o. g. Unterbrechungen der Perfusion [2], wie u. a. von Soto-Gutiérrez et al. beschrieben [9]. In der Literatur variieren die Methoden der Rezellularisierung, was sich durch ebenfalls variierende Dezellularisierung-Protokolle und Versuchstier-Modelle bedingt. In unseren Rezellularisierungsversuchen waren in histologischen Schnitten die Hepatozyten zunächst im Gefäßsystem nachweisbar. Nach etwa 24h konnten Hepatozyten vermehrt im Parenchym-Kompartiment, also außerhalb der dezellularisierten Gefäßstrukturen in clusterartigen Formationen beobachtet werden. Dabei ordneten sich Hepatozyten oft um einen zentral liegenden Ast des Gefäß-Gerüstes, über welchen die Hepatozyten in der sich anschließenden Perfusion mit Sauerstoff angereichertem Medium versorgt werden konnten [2]. Diese Ergebnisse decken sich mit anderen Publikationen [10-12]. Es erscheint hierbei unwahrscheinlich,

dass die Hepatozyten ausschließlich durch den Perfusionsdruck durch ECM-Lücken gepresst wurden, da sie über die Arterie infundiert wurden, die kontinuierliche Medium-Perfusion jedoch über die Portalvene erfolgte [2].

Nach Beginn der Kulturphase und Perfusion mit Medium im Bioreaktor stiegen die Transaminasen sowie die LDH initial an und erreichten ihren Peak nach 1 – 12 h [2]. Ursächlich hierfür war wahrscheinlich ein Untergang von Hepatozyten, die nicht an der ECM adhärierten oder durch Scherstress geschädigt wurden. Zusätzlich waren Zellen, die nicht unmittelbar an das Medium führende Gefäßsystem Anschluss gefunden hatten, stärker von Apoptose betroffen und trugen vermutlich ebenfalls zu dem Transaminasen-Peak bei [2]. Diese Beobachtungen deckten sich mit denen von Robertson et al. [10], welche ähnliche Beobachtungen nach Beginn der Kultur im Perfusionsbioreaktor beschrieben. Nach abgeschlossenem Zell-*Engraftment*, sanken die Transaminasen und die LDH kontinuierlich. Vergleichbar verhielten sich auch die AST, ALT sowie LDH in der statischen zweidimensionalen Zellkultur [2]. Auch hier war eine mangelnde Adhärenz der Zellen und Scherkräfte während des Besiedelungsprozesses ursächlich.

Interessanterweise stieg der Gehalt an Ratten-Albumin in den Mediumproben des Bioreaktors und erreichte seinen *Peak* nach 24 h. Nach diesem Anstieg sank die Albumin-Konzentration bis zur Beendigung des Versuches nach 7 Tagen kontinuierlich [2]. Die Ursache hierfür ist wahrscheinlich die gesteigerte Produktion von Albumin nach abgeschlossenem *Zellengraftment,* nach etwa 24 h, und die in der Histologie nachgewiesenen (TUNEL-Assay) leicht abnehmende Menge viabler Hepatozyten über den Zeitraum der Perfusion [2]. Hepatozyten in der zweidimensionalen Kultur erreichten ihren Albumin-Höchstwert erst nach 2 Tagen und produzierten – verglichen mit den Zellen im Bioreaktor – weniger Albumin [2].

Grundsätzlich sind die hier dargestellten Rezellularisierungs-Versuche als „*proof of concept*“ zu verstehen und bilden keineswegs den Umfang ab, der für die Repopularisierung eines implantierbaren Organs nötig wäre. Für den Aufbau von funktionellem Lebergewebe bedarf es einer größeren Menge Hepatozyten und anderer leberspezifscher Zellen, wie beispielsweise Endothelzellen oder Cholangiozyten, aber auch Kupffer-Zellen. Essentiell ist es daher die Techniken der Rezellularisierung weiter zu entwickeln, sodass auch ein Wiederaufbau der Mikroanatomie möglich wird.

6. Schlussfolgerung

Die Dezellularisierung via A. hepatica mit Anwendung oszillierender Umgebungsdruckschwankungen führte zu einem gleichmäßigeren und schonenderen Ergebnis verglichen mit der bestehenden Dezellularisierungstechnik über die Vena Porta. Die so dezellularisierten ECM konnten zur Wiederansiedelung primärer Hepatozyten genutzt werden. Vermutlich trug die Protein-Struktur der ECM zur dreidimensionalen clusterartigen Anordnung der Hepatozyten bei, die dadurch metabolisch aktiver und weniger von Apoptose betroffen waren. Bevor eine Langzeitimplantation von rezellularisierten Organen möglich wird müssen etliche weitere Hürden (z.B. Wiederaufbau der Mikroanatomie) überwunden werden.

7. Literaturverzeichnis

1 https://www.dso.de/organspende-und-transplantation/transplantation/lebertransplantation.html , zugegriffen am 01.05.2018

Teile dieser Arbeit wurden veröffentlicht in:

2 Butter A, Aliyev K, Hillebrandt KH, Raschzok N, Kluge M, Seiffert N, Tang P, Napierala H, Muhamma AI, Reutzel-Selke A, Andreou A, Pratschke J, Sauer IM, Struecker B: Evolution of graft morphology and function after recellularization of decellularized rat livers. J Tissue Eng Regen Med. 2018 Feb;12(2): e807-e816.

3 Struecker B, Hillebrandt KH, Voitl R, Butter A, Schmuck RB, Reutzel-Selke A, Geisel D, Joehrens K, Pickerodt PA, Raschzok N, Puhl G, Neuhaus P, Pratschke J, Sauer IM Porcine liver decellularization under oscillating pressure conditions: a technical refinement to improve the homogeneity of the decellularization process. Tissue Eng Part C Methods. 2014 Mar;21(3):303-13.

4 Struecker B, Butter A, Hillebrandt K, Polenz D, Reutzel-Selke A, Tang P, Lippert S, Leder A, Rohn S, Geisel D, Denecke T, Aliyev K, Jöhrens K, Raschzok N, Neuhaus P, Pratschke J, Sauer IM: Improved rat liver decellularization by arterial perfusion under oscillating pressure conditions. J Tissue Eng Regen Med. 2014 Feb;11(2):531-541

weitere Quellen:

5 Billecke N, Raschzok N, Rohn S, Morgul MH, Schwartlander R, Mogl M, Wollersheim S, Schmitt KR, Sauer IM; An operational concept for long-term cinemicrography of cells

in mono- and co-culture under highly controlled conditions – the Slide Observer. 2012 J Biotechnol 159: 83–89.

6 Uygun BE, Price G, Saedi N, Izamis ML, Berendsen T, Yarmush M, Uygun K: Decellularization and recellularization of whole livers, J Vis Exp. 2011 Feb 4;(48)

7 De Kock J, Ceelen L, De Spiegelaere W, Casteleyn C, Claes P, Vanhaecke T, et al. Simple and quick method for whole-liver decellularization: a novel in vitro three-dimensional bioengineering tool? Archives of toxicology. 2011;85(6):607–12. Epub 2011/04/23.

8 Crapo PM, Ph.D., Gilbert TW, Badylak SF, D.V.M., Ph.D., M.D. : An overview of tissue and whole organ decellularization, Biomaterials . 2011 April; 32(12): 3233–3243

9 Soto-Gutierrez A, Zhang L, Medberry C, Fukumitsu K, Faulk D, Jiang H, Reing J, Gramignoli R, Komori J, Ross M, Nagaya M, Lagasse E, Stolz D, Strom SC, Fox IJ, Badylak SF: A whole-organ regenerative medicine approach for liver replacement, Tissue Eng Part C Methods. 2011 Jun;17(6):677-86.

10 Robertson MJ, Soibam B, O'Leary JG, Sampaio LC, Taylor DA, Zhao F: Recellularization of rat liver: An in vitro model for assessing human drug metabolism and liver biology PLoS One. 2018; 13(1): e0191892. Published online 2018 Jan 29. doi: 10.1371/journal.pone.0191892

11 Baptista PM, Siddiqui MM, Lozier G, Rodriguez SR, Atala A, Soker S: The use of whole organ decellularization for the generation of a vascularized liver organoid. 2011 Hepatology 53: 604 –617

12 Uygun BE, Soto-Guiterrez A, Yagi H; Organ reeingeneering through development of transplantable recellularized liver graft using decellularized liver matrix Nat Med. 2010 Jul; 16(7): 814–820.

13 Neuhaus, P. Extrakorporale Leberperfusion-Entwicklung und Erprobung eines neuen Modells. 1982

14 Faulk DM, Carruthers CA, Warner HJ, Kramer CR, Reing JE, Zhang L, D'Amore A, Badylak SF: The Effect of Detergents on the Basement Membrane Complex of a Biologic Scaffold Material, Acta Biomater. 2014 Jan; 10(1): 10.1016/j.actbio.2013.09.006.

8. Eidesstattliche Versicherung

„Ich, Antje Butter, versichere an Eides statt durch meine eigenhändige Unterschrift, dass ich die vorgelegte Dissertation mit dem Thema: *Optimierung der Ratten- und Schweineleber-Dezellularisierung durch Anwendung von oszillierenden Umgebungsdruckschwankungen und Analyse der Morphologie und Funktion von parenchymatös rebesiedelten Rattenlebern* selbstständig und ohne nicht offengelegte Hilfe Dritter verfasst und keine anderen als die angegebenen Quellen und Hilfsmittel genutzt habe.
Alle Stellen, die wörtlich oder dem Sinne nach auf Publikationen oder Vorträgen anderer Autoren beruhen, sind als solche in korrekter Zitierung (siehe „Uniform Requirements for Manuscripts (URM)“ des ICMJE -*www.**icmje**.org*) kenntlich gemacht. Die Abschnitte zu Methodik (insbesondere praktische Arbeiten, Laborbestimmungen, statistische Aufarbeitung) und Resultaten (insbesondere Abbildungen, Graphiken und Tabellen) entsprechen den URM (s.o) und werden von mir verantwortet.
Mein Anteil an der ausgewählten Publikation entspricht dem, der in der untenstehenden gemeinsamen Erklärung mit dem/der Betreuer/in, angegeben ist.

Die Bedeutung dieser eidesstattlichen Versicherung und die strafrechtlichen Folgen einer unwahren eidesstattlichen Versicherung (§156,161 des Strafgesetzbuches) sind mir bekannt und bewusst.“

_____

Datum Unterschrift

9. Ausführliche Anteilserklärung an den erfolgten Publikationen

Publikationen:

1. Butter A., Aliyev K., Hillebrandt K., Raschzok N., Kluge M., Seiffert N., Tang P. Napierala H., Ashraf M., Reutzel-Selke A., Andreou A., Pratschke J., Sauer I., Struecker B.:

Evolution of graft morphology and function after recellularization of decellularized rat livers

Journal of Tissue Engineering and Regenerative Medicine, 2016

Anteilserklärung:

- Planung und Aufbau des Bioreaktors sowie des speziellen Perfusionskreislaufes bestehend aus Perfusionskammer, Blasenfalle, Rollerpumpe und Oxygenator
- Operation sämtlicher Ratten in der tierexperimentellen Einheit sowie Dezellularisierung der Lebern im Bioreaktor
- Isolation primärer Ratten-Hepatozyten
- Herstellung der benötigten Lösungen und Verdünnungen der Detergenzien (PBS, Triton X-100 1% und SDS 1%)
- Rezellularisierung der vorher dezellularisierten Rattenlebern
- Aussaat der statischen Zellkultur sowie Medienwechsel und Probengewinnung
- Entnahme von Medium- als auch Gewebeproben aus dem Bioreaktor
- Einbetten der Histopathologischen Schnitte
- Biochemische Analyse der Mediumproben
- Bestimmung des Medium pH-, Kalium und Glukose-Gehaltes mittels BGA-Gerät
- Photometrische Messung der Transaminasen und der LDH
- Mitarbeit bei allen histologischen Färbungen
- Statistische Analyse der Ergebnisse mittels Prism. 6.0
- Fotodokumentation der Versuche
- Dokumentation der makroskopischen Beobachtungen
- Selbstständiges Verfassen der Publikation

2. Struecker B., Hillebrandt K., Voitl R., Butter A., Schmuck R., Reutzel-Selke A., Geisel D., Joehrens K., Pickerodt P., Raschzok N., Puhl G., Neuhaus P., Pratschke J., Sauer I.

Porcine liver decellularization under oscillating pressure conditions: a technical refinement to improve the homogeneity of the decellularization process

Tissue Engineering Part C Methods, 2015

Anteilserklärung:

- Wiederaufbau des speziellen Bioreaktors und des Perfusionssystems in enger Zusammenarbeit mit der Firma Sorin
- Entnahme von Schweinelebern in der Tierexperimentellen Einheit
- Herstellung der benötigten Verdünnungen von Puffern und Detergenzien (u. a. PBS, Triton X-100 und SDS 1%)
- Dezellularisierung von Schweinelebern
- Einbetten histologischer Schnitte
- Mithilfe bei der histologischen Färbung und Analyse der Gewebeproben
- Fotodokumentation der Versuche
- Dokumentation makroskopischer Beobachtungen während der Dezellularisierung
- Mitarbeit bei der Anfertigung eines Ausgusspräparates aus Kunststoff
- Mitverfassen der Publikation

3. Struecker B., Butter A., Hillebrandt K., Polenz D., Reutzel-Selke A., Tang P., Lippert S., Leder A., Rohn S., Geisel D., Denecke T., Aliyev K., Jöhrens K., Raschzok N., Neuhaus P., Pratschke J., Sauer I.

Improved rat liver decellularization by arterial perfusion under oscillating pressure conditions

Journal of Tissue Engineering and Regenerative Medicine, 2014

Anteilserklärung:

- Entwurf und Bau der speziellen Bioreaktoren sowie Aufbau des Perfusionskreislaufes für die Dezellularisierung, bestehend aus Leber-Perfusions-Kammer, Blasenfalle, Rollerpumpe und Beatmungsgerät
- Herstellung aller Lösungen sowie benötigter Verdünnungen der Detergenzien

(PBS, SDS 1%, Triton X-100 1%)

- Operation der Ratten sowie Entnahme der Lebern in der Tierexperimentellen Einheit
- Dezellularisierung aller Rattenlebern im Bioreaktor
- Entnahme aller Gewebe-Proben
- Analyse alle Gewebe-Proben hinsichtlich ihres GAG-, DNA-, HGF-Gehaltes
- Einbetten histologischer Proben
- Färbung histologischer Proben (siehe o. g. Färbungen)
- Auswertung der histologischen Schnitte
- Fotodokumentation der Versuche
- Dokumentation aller makroskopischer Beobachtungen während der Dezellularisierung
- Anfertigung eines Ausgusspräparates aus Kunststoff
- Mitverfassen der Publikation

Unterschrift, Datum und Stempel des betreuenden Hochschullehrers/der betreuenden Hochschullehrerin

_____

Unterschrift des Doktoranden/der Doktorandin

_____

10. Druckexemplar der ausgewählten Publikationen

10.1 Evolution of graft morphology and function after recellularization of decellularized rat livers

JOURNAL OF TISSUE ENGINEERING AND REGENERATIVE MEDICINE
J Tissue Eng Regen Med 2017.
Published online in Wiley Online Library (wileyonlinelibrary.com) **DOI:** 10.1002/term.2383

RESEARCH ARTICLE

Evolution of graft morphology and function after recellularization of decellularized rat livers

Antje Butter[1], Khalid Aliyev[2], Karl-Herbert Hillebrandt[1], Nathanael Raschzok[1], Martin Kluge[1], Nicolai Seiffert[1], Peter Tang[1], Hendrik Napierala[1], Ashraf I. Muhamma[1], Anja Reutzel-Selke[1], Andreas Andreou[1], Johann Pratschke[1], Igor M. Sauer[1]* and Benjamin Struecker[1,3]

[1]*Department of Surgery, Campus Virchow-Klinikum and Campus Charité Mitte, Charité Universitaetsmedizin Berlin, Berlin, Germany*
[2]*Department of General, Visceral and Transplantation Surgery, Johannes Gutenberg Universitaet, Mainz, Germany*
[3]*Berlin Institute of Health (BIH), Berlin, Germany*

Abstract

Decellularization of livers is a well-established procedure. Data on different reseeding techniques or the functional evolution and reorganization processes of repopulated grafts remains limited. A proprietary, customized bioreactor was established to repopulate decellularized rat livers (n = 21) with primary rat hepatocytes (150 × 10^6 cells) via the hepatic artery and to subsequently evaluate graft morphology and function during 7 days of *ex vivo* perfusion. Grafts were analysed at 1 h, 6 h, 12 h, 24 h, 3 days, 5 days and 7 days after recellularization (all n = 3) by immunohistological evaluation, hepatocyte-related enzyme (aspartate transaminase, alanine transaminase and lactate dehydrogenase) and albumin measurement in the perfusate. This appears to be the first available protocol for repopulation of rat livers via the hepatic artery. Within the first 24 h after repopulation, the hepatocytes seemed to migrate out of the vascular network and form clusters in the parenchymal space around the vessels. Graft function increased for the first 24 h after repopulation with a significantly higher function compared to standard two-dimensional culture after 24 h. Thereafter, graft function constantly decreased with significantly lower values after 6 days and 7 days of perfusion, although histologically viable hepatocytes were found even after this period. The data suggests that, owing to a constant loss of function, repopulated grafts should potentially be implanted as soon as cell engraftment and graft re-organization are completed. Copyright © 2016 John Wiley & Sons, Ltd.

Received 3 December 2015; Revised 27 September 2016; Accepted 6 December 2016

Keywords liver decellularization; liver recellularization; arterial perfusion; *ex vivo* perfusion; bioreactor; graft analysis

1. Introduction

Decellularization and recellularization of solid organs is an emerging technique to generate implantable liver tissue *in vitro* (Crapo *et al.*, 2011). The premise of this method is to selectively remove cells and antigenic material from an organ to use the non-immunogenic extracellular matrix (ECM) of the liver as a bioartificial scaffold for cellular repopulation (Bühler *et al.*, 2014; Struecker et al., 2014a, 2014b, 2014c). Although liver decellularization is a well-established procedure in animal models, recellularization remains a challenge, and only limited information on the technical aspects of recellularization is available (Struecker et al., 2014a, 2014b, 2014c; Faulk *et al.*, 2015).

Two generally different approaches for cellular repopulation have been described: (1) direct injection of cells into the ECM and (2) infusion of cells via the conserved vascular network (Soto-Gutierrez *et al.*, 2011; Shirakigawa *et al.*, 2013).

To date, cellular infusion represents the standard procedure for cellular repopulation, but the optimal technique for performing this procedure remains unknown. Different infusion routes have been shown to result in different cellular arrangements inside repopulated grafts, and it appears reasonable that for complete liver re-establishment, all feasible infusion routes (i.e. portal vein, hepatic artery, hepatic veins and bile duct) should be used (Scarritt *et al.*, 2015).

However, no data are yet available on cellular repopulation via the hepatic artery. Furthermore, no information is available on the morphological evolution of grafts after cellular reinfusion and during *ex vivo* perfusion. Thus, it remains unclear how long recellularized grafts should be maturated *ex vivo* before implantation to trigger optimal graft outcomes.

The present study provides the first available data on cellular repopulation of decellularized rat livers via the hepatic artery. Furthermore, the cellular reorganization and graft function was examined over a period of 7 days after recellularization. A bioreactor was developed that allowed perfusion recellularization of liver scaffolds via the hepatic artery and/or the portal vein (see Figure 1). Then, rat liver extracellular matrix (ECM) (n = 21) was recellularized with primary rat hepatocytes (150 × 10^6)

Correspondence to: I. M. Sauer, Department of General, Visceral, and Transplantation Surgery, Charité – Universitaetsmedizin Berlin, Augustenburger Platz 1, D–13353 Berlin, Germany. E-mail: igor.sauer@charite.de

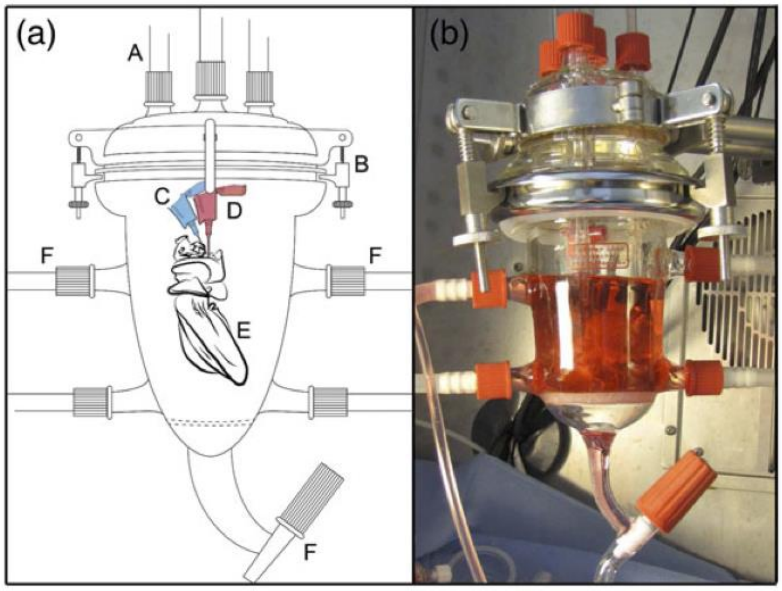

Figure 1. (a) Schematic diagram and (b) photograph of the bioreactor. Culture medium was perfused via the inflow (A) into the sealed chamber (B). The hepatic artery (C) or the portal vein (D) of rat livers (E) were perfused selectively. Perfusate level in the chamber was regulated through the outflow (F). [Colour figure can be viewed at wileyonlinelibrary.com]

via the hepatic artery and the repopulated grafts perfused with oxygenized medium via the portal vein for up to 7 days *ex vivo*. To sequentially evaluate the graft morphology over time, experiments were stopped at several defined time-points (1 h, 6 h, 12 h, 1 d, 3 days, 5 days and 7 days; all $n = 3$), and the grafts were evaluated histologically and functionally.

2. Materials and methods

2.1. Animals

Female Lewis rats (Janvier, St Berthevin Cedex, France) were kept and operated at the Facility for Experimental Medicine (FEM, Charité, Berlin, Germany) in accordance with federal laws and the regulations of the local State Office of Health and Social Affairs (Landesamt für Gesundheit und Soziales Berlin, Germany; Reg. No. O 0365/11).

Female rats weighing 200–300 g ($n = 21$) served as organ donors for liver decellularization to generate cell-free extracellular liver matrices. Female Lewis rats ($n = 21$) of the same weight underwent total liver removal for primary rat hepatocyte isolation.

2.2. Rat liver harvesting

For liver harvesting, rats were anaesthetized via inhalation of isoflurane (3.5% for induction/2% for maintenance) and intraperitoneal injection of (novaminsulfon, metamizole) (100 mg/kg), ketamine (10 mg/kg) and xylazine (2.5 mg/kg).

Liver harvesting was performed as previously described (Bühler *et al.*, 2014; Struecker *et al.*, 2014c). After induction of anaesthesia, the rats underwent longitudinal laparotomy. Liver lobes were prepared and liberated carefully. The bile duct was identified and transected. After ligation, the prepyloric vein was transected. The portal vein was prepared and freed from the abdominal connective tissue. The hepatic artery was prepared and liberated, whereas the lienopancreatic and gastricolienal arteries were ligated and transected. The hepatic artery was prepared and followed to the coeliac trunk and its origin on the abdominal aorta. The inferior vena cava was mobilized and tied with a suture but was not completely ligated. For anticoagulation, 500 Units of heparin (RotexMedica, Luitré, France)/1 ml saline (Braun, Melsungen, Germany) were injected through the inferior vena cava. The abdominal aorta was incised proximal to the coeliac trunk. The portal vein was clamped 3–4 cm distal to the liver and a fish-mouth incision was made; cannulation was performed with an 18 G infusion catheter (BD Venflon™; BD, Eremsbodegem, the Netherlands). The cannulated liver was perfused with 50 ml of saline and freed from the blood. During flushing, the inferior vena cava was incised and used for perfusate outflow. After flushing, perfusion was stopped, and the catheter was fixed to the portal vein with two sutures, which were tied around the valve of the catheter. The inferior vena cava was ligated and transected proximal to its incision. The previously liberated hepatic artery and its origin at the abdominal aorta were incised to generate a patch for cannulation. A plastic tube

DOI: 10.1002/term

(Polythan Tubing, 0.58 mm i.d., 0.96 mm o.d.; SIMS Portex Ltd, Ashford, Kent, UK), which was attached to an 18G infusion catheter, was prefilled with saline and introduced into the hepatic artery through its aortic patch and fixed with a silk suture. Then the hepatic artery was flushed with 5ml of saline to be freed from blood residues.

2.3. Decellularization procedure

To avoid contamination, the decellularization procedure was performed under sterile conditions in a laminar air flow cabinet (Heraeus Instruments, Hanau, Germany).

Rat livers were decellularized via the hepatic artery as previously described (Struecker *et al.*, 2014a). This protocol began with initial perfusion with PBS for 10 min to rinse residual blood. It was followed by 90 min perfusion with 1% Triton X-100 (Roth, Karlsruhe, Germany) and 90 minutes perfusion with 1% sodium dodecyl sulphate (SDS; Roth, Karlsruhe, Germany), with a constant flow rate of 5 ml/min. After decellularization, the cell-free liver extracellular matrices were perfused with phosphate-buffered saline (PBS)/100 U/ml penicillin/100 µg/ml streptomycin (Biochrom GmbH, Berlin, Germany)/100 U/ml gentamicin (Serva, Heidelberg, Germany) overnight.

2.4. Isolation of primary rat hepatocytes

Primary hepatocytes were isolated from the rat livers (female Lewis rats; Janvier). Cell isolation was performed with a previously described isolation protocol (Billecke *et al.*, 2012). Isolated hepatocytes were purified using Percoll (Easycoll Separating Solution; Biochrom GmbH). Hepatocytes with a viability >80% were stored on ice in Dulbecco's Modified Eagle Medium (DMEM; Biochrom GmbH) for a maximum of 1 h before the repopulation experiments.

2.5. Reactor and perfusion system

After hepatocyte isolation, the decellularized liver matrices were connected to the recellularization reactor. This bioreactor was enhanced from previously described systems (Song *et al.*, 2013; Struecker *et al.*, 2014a; Uzarski *et al.*, 2015) and customized to requirements. The main portion of this proprietary bioreactor (Nami 3.0) and perfusion system is a perfusable cylindrical glass chamber that has several adjustable inflows over its screw cab and four lateral outflows that can be connected to perfusion tubing via Luer lock connectors (Figure 1). One advantage of this device is the possibility to selectively perfuse the portal vein and/or the hepatic artery simultaneously. The arterial – as well as the portal venous – system was connected to individual and independent perfusion circuits. The main circuit, which was connected to the portal vein of the decellularized matrix, was constantly recirculating medium (DMEM; Life Technologies GmbH, Darmstadt, Germany). This circuit was driven by a multichannel peristaltic pump (REGLO ICC, Ismatec; IDEX Health and Science GmbH, Wertheim, Germany) and aerated by an oxygenator (neonatal oxygenator, Kids D101; Sorin Group, Arvada, CO, USA) that supplied 95% O_2/5% CO_2 directly to the perfusate.

The arterial perfusion system was connected to a syringe-based perfusion pump with a pressure-path cut-out (Secura FT; Braun) and was used only for hepatocyte seeding.

The portal vein and the hepatic artery were connected to the screw caps of the recellularization chamber, then the reactor chamber was closed and sealed in sterile conditions under laminar air flow.

2.6. Repopulation of decellularized rat livers

Initially, fresh medium perfusion was started via the portal vein to allow the matrix to inflate and warm up to 37°C for 30 min. Isolated primary rat hepatocytes were reseeded on the decellularized matrix via a multistep perfusion technique. For this procedure, 150×10^6 viable rat hepatocytes were placed into a 50 ml syringe (Braun) and infused at a constant flow rate of 1 ml/min into the decellularized matrix via the hepatic artery. During cell seeding via the arterial system the portal venous system was perfused with DMEM at a flow rate of 2 ml/min to prevent the matrix from collapsing. To avoid sedimentation of the hepatocytes, the syringe-based perfusion pump unit was manually rotated during cell seeding. After 15 min, perfusion was paused for 10 min to allow cells to attach to the matrix. The next seeding step was then begun under the same constant arterial and portal venous perfusion conditions as described above. This was repeated four times until all hepatocytes (150×10^6) were distributed into the decellularized matrix. After a final perfusion break of 10 min, only portal venous perfusion was restarted, at a constant flow rate of 2 ml/min for 30 min, to supply the recellularized matrix with fresh, oxygenized medium. This gentle venous perfusion rate was increased to 5 ml/min after 30 min and remained at this level until termination of the experiments. The medium was changed (approximately 180 ml) every 24 h.

2.7. Perfusate sampling

After repopulation of the matrices, samples of medium were taken from the reactor chamber at the beginning of perfusion after 1 h, 6 h, 12 h and 24 h, and then every 24 h thereafter.

2.8. Perfusate analysis

Perfusate samples were analysed with respect to glucose level, pH and potassium using a blood gas analyser (ABL800 FL; Radiometer GmbH, Willich, Germany).

DOI: 10.1002/term

Aspartate transaminase (AST), alanine transaminase (ALT) and lactate dehydrogenase (LDH) were measured photometrically from medium samples with a Fluitest Kit (Analyticon, Lichtenfels, Germany; FLUOSTAR, Optima, BMG Labtech, Ortenberg Germany). Albumin was measured using a Rat Albumin enzyme-linked immunosorbent assay (ELISA) quantification set (Biomol; FLUOSTAR Optima, BMG Labtech).

2.9. Two-dimensional (2D) hepatocyte culture

Cell isolation was performed with a previously described isolation protocol (Billecke *et al.*, 2012). Isolated viable rat hepatocytes were cultured on two six-well cell culture plates (Falcon™ Tissue Culture Plates; Corning Inc, New York, NY, USA) for 7 days ($n = 3$) under cell culture conditions (37°C, 95% O_2/5% CO_2). Each well contained 1×10^6 viable rat hepatocytes and 3 ml cell culture medium (DMEM; Life Technologies GmbH). Medium-change was performed every 24 h. Supernatant medium samples were taken at previously described time-points (1 h, 6 h, 12 h, 24 h, 48 h, 3 days, 4 days, 5 days, 6 days, 7 days).

2.10. Graft harvesting and sampling

Recellularized matrices were harvested after seven previously determined time-points (1 h, 6 h, 12 h, 1 day, 3 days, 5 days and 7 days, each $n = 3$). At each time-point one repopulated rat liver was analysed. Therefore, all repopulated grafts were divided and processed identically: left liver lobes were transected, freeze-dried and mashed carefully to receive homogenous tissue samples. The remaining liver lobes were fixed in 4% formalin at 4°C for histological analysis.

2.11. Histological analysis

For histological analysis, recellularized rat livers were fixed in formalin (4%) for 24 h, dehydrated and embedded in paraffin. Livers were sliced in 5-µm thick sections. These sections were stained with haematoxylin/eosin (H&E) (AppliChem, Darmstadt, Germany) according to standard protocols. To visualize glycoproteins, Alcian blue staining (Morphisto, Frankfurt am Main, Germany) was performed according to the Morphisto customer protocol. Sirius Red staining (Sigma-Aldrich Chemie GmbH, Munich, Germany) was performed to visualize collagen fibres. At first, staining with Weigert's haematoxylin for 8 min was performed and followed by washing for ten minutes and staining in PicroSirius red for 1 h. Two changes of acidified water followed and all sections were dehydrated and mounted with Eukitt (Fluka, Buchs, Switzerland).

Antibodies for collagen IV, laminin and fibronectin were used for immunohistochemistry. The protocol for Collagen IV, Fibronectin and Laminin consisted of deparaffinization, rinsing with hydrogen peroxide, antigen retrieval with a 0.01 M citrate buffer (Agilent Technologies, Glostrup, Denmark) and blocking for 1 h at room temperature in 3% goat serum (Agilent Technologies). The sections were then incubated with a rabbit anti-mouse polyclonal collagen IV antibody at 1:400 dilution (Cat. no. #ab6586; Abcam, Cambridge, UK)/Rabbit polyclonal fibronectin (Cat. no. #ab23751; Abcam) at a dilution 1:100/rabbit anti-mouse polyclonal laminin antibody at 1:100 dilution (Cat. no. #ab11575; Abcam) for 1 hour at 37°C in 3% blocking serum. This was followed by a secondary goat anti-rabbit IgG H&L Horseradish Peroxidase (HRP) at 1:400 dilution (Cat. no. #ab6721; Abcam) in 3% blocking serum at 37°C for 30 min. The HRP substrate used was 3,30-diaminobenzadine (DAB), according to the instructions provided by the manufacturer (Agilent Technologies).

A TdT-mediated-dUTP-biotin-nick-end-labelling (TUNEL) assay (R&D systems, Minneapolis, MN, USA) was used for quantification of apoptosis at the aforementioned time-points during the experiments. To detect proliferation of the recellularized hepatocytes, sections were stained with proliferation cell nuclear antigen (PCNA) antibodies (Dako, Glostrup, Denmark) according to the labelled streptavidin/biotin method. Cytokeratin-18 (CK18) antibody (Abcam) staining of recellularized grafts was performed according to the alkaline phosphate protocol.

2.12. Statistical analysis and graphing

Statistical analysis was performed using GraphPad Prism (Prism 6 for Macintosh Version 6.0b; GraphPad Software, La Jolla, CA, USA). Data are described as means ± standard deviations (SD) in the text and standard error of mean (SEM) in figures. A D'Agostino–Pearson omnibus normality test was used to test for normal distribution. A two-way analysis of variance (two-way ANOVA) was performed to test whether the two independent variables 'group' (2D culture, ReCell Matrix) and 'time' (time of sample collection) affect the course of liver enzyme and albumin production. Two-way ANOVA was followed by multiple comparison *post hoc* tests to compare different time-points within the groups (Tukey) or to compare the two groups at one specific time-point (Sidak). Differences were considered significant at p-values less than 0.05.

3. Results

3.1. Isolation of primary rat hepatocytes

Primary rat hepatocytes had a similar viability after isolation and after performing a Percoll purification protocol (Sigma Aldrich St. Louis, USA) in all groups (Figure 2). After cell isolation and during the recellularization procedure, rat hepatocytes were stored

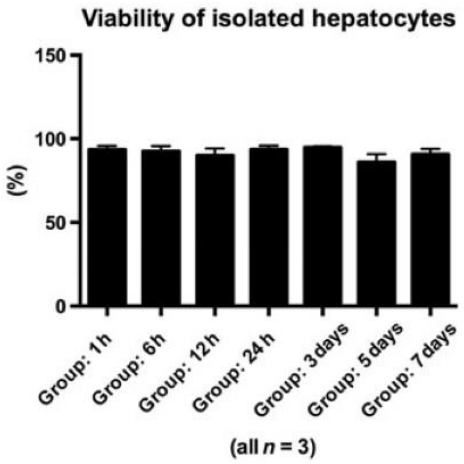

Figure 2. Viability of isolated hepatocytes. Viability ranged from 80.5% to 95.8% with a mean value of 91.6%.

on ice so that cell viability could be preserved until cell seeding was completed.

3.2. Macroscopic observations

Hepatocytes, which were infused via the hepatic artery of the decellularized liver scaffold, spread into all liver lobes. During the first of four infusions, the cells remained mostly inside the vascular network of the ECM (Figure 3a). Then, during the second and third of four infusions, the cells leaked from the vessels and cell clusters formed in the small liver lobes near the arterial inflow (Figure 3b) and during the last infusion in the periphery of the left, right and middle liver lobes (Figure 3c). Clusters appeared as light brownish spots inside the translucent ECM. The cell clusters mainly developed in areas of small capillaries and remained in these macroscopic formations until the end of the experiment. During the first recellularization step, a small quantity of rat hepatocytes left the matrix via the superior vena cava. This cell loss stopped after the initial attachment period and did not recur during subsequent seeding steps.

3.3. Histological evaluation

3.3.1. Decellularization

Haematoxylin and eosin staining showed complete decellularization of the ECM, without cells remaining or cell detritus. The protein structure of the ECM, including the vascular network, was preserved in all specimens (data not shown).

3.3.2. Recellularization

Haematoxylin and eosin staining showed that hepatocytes were attached to both sides of the vascular matrix, near the protein network of the vessels. Some areas of the decellularized liver were not repopulated with cells and remained empty (Figure 4). Cell clusters outside of the vascular network were seen primarily around the medium perfused branches of, presumably, the portal vein. During the first phase of the recellularization process (until 24 h), more cells were found inside the vascular network compared with later time-points, when more cells were found in the parenchymal (extravascular) matrix (Figure 4).

A TUNEL staining was performed to analyse cell apoptosis. At later time-points (24 h and 7 days) more cells appeared TUNEL-positive compared with earlier time-points (1 h and 6 h), indicating that these cells undergo apoptosis. However, even after 7 days of perfusion TUNEL-negative cells were observed inside the recellularized liver graft (Figure 4: pos., positive control; neg., negative control).

Proliferation cell nuclear antigen staining was performed to visualize cell proliferation after recellularization. Even after 7 days of perfusion cells were stained PCNA-positive, showing that these cells proliferate (Figure 4: pos., positive control; neg., negative control).

Immunohistochemical staining for collagen IV, fibronectin and laminin revealed that these typical matrix proteins were detected in decellularized rat liver scaffolds and after recellularization in a comparable pattern.

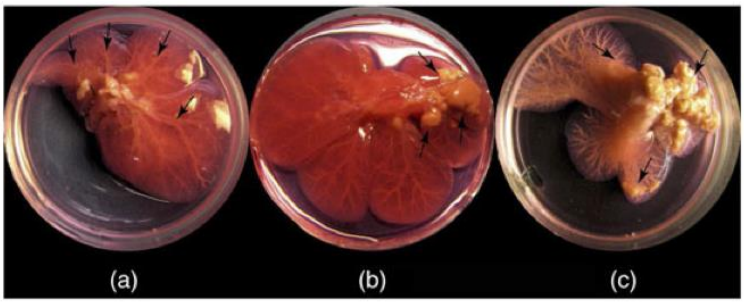

Figure 3. Photographs of recellularized rat livers. (a) After the first of four cell infusions, cells remained mostly inside the vascular network (black arrows). (b) After the third of four infusions, some cells leaked from the vessels and cell clusters formed in the small liver lobes near the arterial inflow (arrows). (c) After infusion of 150 × 106 cells, clusters were found in the periphery of all liver lobes (arrows). [Colour figure can be viewed at wileyonlinelibrary.com]

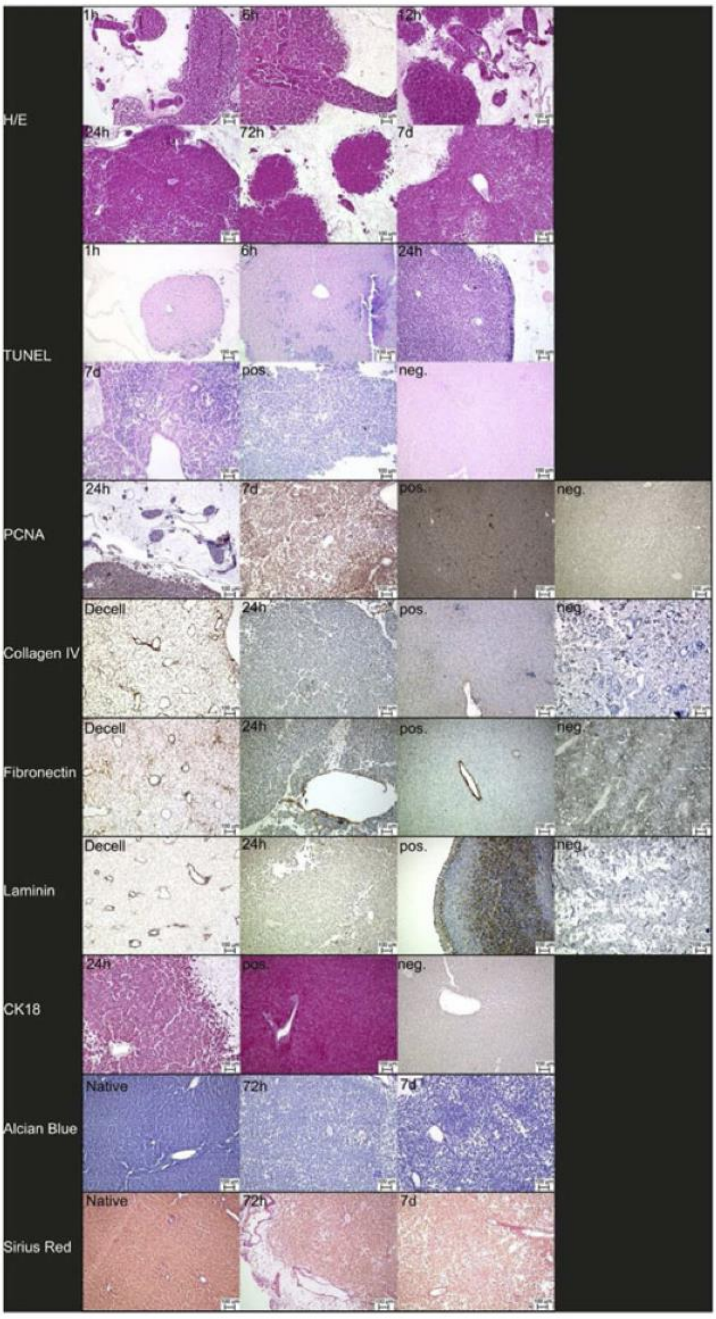

Figure 4. Histological evaluation of recellularized rat livers. H/E: representative images of haematoxylin and eosin stained slices of recellularized rat livers after 1 h, 6 h, 12 h, 24 h, 72 h and 7 days of *ex vivo* perfusion. At early time-points (1, 6 and 12 h) more cells were found inside the vascular framework while at later time points (24 h, 72 h and 7 days) more cells were found in the parenchymal compartment. Owing to the limited cell mass, decellularized areas were observed in any slices at any time point. TUNEL: terminal deoxynucleotidyl transferase dUTP nick-end labelling (TUNEL) staining of slices of recellularized rat livers after 1 h, 6 h, 24 h and 7 days of *ex vivo* perfusion. At later time-points (24 h and 7 days) more cells appear TUNEL-positive compared with earlier time points (1 h and 6 h), meaning that these cells undergo apoptosis. Even after 7 days of perfusion, TUNEL-negative cells were observed inside the recellularized liver graft. PCNA: proliferation cell nuclear antigen staining of slices of recellularized rat livers after 24 h and 7 days of *ex vivo* perfusion. After 7 days of perfusion, cells were stained PCNA-positive, showing that these cells proliferate. Collagen IV: immunohistochemical staining for collagen IV of slices of decellularized rat livers and recellularized rat livers after 24 h of *ex vivo* perfusion. Collagen IV was detected in decellularized rat liver scaffolds and after recellularization in a comparable pattern. Fibronectin: immunohistochemical staining for fibronectin of slices of decellularized rat livers and recellularized rat livers after 24 h of *ex vivo* perfusion. The distribution of fibronectin was comparable in decellularized rat liver scaffolds and after recellularization. Laminin: immunohistochemical staining for laminin of slices of decellularized rat livers and recellularized rat livers after 24 h of *ex vivo* perfusion. Laminin was visualized in decellularized rat liver scaffolds and after recellularization. CK18: immunohistochemical staining for cytokeratin-18 of slices of decellularized rat livers and recellularized rat livers after 24 h of *ex vivo* perfusion. Cells within the recellularized rat livers were stained CK-18 positive. Alcian Blue: Alcian Blue staining to visualize acidic polysaccharides (e.g. glycosaminoglycans); these were found in recellularized rat livers after 72 h and 7 days of perfusion. Sirius Red: Sirius Red staining of recellularized rat livers after 72 h and 7 days of perfusion. Collagen fibres are stained red and visible in native and recellularized liver. pos., Positive control, neg., negative control [Colour figure can be viewed at wileyonlinelibrary.com]

DOI: 10.1002/term

Staining for CK-18 of showed that cells within the recellularized rat livers stained positive.

Acidic polysaccharides (e.g. glycosaminoglycans) and collagen fibres were visualized by Alcian Blue and Sirius Red staining. No significant differences in the distribution of these components were observed after recellularization and subsequent perfusion for up to 7 days.

3.4. Biochemical analysis

3.4.1. Aminotransferases

Aspartate aminotransferase showed elevated levels at the beginning of the experiment in the perfusate and the 2D culture, with peak levels at 1 h after repopulation (ReCell matrix: 23.85 ± 5.68 U/l) and after 24 h, respectively (2D culture: 26.97 ± 3.35 U/l); Figure 5). After peaking, AST levels decreased continuously until they reached a minimum value at 120 h (ReCell matrix: 3.85 ± 1.89 U/l) and 48 h, respectively (2D culture: 2.44 ± 1.24 U/l). Aspartate aminotransferase in the recellularized graft was significantly higher at 1 h compared with 48 h ($p = 0.0079$) and 72 h ($p = 0.0210$). All other differences were not statistically significant and no significant differences between both groups were found.

Alanine aminotransferase levels showed a comparable trend, with an early peak after recellularization (ReCell matrix after 1 h: 20.64 ± 3.52 U/l; 2D culture after 6 h: 14.58 ± 0.29 U/l) and a minimum at 7 days (ReCell matrix after 168 h: 1.91 ± 0.98 U/l; 2D culture after 6 h: 4.92 ± 1.21 U/l). Alanine aminotransferase levels were significantly higher at 1 h compared with 48 h ($p = 0.0005$) and 72 h ($p = 0.0033$) and 120 h ($p = 0.0054$) and 168 h ($p = 0.0421$) in the recellularized graft. All other differences were not statistically significant and no significant differences were found between either group.

3.4.2. Lactate dehydrogenase

Lactate dehydrogenase measurements were comparable to aminotransferases with peak levels at 6 h (ReCell matrix after 6 h: 54.61 ± 30.57 U/l) and 1 h (2D culture: 39.81 ± 16.7 U/l) (Figure 5). After 24 h of perfusion, LDH levels were significantly higher in recellularized grafts than after 120 h of perfusion ($p = 0.0.0384$). All other differences were not statistically significant and no significant differences were found between either group.

3.4.3. Rat albumin

Albumin in recellularized liver grafts peaked at 24 h after repopulation (ReCell matrix: 22966 ± 4361 ng/ml) and then constantly decreased until its lowest value after 7

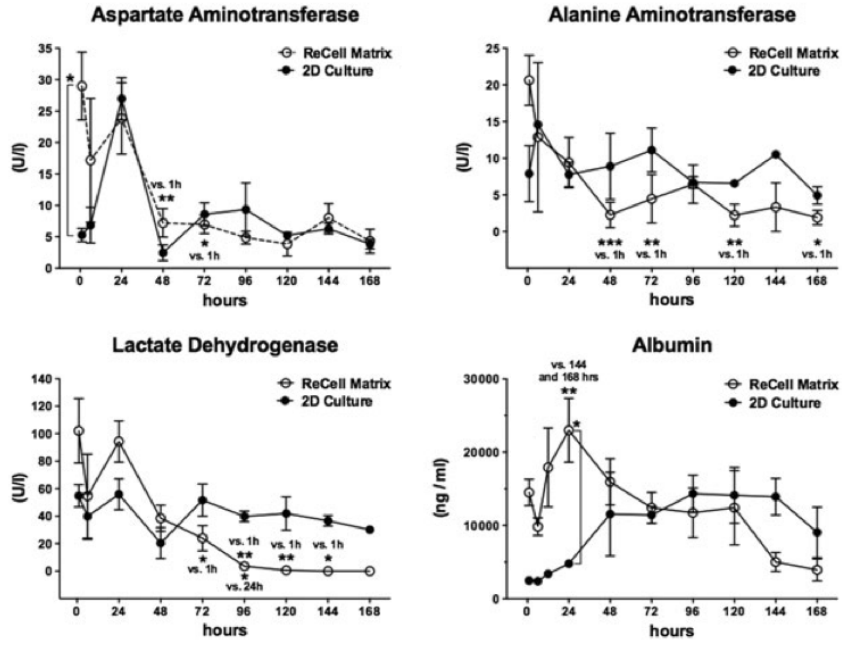

Figure 5. Analysis of intracellular enzymes (aspartate transaminase (AST), alanine transaminase (ALT), lactate dehydrogenase (LDH)) and albumin in the perfusate of recellularized grafts or culture medium of a two-dimensional (2D) hepatocyte culture. Albumin in recellularized rat livers was significantly higher after 24 h than after 144 h ($p = 0.0321$) and 168 h ($p = 0.0176$). Aspartate aminotransferase was significantly higher at 1 h than at 48 h ($p = 0.0079$) and 72 h ($p = 0.0210$). Alanine aminotransferase levels were significantly higher at 1 h than at 48 h ($p = 0.0005$) and 72 h ($p = 0.0033$) and 120 h ($p = 0.0054$) and 168 h ($p = 0.0421$). Furthermore, Albumin at 24 h was significantly higher in the ReCell Matrix compared with the 2D culture ($p = 0.0088$). Lactate dehydrogenase level was significantly higher at 1 h compared with 72 h ($p = 0.0153$), 96 h ($p = 0.0074$), 120 h ($p = 0.0051$) and 144 h ($p = 0.0431$). After 24 h of perfusion, lactate dehydrogenase level was significantly higher than after 120 h of perfusion ($p = 0.0.0384$). All other differences were not statistically significant.

days (ReCell matrix: 3934 ± 1501 ng/ml). Albumin in recellularized rat livers was significantly higher after 24 h than after 144 h ($p = 0.0321$) and 168 h ($p = 0.0176$). In contrast, in the 2D culture the lowest value was measured at 6 h (2D culture: 2390 ± 357.1 ng/ml) with a peak after 96 h (2D culture: 14335 ± 2512 ng/ml). Albumin level at 24 h was significantly higher in the ReCell matrix compared with the 2D culture ($p = 0.0088$) (Figure 5). All other differences were not statistically significant.

3.4.4. Glucose

Glucose levels were relatively stable from the beginning of the perfusion experiments (106.70 ± 5.74 mg/dl) until the end of the experiments at 7 days (105.00 ± 2.83 mg/dl).

3.4.5. pH

The perfusion medium had a slightly alkaline pH. This remained stable after cell seeding (7.59 ± 0.13) and throughout the perfusion period (7.70 ± 0.06; Figure 6).

3.4.6. Potassium

Potassium was stable between 1 h (5.53 ± 0.09) and 12 h (5.7 ± 0.17) after the start of the perfusion experiments. Potassium was then constantly increased until it achieved stable values from 96 h (6.1 ± 0.07) to 7 days (6.1 ± 0.1, Figure 6).

4. Discussion

Liver decellularization and recellularization techniques are evolving quickly, and the amount of available literature in this field is growing constantly. Although liver decellularization is well described, most reports on recellularization are proof-of-concept studies (Uygun *et al.*, 2010; Jiang *et al.*, 2014; Kadota *et al.*, 2014; Ko *et al.*, 2015). Various aspects of liver recellularization (e.g. the optimal infusion route, perfusion pressure, culture conditions, etc.) or implantation (optimal time-point after recellularization, necessary cell types, surgical procedures, etc.) remain unclear, and many issues must be addressed until the long-term survival of an implanted recellularized graft appears feasible.

To date, two different techniques for cellular repopulation have been described: (1) direct injection using a needle (Soto-Gutierrez *et al.*, 2011; Shirakigawa *et al.*, 2012, 2013) or (2) infusion via the vascular network (Bao *et al.*, 2011; Zhou *et al.*, 2011; Barakat *et al.*, 2012; Yagi *et al.*, 2013; Sabetkish *et al.*, 2014; Wang *et al.*, 2014). Although the multistep infusion technique appears to be the current gold-standard for cellular repopulation, only one study comparing these methods is available: Soto-Gutierrez *et al.* (2011) showed that recellularization using a multistep infusion technique resulted in the best cell engraftment and function and reported on the deposition of primary hepatocytes within the parenchymal space and, occasionally, the vessels6. However, Shirakigawa *et al.* (2013) reported that the infusion of hepatocytes via the portal or hepatic vein resulted in clotting of the vascular system and proposed the direct injection of a collagen gel containing hepatocytes as the preferred method of recellularization.

These conflicting observations may be the result of different decellularization and/or recellularization protocols. The decellularization protocol directly affects the integrity of the liver ECM, including the basement membrane, and different recellularization protocols provoke different types of mechanical stress on the matrix. Thus, it appears possible that recellularization with higher flow rates and perfusion pressures pushes cells into the parenchymal ECM through small ruptures in the vascular ECM. However, another interesting finding results from different experimental set-ups after the recellularization process. Whereas Shirakigawa *et al.* (2013) analysed their repopulated grafts after 24 h, Soto-Gutierrez *et al.* (2011) perfused their grafts for 7 days after recellularization before histological analysis.

In the present study, grafts were repopulated using a multistep infusion technique and analysed after 1 h, 6 h,

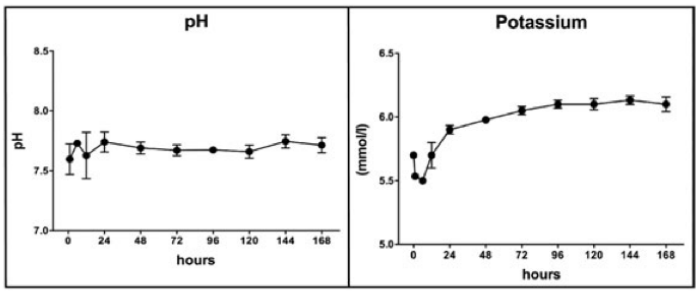

Figure 6. Analysis of pH and potassium in the perfusate over time. The perfusion medium showed a slightly alkaline pH. This remained stable after cell seeding (7.59 ± 0.13) and throughout the perfusion period (7.70 ± 0.06). Potassium was stable between 1 h (5.53 ± 0.09) and 12 h (5.7 ± 0.17) after the start of the perfusion experiments. Potassium then constantly increased until it achieved stable values from 96 h (6.1 ± 0.07) to 7 days (6.1 ± 0.1).

DOI: 10.1002/term

12 h, 24 h, 3 days, 5 days, and 7 days. The results are in agreement with those of both Shirakigawa *et al.* (2013) and Soto-Gutierrez *et al.* (2011) Initially, reseeded hepatocytes could be observed inside the arterial network, but then they appeared to migrate into the parenchymal space within 24 h after recellularization. This observation has been reported by others (Uygun *et al.*, 2010; Baptista *et al.*, 2011; Zhou *et al.*, 2011; Barakat *et al.*, 2012; Yagi *et al.*, 2013). With respect to the set-up of the present study, it appears unlikely that the mechanical force resulting from perfusion pressure was responsible for this effect because the grafts were repopulated via the hepatic artery but perfused via the portal vein. After migration, hepatocytes showed a tendency to form clusters around vascular branches (i.e. within the parenchymal ECM). The cells in these formations appeared to have better long-term survival and function, presumably owing to a sufficient supply of oxygen and nutrients from nearby vessels, as well as cell–cell and cell–matrix interactions. Single hepatocytes inside the ECM or hepatocytes trapped in small vascular branches showed fewer signs of proliferation or metabolism and mostly became apoptotic during the course of experiment.

Re-establishing the complex micro-architecture of the liver, including the parenchymal space, the biliary system and the vascular system, is still an unresolved issue and is the subject of ongoing studies. Baptista *et al.* (2011) showed that it was possible to selectively re-endothelialize the hepatic or portal vein of a decellularized liver by selective infusion of green fluorescent protein (GFP)-labelled endothelial cells via these vessels. They concluded that simultaneous utilization of both vascular routes for cell seeding enables complete access to the entire length of the vascular network, although they did not mention the arterial system. (Baptista *et al.*, 2011) However, it has already been shown that rat liver decellularization via the hepatic artery resulted in more homogeneous results compared with the portal vein (Struecker *et al.*, 2014a). It appears likely that the application of different perfusion routes may be necessary for a complete re-establishment of the complex liver microarchitecture (Scarritt *et al.*, 2015). The study presented here demonstrated that arterial recellularization is a feasible concept and showed results that were similar to those in existing literature. However, repopulation of livers implicates many different parameters (e.g. cell mass, cell concentrations, perfusion rate, etc.) and, to date, no statistically relevant data on the optimization of these parameters is available.

The ultimate goal of liver decellularization and recellularization is the implantation of a repopulated graft and the consecutive evaluation *in vivo*. However, to date, insufficient information is available on the evolution of repopulated grafts *ex vivo* and on the optimal time-point for implantation after recellularization. The present study analysed the morphology and function of repopulated liver grafts during 7 days of *ex vivo* perfusion to deliver references regarding this question.

During the first 24 h after repopulation, strong cytotoxicity was observed, which was analysed by the measurement of intra-hepatocellular enzymes (aminotransferases and lactate dehydrogenase) in the perfusate. Because the histological analysis of grafts did not reveal many apoptotic or lytic cells during this period, it is hypothesized that the increase in the enzyme levels in the perfusate was caused by hepatocytes that did not engraft on the ECM and consequently died because of hypoxia, shear stress or anoikis. Analysis of albumin secretion in the perfusate revealed an increase in cell function within the first 24 h after repopulation, which was followed by a constant decrease until the end of the experiment. Interestingly, compared with standard 2D culture, the repopulated grafts secreted significantly more albumin at 24 h, showing a potential benefit of the ECM for the cells. In their studies, Soto-Gutierrez (2011) and Uygun *et al.* (2010) showed comparable effects, although these authors presented cumulative albumin levels, which complicates a direct comparison between the studies.

Building a liver hybrid based on ECM and primary cells with a relevant function will require a greater quantity of hepatocytes, endothelial cells and liver specific cells (e.g. cholangiocytes, sinusoidal endothelial cells, Kupffer cells and hepatic stellate cells). These cells will have an impact on graft re-establishment after cell seeding, and more experimental results are needed to provide clear insight regarding when to implant repopulated grafts. However, it appears reasonable that the general processes of cell engraftment, migration, organization and function after repopulation of decellularized scaffolds is comparable for different cell types. Although we present a proof-of-concept study and many more data are needed to provide definitive answers on when to implant repopulated grafts, the data presented at least give a first impression of the morphological and functional processes within liver grafts after repopulation. It appears reasonable that repopulated grafts should be implanted 12–24 h after repopulation, although it is not yet possible to present definitive evidence for this statement.

5. Conclusion

A customized, proprietary bioreactor was developed for the selective decellularization and recellularization of rat livers via different perfusion routes. The present study is the first to show a proof-of-concept for arterial repopulation in rat livers. The data indicate that hepatocyte engraftment and reorganization is implemented within 24 h after repopulation. The function of repopulated grafts during *ex vivo* perfusion increases for up to 24 h but then constantly decreases. It is hypothesized that repopulated rat livers should be implanted within the first 24 h after repopulation, although definitive evidence is not yet available to support this for this statement.

Conflict of interest

The authors have declared that there is no conflict of interest

Acknowledgements

B.S. is participant in the BIH Charité Clinical Scientist Program funded by the Charité – Universitätsmedizin Berlin and the Berlin Institute of Health. The authors thank Steffen Lippert, Dietrich Polenz, Annekatrin Leder and Katharina Struecker for their help during this project.

References

Bao J, Shi Y, Sun H, *et al.* 2011; Construction of a portal implantable functional tissue-engineered liver using perfusion-decellularized matrix and hepatocytes in rats. *Cell Transplant* **20**: 753–766.

Baptista PM, Siddiqui MM, Lozier G, *et al.* 2011; The use of whole organ decellularization for the generation of a vascularized liver organoid. *Hepatology* **53**: 604–617.

Barakat O, Abbasi S, Rodriguez G, *et al.* 2012; Use of decellularized porcine liver for engineering humanized liver organ. *J Surg Res* **173**: 11–25.

Billecke N, Raschzok N, Rohn S, *et al.* 2012; An operational concept for long-term cinemicrography of cells in mono- and co-culture under highly controlled conditions – the SlideObserver. *J Biotechnol* **159**: 83–89.

Bühler NE, Schulze-Osthoff K, Königsrainer A, *et al.* 2014; Controlled processing of a full-sized porcine liver to a decellularized matrix in 24 h. *J Biosci Bioeng* **119**: 609–613.

Crapo PM, Gilbert TW, Badylak SF. 2011; An overview of tissue and whole organ decellularization processes. *Biomaterials* **32**: 3233–3243.

Faulk D, Wildemann J, Badylak S. 2015; Decellularization and cell seeding of whole liver biologic scaffolds composed of extracellular matrix. *J Clin Exp Hepatol* **5**: 69–80.

Jiang, W-CC, Cheng YHH, Yen, MHH, *et al.* 2014; Cryo-chemical decellularization of the whole liver for mesenchymal stem cells-based functional hepatic tissue engineering. *Biomaterials* **35**: 3607–3617.

Kadota Y, Yagi H, Inomata K, *et al.* 2014; Mesenchymal stem cells support hepatocyte function in engineered liver grafts. *Organogenesis* **10**: 268–277.

Ko IK, Peng L, Peloso A, *et al.* 2015; Bioengineered transplantable porcine livers with re-endothelialized vasculature. *Biomaterials* **40**: 72–79.

Sabetkish S, Kajbafzadeh AMM, Sabetkish N, *et al.* 2014; Whole-organ tissue engineering: decellularization and recellularization of three-dimensional matrix liver scaffolds. *J Biomed Mater Res A* **173**: 11–25.

Scarritt M, Pashos N, Bunnell B. 2015; A review of cellularization strategies for tissue engineering of whole organs. *Front Bioeng Biotechnol* **3**: 83–89

Shirakigawa N, Ijima H, Takei T. 2012; Decellularized liver as a practical scaffold with a vascular network template for liver tissue engineering. *J Biosci Bioeng* **114**: 546–551.

Shirakigawa N, Takei T, Ijima H. 2013; Base structure consisting of an endothelialized vascular-tree network and hepatocytes for whole liver engineering. *J Biosci Bioeng* **5**: 69–80

Song JJ, Guyette JP, Gilpin SE, *et al.* 2013; Regeneration and experimental orthotopic transplantation of a bioengineered kidney. *Nat Med* **19**: 646–651.

Soto-Gutierrez A, Zhang L, Medberry C, *et al.* 2011; A whole-organ regenerative medicine approach for liver replacement. *Tissue Eng Part C Methods* **17**: 677–686.

Struecker B, Butter A, Hillebrandt K, *et al.* 2014a. Improved rat liver decellularization by arterial perfusion under oscillating pressure conditions. *J Tissue Eng Regen Med* **35**: 3607–3617

Struecker B, Hillebrandt KH, Voitl R, *et al.* 2014b. Porcine liver decellularization under oscillating pressure conditions: a technical refinement to improve the homogeneity of the decellularization process. *Tissue Eng Part C Methods* **53**: 604–617

Struecker B, Raschzok N, Sauer IM. 2014c. Liver support strategies: cutting-edge technologies. *Nat Rev Gastroenterol Hepatol* **11**: 166–176.

Uygun BE, Soto-Gutierrez A, Yagi H, *et al.* 2010; Organ reengineering through development of a transplantable recellularized liver graft using decellularized liver matrix. *Nat Med* **16**: 814–820.

Uzarski JS, Bijonowski BM, Wang B, *et al.* 2015; Dual-purpose bioreactors to monitor noninvasive physical and biochemical markers of kidney and liver scaffold recellularization. *Tissue Eng Part C Methods* **21**: 1032–1043.

Wang X, Cui J, Zhang, B-QQ, *et al.* 2014; Decellularized liver scaffolds effectively support the proliferation and differentiation of mouse fetal hepatic progenitors. *J Biomed Mater Res A* **102**: 1017–1025.

Yagi H, Fukumitsu K, Fukuda K, *et al.* 2013; Human-scale whole-organ bioengineering for liver transplantation: a regenerative medicine approach. *Cell Transplant* **22**: 231–242.

Zhou P, Lessa N, Estrada DC, *et al.* 2011; Decellularized liver matrix as a carrier for the transplantation of human fetal and primary hepatocytes in mice. *Liver Transpl* **17**: 418–427.

10.2 Porcine Liver Decellularization Under Oscillating Pressure Conditions: A Technical Refinement to Improve the Homogeneity of the Decellularization Process

TISSUE ENGINEERING: Part C
Volume 21, Number 3, 2015

DOI: 10.1089/ten.tec.2014.0321

Porcine Liver Decellularization Under Oscillating Pressure Conditions: A Technical Refinement to Improve the Homogeneity of the Decellularization Process

Benjamin Struecker, MD,[1,*] Karl Herbert Hillebrandt,[1,*] Robert Voitl,[1] Antje Butter,[1] Rosa B. Schmuck, MD,[1] Anja Reutzel-Selke,[1] Dominik Geisel, MD,[2] Korinna Joehrens, MD, PhD,[3] Philipp A. Pickerodt, MD,[4] Nathanael Raschzok, MD,[1] Gero Puhl, MD, PhD,[1] Peter Neuhaus, MD, PhD,[1] Johann Pratschke, MD, PhD, FACS,[1] and Igor M. Sauer, MD, PhD[1]

Decellularization and recellularization of parenchymal organs may facilitate the generation of autologous functional liver organoids by repopulation of decellularized porcine liver matrices with induced liver cells. We present an accelerated (7 h overall perfusion time) and effective protocol for human-scale liver decellularization by pressure-controlled perfusion with 1% Triton X-100 and 1% sodium dodecyl sulfate via the hepatic artery (120 mmHg) and portal vein (60 mmHg). In addition, we analyzed the effect of oscillating pressure conditions on pig liver decellularization ($n = 19$). The proprietary perfusion device used to generate these pressure conditions mimics intra-abdominal conditions during respiration to optimize microperfusion within livers and thus optimize the homogeneity of the decellularization process. The efficiency of perfusion decellularization was analyzed by macroscopic observation, histological staining (hematoxylin and eosin [H&E], Sirius red, and alcian blue), immunohistochemical staining (collagen IV, laminin, and fibronectin), and biochemical assessment (DNA, collagen, and glycosaminoglycans) of decellularized liver matrices. The integrity of the extracellular matrix (ECM) postdecellularization was visualized by corrosion casting and three-dimensional computed tomography scanning. We found that livers perfused under oscillating pressure conditions (P^+) showed a more homogenous course of decellularization and contained less DNA compared with livers perfused without oscillating pressure conditions (P^-). Microscopically, livers from the (P^-) group showed remnant cell clusters, while no cells were found in livers from the (P^+) group. The grade of disruption of the ECM was higher in livers from the (P^-) group, although the perfusion rates and pressure did not significantly differ. Immunohistochemical staining revealed that important matrix components were still present after decellularization. Corrosion casting showed an intact vascular (portal vein and hepatic artery) and biliary framework. In summary, the presented protocol for pig liver decellularization is quick (7 h) and effective. The application of oscillating pressure conditions improves the homogeneity of perfusion and thus the outcome of the decellularization process.

Introduction

Decellularization and recellularization of solid organs is a recent and evolving tissue engineering concept used to generate functional organoids *in vitro*.[1] It is based on removing cellular and other immunogenic materials (e.g., DNA and alpha-Gal epitopes) from tissues to obtain the extracellular matrix (ECM).[2] The ECM is mainly composed of proteins (e.g., collagens, elastin, and fibronectin), polysaccharides (e.g., hyaluronic acids), and proteoglycans (e.g., glycosaminoglycans [GAGs] and heparan sulfate). It preserves the microanatomical organ framework, including the vascular structure and, in case of the liver, the biliary tract.[3] Because ECM components are highly conserved across species, the ECM is less or even nonimmunogenic to possible host organisms, even if the ECM is of xenogeneic origin.[4] Further, the ECM can determine cell fates based on its specific deposition of growth factors and

[1]Department of General, Visceral, and Transplantation Surgery, Charité–Universitätsmedizin Berlin, Berlin, Germany.
[2]Institute of Radiology, Charité–Universitätsmedizin Berlin, Berlin, Germany.
[3]Institute of Pathology, Charité–Universitätsmedizin Berlin, Berlin, Germany.
[4]Department of Anesthesiology and Operative Intensive Care Medicine, Charité–Universitätsmedizin Berlin, Berlin, Germany.
*Both authors contributed equally to this work.

serves as an ideal biomatrix for cellular repopulation.[5] Thus, in the future, this technique may facilitate the generation of functional, autologous liver organoids *in vitro* by the recellularization of a porcine liver ECM with (induced stem) cells from a patient who is on a waiting list for liver transplantation.[6]

However, despite inspiring reports on the experimental implantation of recellularized liver grafts,[3,7,8] much technical refinement is necessary before these approaches can be translated into the clinical setting. Two significant steps include (1) the upscaling and (2) the improvement of existing decellularization methodology. In contrast to several reports on mouse, rat, and ferret liver decellularization,[9–15] to date, only a limited number of protocols for pig liver decellularization have been published.[8,16–19] The recently favored method for whole organ or liver lobe decellularization is portal venous or arterial perfusion with alkaline detergents (i.e., sodium dodecyl sulfate [SDS] and Triton-X 100) in varying combinations with hypotonic or enzymatic solutions with perfusion times lasting from 16 h up to several days. In addition, all published methods for decellularization cause alterations and damage to ECM components, yet the "optimal decellularization protocol" should be fast and effective at removing cells and immunogenic material but avoid any damage of the ECM.[1]

Here, we report on a novel protocol for fast and homogenous whole pig liver decellularization by simultaneous, pressure-controlled perfusion of detergents (i.e., 1% Triton X-100 and 1% SDS) via the portal vein and the hepatic artery. Livers were perfused under oscillating pressure conditions to improve the homogeneity and increase the effectiveness of the decellularization process. The oscillating pressure was generated by a vane-type pump, which improves microperfusion within livers by mimicking intra-abdominal conditions during respiration. *In situ*, the liver is located under the copula of the diaphragm and follows the movement of the diaphragm during respiration. Thus, due to the lowering of the diaphragm and the increase in the intra-abdominal pressure during inspiration, the liver is squeezed to optimize outflow of blood into the liver veins. During expiration, the diaphragm elevates the liver, the intra-abdominal pressure decreases, and the inflow of portal venous blood into the liver is subsequently increased.[20]

Two experimental groups were investigated, and livers were decellularized with (P^+) or without (P^-) the application of sinusoidal pressure changes to verify whether the application of oscillating pressure conditions improves the effectiveness of pig liver decellularization.

Materials and Methods

Sample harvest

Pig livers weighing 600–1500 g were obtained from male and female domestic pigs ($n = 19$) weighing 20–60 kg. All animals were kept at the Facility for Experimental Medicine (FEM, Charité–Universitätsmedizin Berlin). The experiments were performed in accordance with federal law regarding the protection of animals and were approved by the federal authorities for animal research (G 0116/14, G 0249/13; Landesamt für Gesundheit und Soziales–LAGeSo, Berlin, Germany). Livers were harvested after the animals were euthanized. After cardiac arrest (~2–3 min), the abdominal cavity was opened using a median laparotomy. First, the hepatoduodenal ligament was prepared to selectively incise the portal vein. Next, a catheter (100% silicone, 6.7 mm; Rüsch, Teleflex Medical GmbH, Kernen, Germany) was inserted into the portal vein to flush livers with 2 L of heparinized (5000 I.E., heparin/liter) balanced electrolyte solution (Jonosteril; Fresenius SE & Co. KGaA, Bad Homburg, Germany). After initialization of liver rinsing, the infrahepatic inferior vena cava was incised and finally dissected to permit perfusate and blood outflow. Livers were rinsed *in situ* until the parenchyma appeared to be homogenously clear of blood residues. Then, the hepatoduodenal ligamentum was further prepared to selectively dissect the hepatic artery and the common bile duct as distant to the liver as possible. The suprahepatic inferior vena cava was dissected, and livers were freed from residual ligaments and finally removed. For logistical reasons, three livers from each experimental group were primarily stored at −80°C for at least 24 h, while three livers from each group were used directly for decellularization experiments. Cold-stored livers were thawed slowly over 24 h. Before perfusion in the decellularization device the portal vein and the suprahepatic and infrahepatic vena cava inferior were cannulated with catheters (100% silicone, 6.7 mm; Rüsch, Teleflex Medical GmbH). The hepatic artery was cannulated using a metal tube connector (3.0 mm; Carl Roth GmbH & Co. KG, Karlsruhe, Germany).

Perfusion/decellularization device

Whole pig livers were decellularized in a proprietary device for extracorporeal human-scale liver perfusion (Fig. 1). This device is a customized and remodeled cardiovascular bypass system (SIII; Sorin Group, Milan, Italy) and consists of four peristaltic double pumps (Ref. 10-65-00;

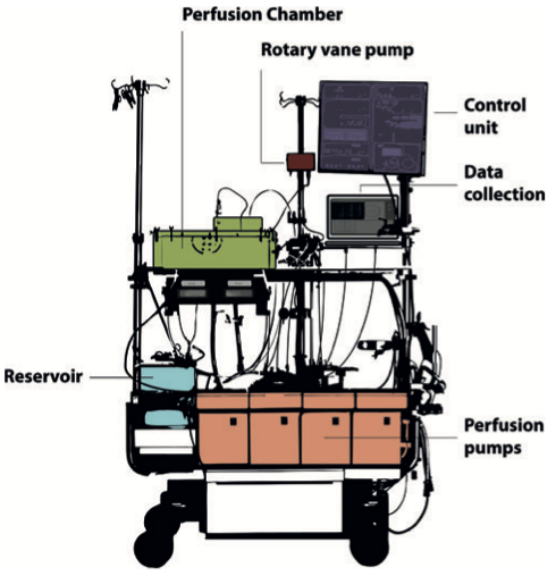

FIG. 1. Illustration of the device for human-scale extracorporeal liver perfusion. The device is a customized and remodeled cardiovascular bypass system. Color images available online at www.liebertpub.com/tec

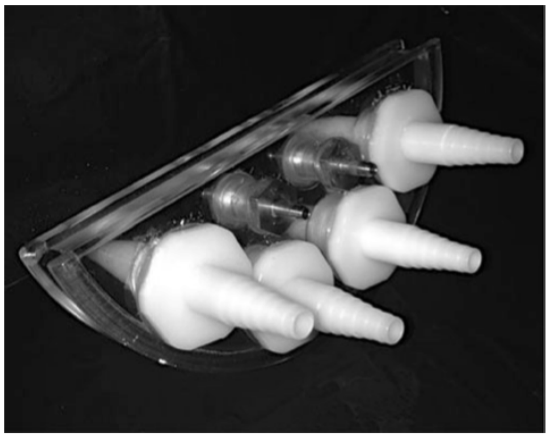

FIG. 2. Photograph of the passage tile through which the catheters are diverted.

Sorin Group), a peristaltic roller pump (Ref. 10-60-00; Sorin Group), a sealed perfusion chamber (proprietary construction), a vane-type pump (customized from Helmut Brey GmbH, Memmingen, Germany), and a control unit (customized S3 control panel; Sorin Group). Livers were placed in the sealed chamber, and perfusion catheters were diverted through a special passage tile (Fig. 2). For livers that were perfused under oscillating pressure conditions (P^+), the perfusion chamber was filled with tap water at room temperature. Further, in these cases, the chamber was connected to a vane-type pump to apply oscillating pressure via a plastic tube. The perfusion tubing was connected as illustrated in Figure 3, and the perfusion was initiated according to our protocol (Table 1). The perfusion pressures within the portal vein (60 mmHg) and the hepatic artery (120 mmHg) were continuously measured, and the control unit automatically adapted the continuously monitored flow rates to maintain these perfusion pressures at a constant level.

Decellularization protocols and experimental groups

Pig livers, regardless of their size and weight, were decellularized according to the following protocol.

Livers of experimental group P^- ($n=6$) were perfused without the application of oscillating pressure conditions. Livers of experimental group P^+ ($n=6$) were perfused with the application of oscillating pressure conditions generated by the rotary vane pump ($f=12$/min; $P_{max}=20$ mmHg, $P_{min}=0$ mmHg). After 90 and 270 min of detergent perfusion, livers of both groups were rotated manually upside-down

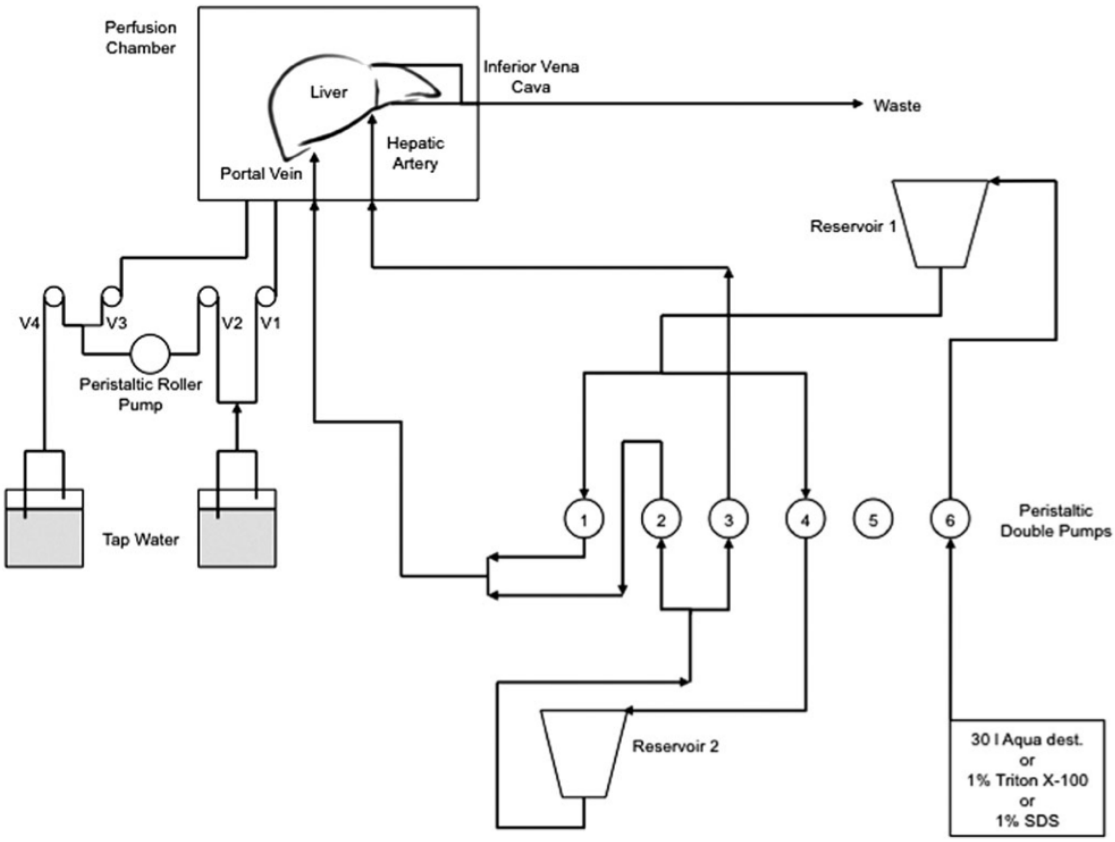

FIG. 3. Illustration of the perfusion draft used for decellularization experiments.

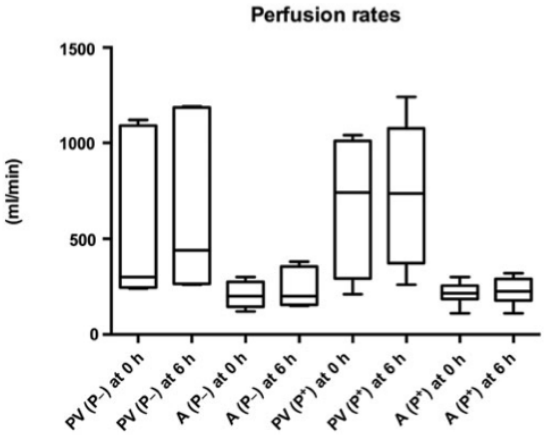

FIG. 4. Perfusion rates of the different routes at different time points (PV, portal vein; A, hepatic artery; P^-, perfusion without oscillating pressure conditions; P^+, perfusion with oscillating pressure conditions).

within the perfusion device to improve perfusion in the depending parts of the livers (Table 1).

Untreated native pig livers ($n=5$) that were stored at −80°C were thawed slowly over 24 h and used as controls.

Histological analyses

Randomly obtained samples of decellularized liver matrices (DLMs) and native liver tissue were fixed with 4% formalin, embedded in paraffin, and sliced. Hematoxylin and eosin (H&E) staining was performed (Institute for Pathology, Charité–Universitätsmedizin Berlin), according to standard procedures. To visualize the collagen fibers and estimate the disruption of DLMs, Sirius red staining (Sigma-Aldrich, Inc., St. Louis, MO) was performed according to standard procedures (collagen was stained red, and the remaining cytoplasms were stained yellow). Immunohistochemical staining of collagen IV, laminin, and fibronectin was performed using the following antibodies: anti-collagen IV antibody (Cat.: ab6586), anti-laminin antibody (Cat.: ab11575), and anti-fibronectin antibody (Cat.: ab23751) (all from Abcam, Cambridge, United Kingdom). Goat anti-rabbit IgG H&L (horseradish peroxidase) (Cat.: ab6721; Abcam) was used as a secondary antibody. Alcian blue/PAS staining was performed to visualize GAGs, and Van-Gieson staining was performed according to the manufacturer's instructions (Morphisto GmbH, Frankfurt am Main, Germany).

Images were acquired using a BZ-9000 microscope (Keyence Deutschland GmbH, Neu-Isenburg, Germany).

Biochemical evaluation of DLMs

Two tissue samples ($\sim 1\,cm^3$) from each DLM ($n=12$; total $n=24$) and four samples from each native liver ($n=5$; total $n=20$) were randomly selected, lyophilized (Lyovac GT2; Finn-Aqua Santasalo-Sohlberg GmbH, Hürth, Germany), weighed, and stored at −20°C until further analysis. DNA was isolated using the QiAmp DNA FFPE tissue kit (Qiagen, Hilden, Germany) according to the manufacturer's instructions. The DNA content was measured using a Nanodrop spectrophotometer (ND-1000; Peq-Lab Biotechnologie, Erlangen, Germany). To quantify the sulfated GAG content, one homogenized tissue sample from each decellularized ($n=12$) and native liver ($n=5$) was weighed, digested with papain, and measured as described by Farndale *et al.*[21] Collagen was measured using the Total Collagen Assay (Quickzyme Biosciences, Leiden, The Netherlands).

Three-dimensional computed tomography scan and corrosion casting

To determine whether the ECM of the (micro-)vasculature and bile duct system were still patent after decellularization, corrosion casts of the DLMs were made using the Biodur E20 kit (Biodur Products GmbH, Heidelberg, Germany).

A maximum-intensity three-dimensional computed tomography (CT) projection (64×0.625 mm slices) of DLMs

TABLE 1. PERFUSION PROTOCOLS

Group	P^-	P^+
Oscillating pressure $f=12$/min P_{max}: 20 mmHg P_{min}: 0 mmHg	No	Yes
Both groups	Perfusion pressure on the portal vein: 60 mmHg Perfusion pressure on the hepatic artery: 120 mmHg Perfusion with distilled water for 30 min Perfusion with 1% Triton X-100 (Carl Roth GmbH & Co. KG, Karlsruhe, Germany) for 90 min Manual rotation (180°) of the liver inside the perfusion chamber Perfusion with Triton X-100 for 90 min Perfusion with 1% SDS (Carl Roth GmbH & Co. KG) for 90 min Manual rotation (180°) of the liver inside the perfusion chamber Perfusion with 1% SDS for 90 min Perfusion with distilled water for 30 min	

SDS, sodium dodecyl sulfate.

TABLE 2. PERFUSION RATES DURING DECELLULARIZATION

Parameter	*PV (P^-)*	*PV (P^+)*	p	*A (P^-)*	*A (P^+)*	p
Min. perfusion rate (mL/min)	230	210	n.s.	90	90	n.s.
Max. perfusion rate (mL/min)	1210	1240	n.s.	380	330	n.s.
Perfusion rate at the beginning of perfusion (mL/min)	594 ± 203	733 ± 146	n.s.	208 ± 31	215 ± 25	n.s.
Perfusion rate after 6 h of detergent perfusion (mL/min)	668 ± 214	733 ± 157	n.s.	244 ± 47	227 ± 30	n.s.

PV (P^-), portal venous perfusion rate in the (P^-) group; PV (P^+), portal venous perfusion rate in the (P^+) group; A (P^-), arterial perfusion rate in the (P^-) group; A (P^+), arterial perfusion rate in the (P^+) group; *p*, statistical difference; n.s., not significant.

was constructed. The cannulated portal vein was contrasted with a 1:2 mixture of butyl cyanoacrylate (histoacryl) and Lipiodol (Guerbet GmbH, Sulzbach/Taunus, Germany).

Statistical analyses

Analysis and graphing of the statistical data were performed using Prism for Mac OS X (Version 6.0b; GraphPad Software, Inc., La Jolla, CA). Numerical data are expressed as the mean ± standard deviation of the mean within the text and graphically displayed as box and whisker plots. Due to the small group size ($n = 6$/experimental group), normal distribution of the data could not be assumed. Thus, group comparison was performed using the nonparametric Kruskal–Wallis test followed by Dunn's multiple-comparison analysis. Differences were considered significant at p-values < 0.05.

Results

Operational parameters: perfusion rates

All perfusions were performed using a clinical-scale perfusion device. Depending on the liver size (and weight), perfusion rates via the portal vein ranged from 210 to 1240 mL/min and from 90 to 380 mL/min via the hepatic artery. However, the flow rates did not significantly differ in the two experimental groups neither at the beginning of perfusion (at 0 h) nor at the end of the decellularization process (after 6 h of perfusion with detergents) (Table 2 and Fig. 4). During decellularization, the flow rates slightly increased, although the differences were not significant in any of the groups Table 2.

Macroscopic observation

At the beginning of the perfusion, the remaining blood clots were washed out, producing a brownish, thick perfusate.

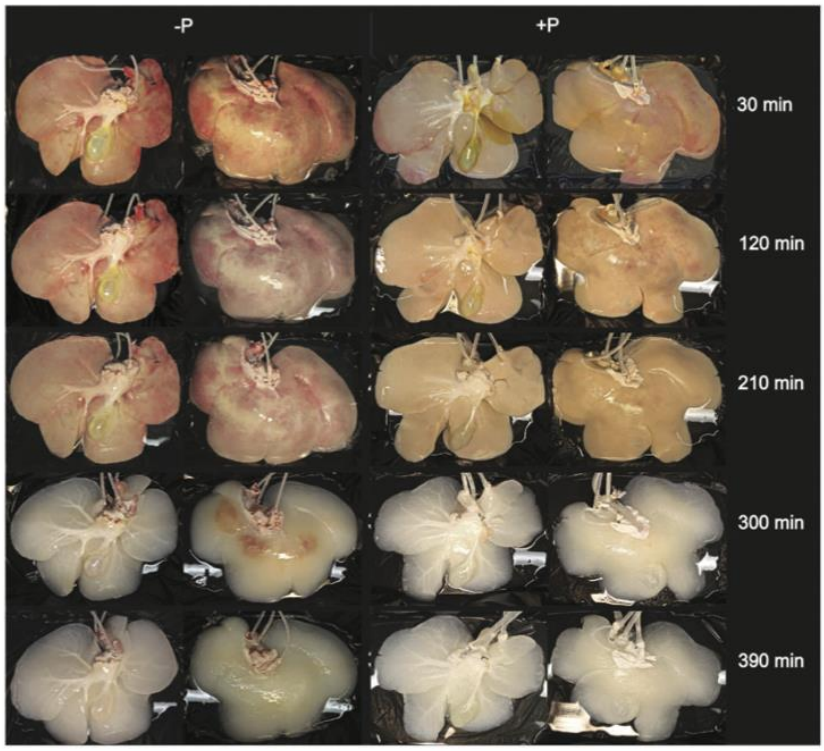

FIG. 5. Photograph of two exemplarily chosen pig livers during the course of decellularization (P^-, perfusion without oscillating pressure conditions; P^+, perfusion with oscillating pressure conditions).

After 30 min of perfusion with *Aqua dest.*, the perfusate was clear and thin. After initialization of perfusion with Triton X-100, the perfusate became thicker again, and the perfused livers began to elucidate (Fig. 5). After manual rotation of the livers (after 90 and 270 min), more cell debris was visible within the perfusate. At the end of the perfusion with Triton X-100, the livers appeared to have less color but were still not colorless. The livers perfused with oscillating pressure changes (P^+) appeared to have less color, and the elucidation was more homogenous compared with livers perfused without oscillating pressure changes (P^-) (Fig. 5). After the initialization of SDS perfusion, a very soapy perfusate enriched with a large amount of cell debris was visible, and the livers continued to elucidate. Again, elucidation of livers of the (P^+) experimental group appeared more homogenous compared with that of livers from the (P^-) group (Fig. 5). At the end of 6 h of detergent perfusion (3 h Triton X-100 and 3 h SDS), the perfusate was soapy but clear, and DLMs of both experimental groups were clear and white without macroscopically visible cell clusters.

Histological analyses

H&E staining of DLMs revealed an intact ECM for the livers of both experimental groups, although the ECMs of livers from the (P^-) group appeared to be more disrupted (Fig. 6). In some slices of DLMs of the (P^-) group, rests of cells and cell skeletons were found, although most of the cell nuclei were not visible. No remaining cells or nuclei were found in any of the slices from livers of the (P^+) group. These observations were confirmed with Van-Gieson stains (Fig. 7). Sirius red staining revealed that collagen was mostly preserved after the decellularization process (Fig. 8). No relevant differences were found with respect to the visual aspects of collagen distribution within DLMs of the two experimental groups, although DLMs of the (P^-) group showed more remnant parenchymal cell rests. These findings were confirmed by immunohistochemical staining for collagen IV (Fig. 9). Laminin and fibronectin were visualized by immunohistochemical staining and were observed in DLMs of both experimental groups (Figs. 10 and 11). The distribution pattern of laminin and fibronectin appeared to be more comparable to that observed in native livers in DLMs of the (P^+) group. Further, the extracellular network appeared to be less disrupted in the (P^+) group, and it lacked cell residues. Alcian blue staining showed a normal distribution of GAGs in DLMs of both groups; however, again, residual cell rests were only observed in the (P^-) group (Fig. 12).

Biochemical evaluation of DLMs

The measured DNA content of native livers was 4774 ± 3354 ng/mg (Fig. 13). The DNA content of DLMs of the (P^-) experimental group was significantly lower (659 ± 744.7 ng/mg; $p = 0.0003$). Livers perfused with oscillating pressure conditions showed the lowest amount of remnant DNA (400.9 ± 587.8 ng/mg; native vs. [P^+]: $p < 0.0001$), although the difference between the experimental groups was not statistically significant ([P^-] vs. [P^+]: n.s.).

Decellularization increased the fraction of collagen per mg of liver matrix in both experimental groups (Fig. 14). While this difference was not statistically significant for livers of the (P^-) group (native: 2.92 ± 0.40 µg/mg vs. [P^-]: 35.44 ± 25.35 µg/mg; p: n.s.), a statistically significant difference was observed for livers of the (P^+) group (native vs. [P^+]: 52.19 ± 11.18 µg/mg; $p = 0.0193$). Differences between the experimental groups were not statistically significant.

The content of GAGs per milligram was not significantly different between the two experimental groups and was not significantly different compared with native liver tissue (native: 7.39 ± 2.33 µg/mg; [P^-]: 5.62 ± 0.65 µg/mg; [P^+]: 5.49 ± 0.39 µg/mg), although there was a trend toward lower GAG content (per milligram of liver matrix) in the experimental groups compared with native livers (Fig. 15).

Three-dimensional CT scan and corrosion casting

The CT scan of a DLM from the (P^+) group revealed homogenous distribution of contrast agent within the major and minor branches of the portal vein (Fig. 16). Corrosion casting of another DLM from the (P^+) group showed intact frameworks of the portal vein (blue), the hepatic artery (red), and the biliary tract (yellow) after decellularization (Fig. 17).

Discussion

Our perfusion device mimics physiological, intra-abdominal conditions by generating slow-oscillating pressures paralleling resting respiratory rates in humans. The effects of this device have previously been evaluated in extracorporeally perfused pig livers in *in vitro* and preclinical transplant models.[20,22] Neuhaus, who developed this perfusion model, showed that oscillating pressure changes interfered reciprocally with portal venous and arterial perfusion flow (an effect that was confirmed in our experiments; data not shown) and significantly improved the homogeneity of liver perfusion. He observed less cell damage and improved functionality in livers perfused for 24 h under oscillating pressure conditions compared with livers perfused without oscillating pressure. Further, he showed that the application of this device as an extracorporeal liver support improved the survival of hepatectomized pigs.[20] Schon *et al.* confirmed these results by using a modified version of the Neuhaus perfusion chamber. In his experiments, livers perfused under oscillating pressure conditions showed less endothelial cell damage compared with cold-stored livers. Further, in an orthotopic transplant model, pigs showed improved survival if livers (warm ischemic time of 1 h) were perfused for 4 consecutive hours under oscillating pressure conditions prior to implantation as compared with 4 h of cold storage only.[22] Thus, Schon proposed that his normothermic extracorporeal liver perfusion model could serve as a conservation method for livers of nonheartbeating donors.

Based on these results, we evaluated the effect of oscillating pressure conditions on the homogeneity and effectiveness of pig liver perfusion decellularization. Of note, to our knowledge the homogeneity of decellularization processes has not been quantified previously. Importantly, in case of an inhomogenous perfusion, cells are removed effectively in the well-perfused areas but may remain in underperfused areas. To remove these cells, either the perfusion pressure or the perfusion duration must be increased. However, any possible deleterious effect of the decellularization agents will then be aggravated in well-perfused areas, possibly limiting the quality of the generated ECM. Of importance,

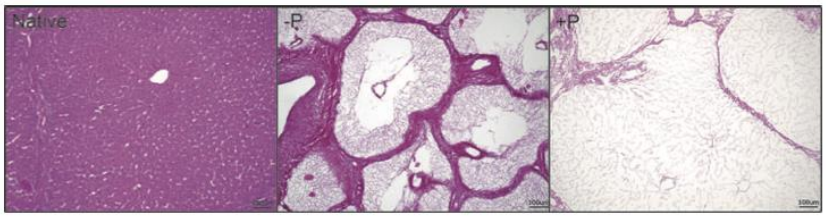

FIG. 6. Hematoxylin and eosin (H&E) stainings (Native, native pig liver; P^-, perfusion without oscillating pressure conditions; P^+, perfusion with oscillating pressure conditions).

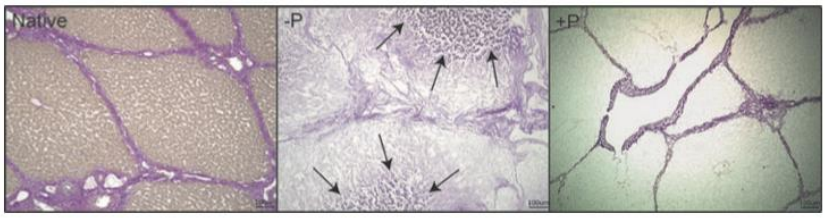

FIG. 7. Van-Gieson stainings (Native, native pig liver; P^-, perfusion without oscillating pressure conditions; P^+, perfusion with oscillating pressure conditions; *black arrows*, remaining cells, cell cluster, and/or nuclei within decellularized liver matrices).

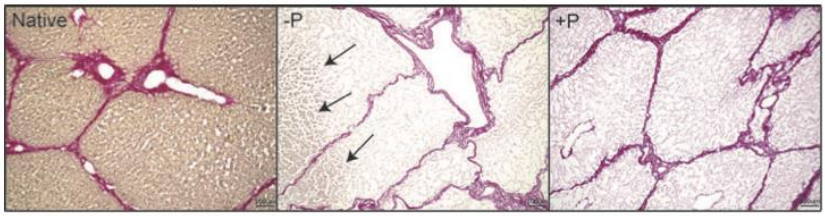

FIG. 8. Sirius red staining (Native, native pig liver; P^-, perfusion without oscillating pressure conditions; P^+, perfusion with oscillating pressure conditions; *black arrows*, remaining cells, cell cluster, and/or nuclei within decellularized liver matrices).

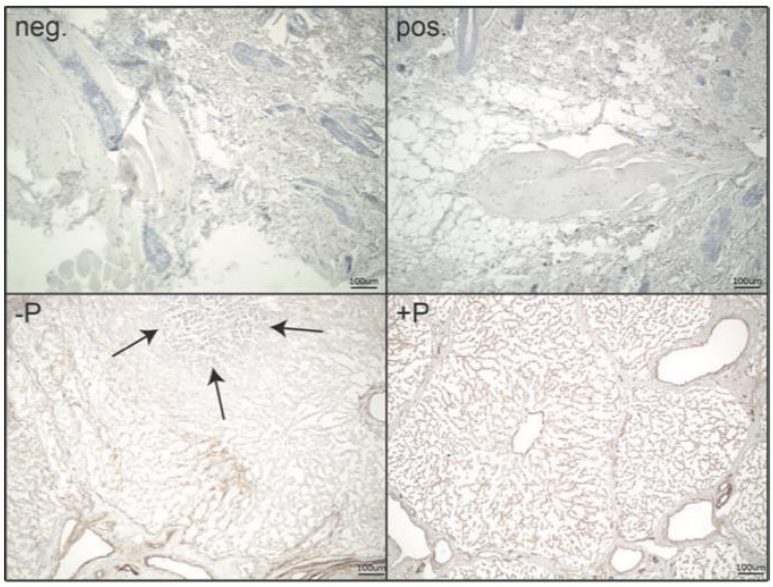

FIG. 9. Immunohistochemical staining of collagen IV (neg., Negative control [rat skin]; pos., positive control [rat skin]; P^-, perfusion without oscillating pressure conditions; P^+, perfusion with oscillating pressure conditions; *black arrows*, remaining cells, cell cluster, and/or nuclei within decellularized liver matrices).

ECM composition has an impact on cell function after repopulation[23] and should be altered as little as possible.[1]

In our experiments, the decellularization was faster and more homogenous in livers perfused under oscillating pressure conditions, an effect that we have previously shown for rodent (rat) liver decellularization.[24] Further, remnant cells were only found within slices of livers of the (P^-) group, although various randomly selected slices from various livers of both groups have been analyzed. This result is supported by the fact that livers of the (P^+) group show less

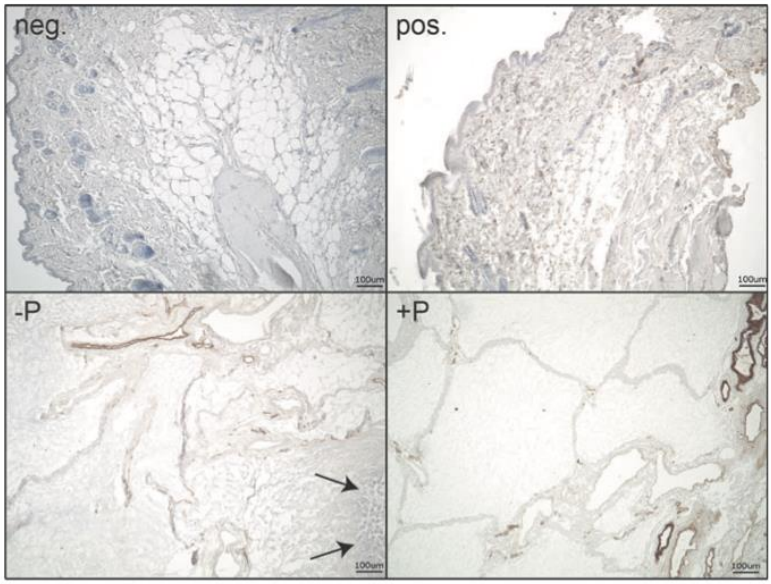

FIG. 10. Immunohistochemical staining of laminin (neg., Negative control [rat skin]; pos., positive control [rat skin]; P^-, perfusion without oscillating pressure conditions; P^+, perfusion with oscillating pressure conditions; *black arrows*, remaining cells, cell cluster, and/or nuclei within decellularized liver matrices).

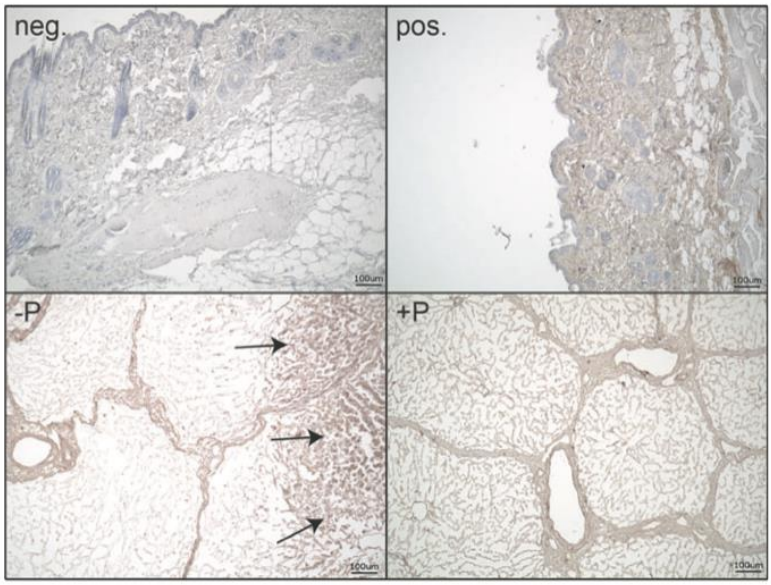

FIG. 11. Immunohistochemical staining of fibronectin (neg., Negative control [rat skin]; pos., positive control [rat skin]; P^-, perfusion without oscillating pressure conditions; P^+, perfusion with oscillating pressure conditions; *black arrows*, remaining cells, cell cluster, and/or nuclei within decellularized liver matrices).

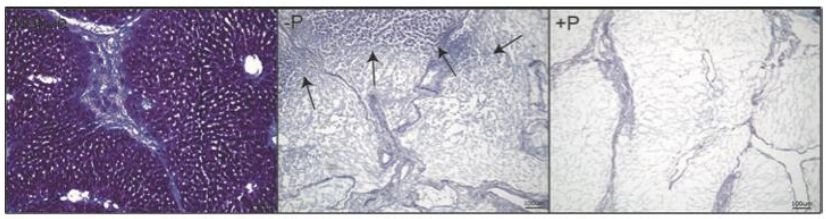

FIG. 12. Alcian blue staining (Native, native pig liver; P^-, perfusion without oscillating pressure conditions; P^+, perfusion with oscillating pressure conditions; *black arrows*, remaining cells, cell cluster, and/or nuclei within decellularized liver matrices).

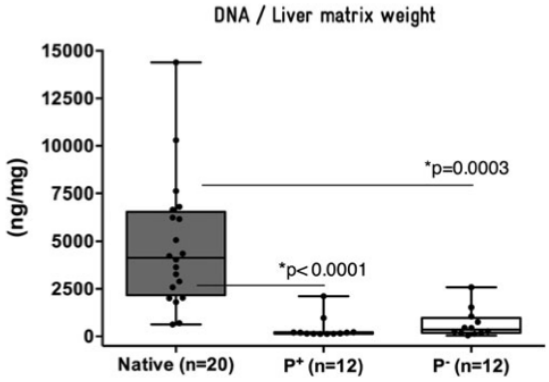

FIG. 13. Content of DNA per liver matrix weight.

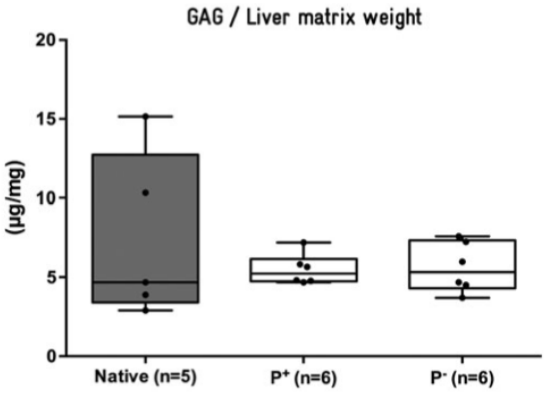

FIG. 15. Content of glycosaminoglycans per liver matrix weight.

remaining DNA content compared with livers from the (P^-) group, although the differences were not statistically significant. The standard deviation of the DNA content in livers of the (P^-) group was higher, again indicating inhomogenous decellularization. One possibly confusing result of the biochemical DLM analysis was a higher level of collagen in DLMs compared with native livers. Since the total amount of collagen will not be increased by decellularization, this finding is explicable due to a relevant loss of cell mass and cell protein and thus a higher fraction of collagen per weight of the DLM. This finding is supported by Baptista *et al.*, who made the same observation.[19]

Another question was that whether freezing and thawing could have had an impact on the course of pig liver decellularization since some livers of both groups were frozen before decellularization due to organizational reasons. Thus, data were analyzed with respect to this concern by dividing livers from the P^+ and P^- groups into two groups [frozen ($n=6$) vs. fresh ($n=6$)]. For none of the analyzed parameters (i.e., DNA, collagen, and GAGs) statistically significant differences were observed (data not shown). Thus, four groups were built (P^+, fresh; P^+, frozen; P^-, fresh; and P^-, frozen) and analyzed. Again no significant differences between none of the groups for none of the above mentioned parameters could be observed (data not shown). Although group numbers were small when divided into four groups (each $n=3$), the data reveal that one cycle of freezing to −80°C for 24 h has no significant impact on the course of pig liver decellularization.

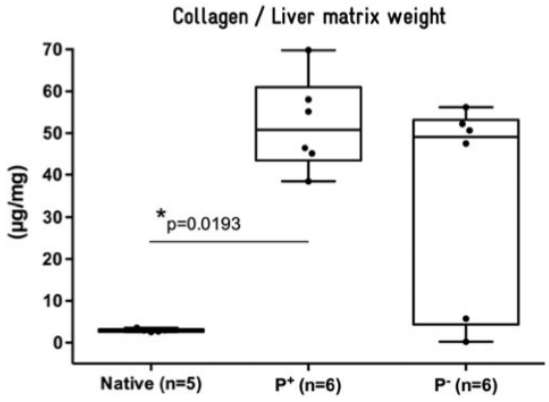

FIG. 14. Content of collagen per liver matrix weight. Spots represent measured values *n* data points.

Since perfusion decellularization of parenchymal organs was introduced by Ott *et al.*,[2] this technique has quickly evolved and has been applied to many parenchymal organs[3,25–27] and first reports on the clinical application of decellularized and recellularized tissue provided evidence for the immense potential of this concept.[26,28–30] However, before translation from bench to bedside is possible, various issues must be addressed.[31,32] One problem is the upscaling of available small-animal models to clinically relevant scales. Although current reports on liver decellularization and recellularization include the use of sheep[33] or ferret livers[34] for human-scale organoid generation, we suggest that pig livers are an adequate source for potential future large-scale scaffold generation. Pigs are readily available, and their livers are comparable to human livers with respect to size and weight.

Regarding perfusion duration, our protocol is the fastest protocol for human-scale liver decellularization (7 h of overall perfusion time) compared with other published protocols (ranging from 16 h to several days).[8,17,18,33–36] This difference in perfusion length might result from the fact that we perfused simultaneously via the portal vein and the hepatic artery and not only via the portal vein, as proposed in the majority of available publications.[8,17,18,33–36]

Another interesting aspect of our data is the fact that we only used livers of deceased animals that were not heparinized before sacrifice. Because our perfusion device enables high simultaneous perfusion pressures via the portal vein (60 mmHg) and the hepatic artery (120 mmHg), blood clots and cell debris could effectively be removed from livers, resulting in macroscopically well DLMs in the (P^+) group and even in the (P^-) group. Because perfusion was pressure controlled, the size and weight of the perfused livers resulted in different perfusion rates; however, our

FIG. 16. Reconstructed three-dimensional, high-resolution computed tomography scan.

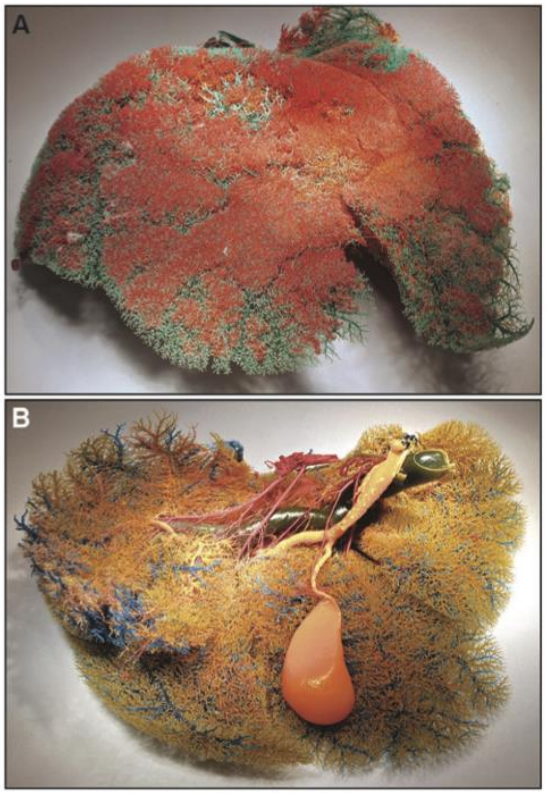

FIG. 17. Photograph of a corrosion cast of a decellularized pig liver matrix (P^+ group). **(A)** *Ventral view*; **(B)** *dorsal view*: frameworks of the portal vein (*blue*), the hepatic artery (*red*), and the biliary tract (*yellow*) after decellularization.

protocol was applicable to all livers without any modifications. Thus, the perfusion device and an adapted version of our protocol could be used for the generation of clinically applicable decellularized liver scaffolds even from the discarded livers of deceased donors.

Our study has important limitations. First, whether the application of oscillating pressure conditions during decellularization has an impact on the quality of generated ECMs must ultimately be addressed in future repopulation experiments. Second, the effect of oscillating pressure conditions on the survival and functionality of recellularized organoids, including the optimal frequency and force of pressure changes (e.g., $f = 12$/min; P_{max}: 20 mmHg as in our recent experiments), must be evaluated further.

Because our perfusion device has been used in sterile transplant models, it could be used for these experiments without modifications if the recellularization experiments are performed in a perfusion chamber within a sterile unit.

Conclusions

The presented protocol for pig liver decellularization is quick (7 h) and effective. The application of oscillating pressure conditions improves the homogeneity of perfusion and thus the outcome of the decellularization process. The presented DLMs could serve as scaffolds for organoid generation on a clinically relevant scale. Further, an adapted version of our perfusion settings may be applied for the decellularization of discarded human livers.

Acknowledgments

The authors gratefully thank Peter Tang, Steffen Lippert, Peter Baer, Ingo Steffen, and Katharina Struecker for their help.

Disclosure Statement

No competing financial interests exist.

References

1. Crapo, P.M., Gilbert, T.W., and Badylak, S.F. An overview of tissue and whole organ decellularization processes. Biomaterials **32,** 3233, 2011.
2. Ott, H.C., *et al.* Perfusion-decellularized matrix: using nature's platform to engineer a bioartificial heart. Nat Med **14,** 213, 2008.
3. Uygun, B.E., *et al.* Organ reengineering through development of a transplantable recellularized liver graft using decellularized liver matrix. Nat Med **16,** 814, 2010.
4. Badylak, S.F. Decellularized allogeneic and xenogeneic tissue as a bioscaffold for regenerative medicine: factors that influence the host response. Ann Biomed Eng **42,** 1517, 2014.
5. Wang, Y., *et al.* Lineage restriction of human hepatic stem cells to mature fates is made efficient by tissue-specific biomatrix scaffolds. Hepatology **53,** 293, 2011.
6. Struecker, B., Raschzok, N., and Sauer, I.M. Liver support strategies: cutting-edge technologies. Nat Rev Gastroenterol Hepatol **11,** 166, 2014.
7. Bao, J., *et al.* Construction of a portal implantable functional tissue-engineered liver using perfusion-decellularized matrix and hepatocytes in rats. Cell Transplant **20,** 753, 2011.

8. Barakat, O., *et al.* Use of decellularized porcine liver for engineering humanized liver organ. J Surg Res **173,** e11, 2012.
9. Zhou, P., *et al.* Decellularized liver matrix as a carrier for the transplantation of human fetal and primary hepatocytes in mice. Liver Transpl **17,** 418, 2011.
10. Ji, R., *et al.* The differentiation of MSCs into functional hepatocyte-like cells in a liver biomatrix scaffold and their transplantation into liver-fibrotic mice. Biomaterials **33,** 8995, 2012.
11. Shupe, T., Williams, M., Brown, A., Willenberg, B., and Petersen, B.E. Method for the decellularization of intact rat liver. Organogenesis **6,** 134, 2010.
12. Soto-Gutierrez, A., *et al.* A whole-organ regenerative medicine approach for liver replacement. Tissue Eng Part C Methods **17,** 677, 2011.
13. Park, K.M., and Woo, H.M. Systemic decellularization for multi-organ scaffolds in rats. Transplant Proc **44,** 1151, 2012.
14. Shirakigawa, N., Ijima, H., and Takei, T. Decellularized liver as a practical scaffold with a vascular network template for liver tissue engineering. J Biosci Bioeng **114,** 546, 2012.
15. Ren, H., *et al.* Evaluation of two decellularization methods in the development of a whole-organ decellularized rat liver scaffold. Liver Int **33,** 448, 2013.
16. Park, K.M., and Woo, H.M. Porcine bioengineered scaffolds as new frontiers in regenerative medicine. Transplant Proc **44,** 1146, 2012.
17. Mirmalek-Sani, S.H., Sullivan, D.C., Zimmerman, C., Shupe, T.D., and Petersen, B.E. Immunogenicity of decellularized porcine liver for bioengineered hepatic tissue. Am J Pathol **183,** 558, 2013.
18. Yagi, H., *et al.* Human-scale whole-organ bioengineering for liver transplantation: a regenerative medicine approach. Cell Transplant **22,** 231, 2013.
19. Baptista, P.M., *et al.* The use of whole organ decellularization for the generation of a vascularized liver organoid. Hepatology **53,** 604, 2011.
20. Neuhaus, P. Extrakorporale Leberperfusion—Entwicklung und Erprobung eines neuen Modells. 1982.
21. Farndale, R.W., Buttle, D.J., and Barrett, A.J. Improved quantitation and discrimination of sulphated glycosaminoglycans by use of dimethylmethylene blue. Biochim Biophys Acta **883,** 173, 1986.
22. Schon, M.R., *et al.* Liver transplantation after organ preservation with normothermic extracorporeal perfusion. Ann Surg **233,** 114, 2001.
23. Jarvelainen, H., Sainio, A., Koulu, M., Wight, T.N., and Penttinen, R. Extracellular matrix molecules: potential targets in pharmacotherapy. Pharmacol Rev **61,** 198, 2009.
24. Struecker, B., *et al.* Improved rat liver decellularization by arterial perfusion under undulating pressure conditions. J Tissue Eng Regen Med 2014. [Epub ahead of print]; DOI: 10.1002/term.1948.
25. Song, J.J., *et al.* Regeneration and experimental orthotopic transplantation of a bioengineered kidney. Nat Med **19,** 646, 2013.
26. Gonfiotti, A., *et al.* The first tissue-engineered airway transplantation: 5-year follow-up results. Lancet **383,** 238, 2014.
27. Mirmalek-Sani, S.H., *et al.* Porcine pancreas extracellular matrix as a platform for endocrine pancreas bioengineering. Biomaterials **34,** 5488, 2013.
28. Jungebluth, P., *et al.* Tracheobronchial transplantation with a stem-cell-seeded bioartificial nanocomposite: a proof-of-concept study. Lancet **378,** 1997, 2011.
29. Macchiarini, P., *et al.* Clinical transplantation of a tissue-engineered airway. Lancet **372,** 2023, 2008.
30. Olausson, M., *et al.* Transplantation of an allogeneic vein bioengineered with autologous stem cells: a proof-of-concept study. Lancet **380,** 230, 2012.
31. Vogel, G. Trachea transplants test the limits. Science **340,** 266, 2013.
32. Ott, H.C., and Mathisen, D.J. Bioartificial tissues and organs: are we ready to translate? Lancet **378,** 1977, 2011.
33. Kajbafzadeh, A.-M., Javan-Farazmand, N., Monajemzadeh, M., and Baghayee, A. Determining the optimal decellularization and sterilization protocol for preparing a tissue scaffold of a human-sized liver tissue. Tissue Eng Part C Methods **19,** 642, 2013.
34. Baptista, P.M., Vyas, D., Moran, E., Wang, Z., and Soker, S. Human liver bioengineering using a whole liver decellularized bioscaffold. Methods Mol Biol **1001,** 289, 2013.
35. Park, K.M., Park, S.M., Yang, S.R., Hong, S.H., and Woo, H.M. Preparation of immunogen-reduced and biocompatible extracellular matrices from porcine liver. J Biosci Bioeng **115,** 207, 2013.
36. Uzarski, J.S., Van de Walle, A.B., and McFetridge, P.S. *In vitro* method for real-time, direct observation of cell-vascular graft interactions under simulated blood flow. Tissue Eng Part C Methods **20,** 116, 2014.

Address correspondence to:
Benjamin Struecker, MD
Department of General, Visceral, and Transplantation Surgery
Charité–Universitätsmedizin Berlin
Augustenburger Platz 1
Berlin 13353
Germany

E-mail: benjamin.struecker@charite.de

Received: June 2, 2014
Accepted: August 11, 2014
Online Publication Date: October 14, 2014

10.3 Improved rat liver decellularization by arterial perfusion under oscillating pressure conditions

JOURNAL OF TISSUE ENGINEERING AND REGENERATIVE MEDICINE
J Tissue Eng Regen Med 2017; **11**: 531–541.
Published online 4 September 2014 in Wiley Online Library (wileyonlinelibrary.com) **DOI:** 10.1002/term.1948

RESEARCH ARTICLE

Improved rat liver decellularization by arterial perfusion under oscillating pressure conditions

Benjamin Struecker, Antje Butter, Karl Hillebrandt, Dietrich Polenz, Anja Reutzel-Selke, Peter Tang, Steffen Lippert, Anne Leder, Susanne Rohn, Dominik Geisel, Timm Denecke, Khalid Aliyev, Korinna Jöhrens, Nathanael Raschzok, Peter Neuhaus, Johann Pratschke and Igor M. Sauer*
General, Visceral, and Transplantation Surgery, Charité – Campus Virchow, Berlin, Germany

Abstract

One approach of regenerative medicine to generate functional hepatic tissue *in vitro* is decellularization and recellularization, and several protocols for the decellularization of livers of different species have been published. This appears to be the first report on rat liver decellularization by perfusion under oscillating pressure conditions, intending to optimize microperfusion and minimize damage to the ECM. Four decellularization protocols were compared: perfusion via the portal vein (PV) or the hepatic artery (HA), with (+P) or without (–P) oscillating pressure conditions. All rat livers ($n = 24$) were perfused with 1% Triton X-100 and 1% sodium dodecyl sulphate, each for 90 min with a perfusion rate of 5 ml/min. Perfusion decellularization was observed macroscopically and the decellularized liver matrices were analysed by histology and biochemical analyses (e.g. levels of DNA, glycosaminoglycans and hepatocyte growth factor). Livers decellularized via the hepatic artery and under oscillating pressure showed a more homogeneous decellularization and less remaining DNA, compared with the livers of the other experimental groups. The novel decellularization method described is effective, quick (3 h) and gentle to the extracellular matrix and thus represents an improvement of existing methodology.

Received 7 November 2013; Revised 27 May 2014; Accepted 16 June 2014

Keywords **rat liver decellularization; rat liver perfusion device; oscillating pressure conditions; rat liver recellularization; liver engineering; future liver support**

1. Introduction

Orthotopic liver transplantation (OLT) remains the only definitive treatment option for end-stage liver failure but has become a victim of its own success (Lechler *et al.*, 2005). With improving results over the last few decades, the indications for liver transplant have been widely expanded, and the disparity between organ supply and demand has continued to grow (Adam and Hoti, 2009). The urgent demand for new sources of transplantable organs is demonstrated by the fact that post-OLT outcomes began to deteriorate in the 'high MELD (model of end-stage liver disease) era' because only severely ill patients will receive a donor organ (Bahra and Neuhaus, 2011). Thus, more than ever, different strategies to overcome organ scarcity and to prevent the death of patients on transplant waiting lists are needed (Struecker *et al.*, 2013).

One promising approach of regenerative medicine to generate transplantable tissue and organs *in vitro* is decellularization and recellularization (Badylak *et al.*, 2011). This concept is based on the idea of generating biological scaffolds by removing cellular and antigen-presenting components from tissues or organs and obtaining the organs' extracellular matrix (ECM). The ECM serves as an interactive scaffold for resident cells and preserves the complex architecture and three-dimensional structure of the organ. Furthermore, the ECM is in a state of dynamic reciprocity with cells and possibly can induce proliferation and differentiation processes. These properties suggest that the ECM can function as a biomatrix ideally suited for repopulation with cells (Bissell and Aggeler, 1987; Ross *et al.*, 2009; Stern *et al.*, 2009; Cortiella *et al.*, 2010; Crapo *et al.*, 2011; Wang *et al.*, 2011, 2013).

*Correspondence to: Igor Maximilian Sauer, General, Visceral, and Transplantation Surgery, Charité – Campus Virchow, Augustenburger Platz 1, D–13353 Berlin, Germany. E-mail: Igor.Sauer@charite.de

Decellularization of whole organs is usually achieved by the perfusion of alkaline detergents [e.g. Triton X-100, sodium dodecyl sulphate (SDS), cholamidopropyl)dimethylammonium)-1-propanesulfonate (CHAPS)] and, optionally, enzymatic solutions (e.g. trypsin, nucleases, etc.) via the organ's vascular system. Since 2010, various protocols for the decellularization of mouse (Zhou *et al.*, 2011; Ji *et al.*, 2012), rat (Shupe *et al.*, 2010; Uygun *et al.*, 2010; Bao *et al.*, 2011; Baptista *et al.*, 2011; De Kock *et al.*, 2011; Soto-Gutierrez *et al.*, 2011; Wang *et al.*, 2011; Park and Woo, 2012b; Shirakigawa *et al.*, 2012; Ren *et al.*, 2013), ferret (Baptista *et al.*, 2011), pig (Baptista *et al.*, 2011, Barakat *et al.*, 2012, Park and Woo, 2012a, Yagi *et al.*, 2012, Park *et al.*, 2013) and sheep livers (Kajbafzadeh *et al.*, 2013) have been published. With the except of one report (Mirmalek-Sani *et al.*, 2013), the commonality between these studies was that decellularization was achieved by the perfusion of alkaline detergents and/or enzymatic solutions via the portal vein. The duration of rat liver decellularization varied between 1 h (De Kock *et al.*, 2011) and 72 h (Uygun *et al.*, 2010), with perfusion rates ranging from 1 ml/min to 30 ml/min. There do not appear to have been reports on either decellularization techniques applying oscillating pressure conditions or rat liver decellularization via the hepatic artery.

This paper reports on a novel decellularization technique by perfusing with Triton X-100 and SDS via the hepatic artery under oscillating pressure conditions in a proprietary decellularization device. This device is designed to generate pressure changes on the perfused organ by mimicking intra-abdominal conditions. *In situ*, the liver is adherent to the diaphragm and 'hangs' in its copula; the liver is affected mechanically by movement of the diaphragm during respiration. Whereas exhaling leads to lower intra-abdominal pressure and increased portal-venous flow, inhaling (or increasing the intra-abdominal pressure) causes higher outflow via the hepatic veins into the vena cava. This mechanism leads to a physiological aspiration of portal venous blood during expiration and a 'squeezing' of venous blood during inspiration, which can be likened to a 'sponge' and results in optimal perfusion of the liver.

The notion that changes in intra-abdominal pressure and the movement of the diaphragm during respiration could affect liver perfusion has been mentioned previously (Fishman and Dickinson, 1988), and the benefit of oscillating pressure conditions on extracorporeally perfused pig livers was confirmed experimentally by Neuhaus and others (Neuhaus, 1982, Schon *et al.*, 2001). It was shown that oscillating pressure conditions improve the microperfusion within these organs and homogenize perfusions under physiological perfusion rates. Homogeneity of extracorporeal perfusion is important because cells in poorly perfused areas are ischaemic and are more likely to perish. During perfusion decellularization, cells in poorly perfused areas do not come in contact with detergents and remain within the organ. Thus, to dissolve these remaining cells, either the perfusion rate (or pressure) can be increased or the perfusion can be extended.

However, every known agent for cellular removal confers damage to the ECM and leads to an alteration of the ECM composition (Badylak *et al.*, 2011). Thus, if the decellularization process is not homogeneous, additional detergents to remove cells in poorly perfused areas could augment the harm to optimally perfused areas within the organ. One requirement to optimize existing decellularization techniques is to minimize these deleterious effects (Badylak *et al.*, 2011). Improving microperfusion and the homogeneity of decellularization by applying oscillating pressure conditions could enable gentler decellularization protocols and decrease the damage to the ECM.

Four different perfusion protocols [perfusion via the portal vein either without (PV – P) or with oscillating pressure (PV + P) and perfusion via the hepatic artery either without (A – P) or with oscillating pressure (A + P)] were compared. Aside from the route of perfusion and application of pressure, all of the livers ($n = 24$) were perfused in the custom-made device under identical conditions with a perfusion rate of 5 ml/min. Initially, 90 min with 1% Triton X-100 were followed by 90 min with 1% SDS (3 h total). Livers were observed macroscopically during the process, and decellularized liver matrices (DLMs) were examined by histological and immunohistochemical staining. Furthermore, biochemical analyses [e.g. DNA content, glycosaminoglycan (GAG) content, hepatocyte growth factor content (HGF)] of the decellularized liver matrices were performed and statistically evaluated. Corrosion casting was used to determine the integrity of the remaining ECM vasculature.

2. Materials and methods

Livers ($n = 24$) were harvested from male Lewis rats weighing 300–400 g (Janvier, St Berthevin Cedex, France). Animals were kept at the Facility for Experimental Medicine (FEM, Charité, Berlin, Germany) and all experimental protocols were reviewed and approved by the State Office of Health and Local Affairs (LAGeSo, Berlin, Germany; Reg. No. O 0365/11).

2.1. Surgical procedure

Rats were anaesthetized by inhalation of isoflurane (3.5% for induction/2% for maintenance) and administered an intraperitoneal injection of novaminsulfone (100mg/kg) and ketamine (10 mg/kg). After a longitudinal laparotomy with lateral expansions, the left lateral and caudal liver lobes were mobilized and the common bile duct was ligated and transected. The prepyloric vein was ligated and transected; the portal vein was prepared and mobilized. The superior pancreaticoduodenal, lienopancreatic and gastricolienal arteries were liberated, ligated and transected. The celiac trunk was prepared onto the aortic origin, and 500 units of heparin in 1 ml saline were infused through a puncture of the infrahepatic vena cava inferior (IHVCI). The portal vein was clamped at the level of the inferior mesenteric vein, incised, cannulated with an 18 G infusion catheter

(Venflon™; BD, Heidelberg, Germany) and perfused with 50 ml PBS. To secure the catheter in the portal vein, two stay sutures were placed firmly and connected to the neck of the catheter. The IHVCI was then incised to permit blood and perfusate outflow. After complete exsanguination of the liver, the IHVCI was ligated close to the liver. The coeliac trunk with a remaining aortic patch was lifted up, excised and perfused with 1 ml of heparinized saline using a 24 G BD Venflon infusion catheter. The hepatic artery was then cannulated through the aortic patch with a plastic tube prefilled with saline (Polythan Tubing, 0.58 mm i.d.; 0.96 mm o.d.; Smith Portex Ltd., Kent, UK) that was fixed and sealed on the aortic patch with a 6–0 Prolene® (Ethicon, Hamburg, Germany) stitch and Histoacryl® glue (Braun, Kronberg/Taunus, Germany) and, on the other end, sealed and connected with an 18 G infusion catheter (BD Venflon). Finally, the liver was removed and stored in a saline-filled beaker for transport to the decellularization reactor.

2.2. Proprietary decellularization device

Rat liver decellularization by perfusion was performed in a proprietary decellularization device (Figure 1). This device consists of four upright sealed tubes (i.e. the perfusion chamber), each with four Luer-Lock connectors on the cover plate and another Luer-Lock connector on the bottom plate. The cover plate connectors were used for selective perfusion of either the portal vein or hepatic artery, infusion of medium within the perfusion chamber and application of pressure. The connector on the bottom plate was used for perfusate and waste removal. At the centre of the four perfusion chambers, a fifth tube (pressure distributor) was placed for the distribution of applied pressure to the perfusion chambers. A respirator (Smartair ST Airox, ResMed Germany Inc., Martinsried, Germany) was used to generate oscillating pressure ranging from 0 to 35 mbar and connected to the pressure distributor with silicone tubes. The distributor was then connected to each perfusion chamber with silicone tubes and pressure was applied.

2.3. Decellularization protocols

Decellularization was achieved by perfusion via either the portal vein (PV) or the hepatic artery (A). Each group was decellularized either with (+P) or without (–P) oscillating pressure conditions, resulting in four experimental groups: (PV – P, PV + P, A – P, A + P; $n = 6$ for all groups) (Table 1). After explantation and initial perfusion via the portal vein, four harvested rat livers were placed into the proprietary decellularization device (Figure 1), and perfusion was initiated with PBS (5 ml/min) for 10 minutes to wash out residual blood. All of the livers were hung in PBS inside the perfusion chambers for decellularization. Depending on the experimental group, the oscillating pressure was enabled by connecting the tubes to a respirator (ResMed Smartair ST Airox; frequency: 15/s; maximum pressure

Table 1. Definition of the experimental groups

Group	PV – P ($n = 6$)	PV + P ($n = 6$)	A – P ($n = 6$)	A + P ($n = 6$)
Perfusion route	Portal Vein	Portal Vein	Hepatic Artery	Hepatic Artery
Oscillating pressure	No	Yes	No	Yes

All groups: perfusion rate 5 ml/min, 10 min phosphate-buffered saline (PBS), 90 min 1% Triton X-100, 90 min 1% sodium dodecyl sulphate (SDS), PBS overnight.

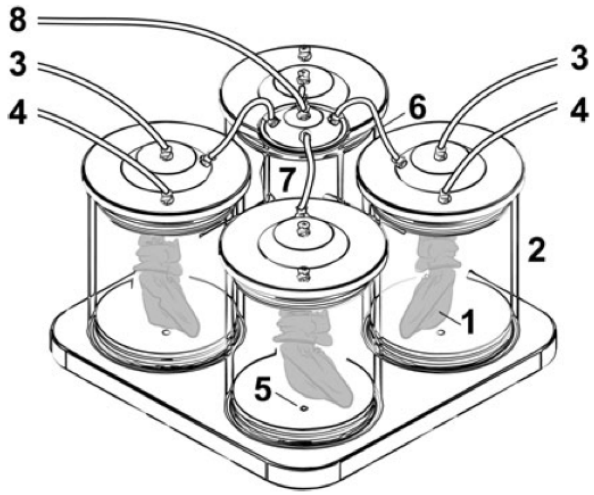

Figure 1. Proprietary perfusion device (Nami R1.0) enabling oscillating pressure conditions. (1) Perfused rat liver 'hanging' inside the sealed perfusion chamber (2) that is filled with sterile 0.9% NaCl solution. Tubes (3) for the selective perfusion of the portal vein and the hepatic artery (4). Luer-Lock connectors are available for waste removal (5). A tube (6) connects the pressure distributor (7) with the perfusion chambers (2). A further tube (8) connects the pressure distributor (7) to the respirator (not shown)

applied: 35 mbar; minimum pressure applied: 0 mbar). Perfusion using a peristaltic pump (IPC ISM 932, Ismatec, Switzerland) with 1% Triton X-100 (5 ml/min) was then initiated via either the portal vein or hepatic artery for 90 min, followed by a 90-min perfusion of 1% SDS (5 ml/min).

2.4. Histological analyses

One entire liver of each experimental group ($n = 4$) was fixed in formalin and completely embedded in paraffin wax. Thirty deeper sections of each liver were cut. Every fifth section of these 30 was stained with haematoxylin and eosin (Figure 2). These stained sections were blinded and then evaluated by an experienced pathologist at the Institute for Pathology (Charité – Universitätsmedizin Berlin). To quantify the efficiency of the decellularization process the pathologist identified clusters of remaining cells within the stains and optically estimated the area of the remaining cell clusters and the decellularized area. Thus, the percentage of decellularization was quantified by optical estimation of six blinded sections per DLM by an experienced pathologist. Furthermore, Gömöri stains were performed according to standard procedures to visualize the collagen fibres in order to estimate the disruption of decellularized liver matrices. Sirius red staining (Sigma-Aldrich Inc., St Louis, MO, USA), was performed according to standard procedures. Immunohistochemical staining of collagen IV, laminin and fibronectin was performed using the following antibodies: anti-collagen IV antibody (Cat no. ab6586), anti-laminin antibody (Cat no. ab11575) and anti-fibronectin antibody (Cat no. ab23751) (all from Abcam, Cambridge, UK). As a secondary antibody goat anti-rabbit IgG H&L (HRP) (Cat no. ab6721; Abcam) was used.

Images from stained sections were taken using a Keyence microscope (BZ-9000; Keyence Deutschland GmbH, Neu-Isenburg, Germany).

2.5. Biochemical analyses of DLMs and native liver

Six complete decellularized liver matrices of each experimental group ($n = 24$) as well as native livers ($n = 9$) were separately homogenized in PBS using a digital homogenizer (Ultra-Turax T25; IKA Werke GmbH & Co. KG, Staufen, Germany).

DNA was isolated using the QiAmp DNA FFPE tissue kit (Qiagen, Hilden, Germany), according to the manufacturer's instructions. The DNA content was measured using a nanodrop spectrophotometer (ND-1000; Peq-Lab Biotechnologie, Erlangen, Germany). Two samples of each decellularized liver ($n = 6$) were taken and measured. Then means of both values were taken for further statistical evaluation. To quantify the sulphated GAG content, homogenized tissue samples were digested with papain and measured as described by Farndale *et al.*, 1986 The HGF content was measured using an assay according to the

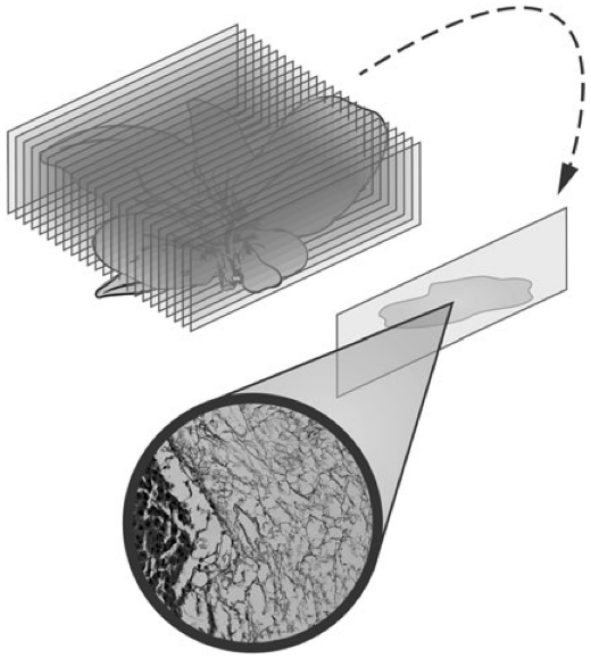

Figure 2. Illustration of the histological analysis. One entire liver of each experimental group ($n = 4$) was fixed in formalin and completely embedded in paraffin wax. Thirty deeper sections of each liver were cut. Every fifth section of these 30 was stained with haematoxylin and eosin. These stains were blinded and then evaluated by an experienced pathologist at the Institute for Pathology (Charité – Universitätsmedizin Berlin). To quantify the efficiency of the decellularization process the pathologist identified clusters of remaining cells within the stains and optically estimated the area of the remaining cell clusters and the decellularized area

manufacturer's protocol (Ref.-No. K2002-1; B-Bridge International, Inc., Cupertino, CA, USA). For measurements of HGF and GAG contents only one sample per DLM was analysed.

2.6. Statistical analyses

Analysis and graphing of the statistical data were performed using Prism 6.0b for Mac OS X (GraphPad Software, Inc., La Jolla, CA, USA).

Numeric data were expressed as mean ± standard deviation of mean (SD) within the text and graphically displayed as box and whisker plots. Owing to the small group size ($n = 6$/experimental group) normal distribution of the data could not be assumed. Thus, group comparison was performed using the non-parametric Kruskal–Wallis test followed by Dunn's multiple comparison analysis. Differences were considered significant at p less than 0.05.

2.7. Corrosion casting

To determine if the ECM of the (micro-)vasculature was still patent after decellularization, corrosion casts of the decellularized liver matrices were made using the BIODUR® E20 kit (BIODUR Products GmbH, Heidelberg, Germany).

3. Results

3.1. Macroscopic observations

During perfusion of rat livers with SDS and Triton X-100 a blanching of livers was observed (Figure 3A) and perfusion was continued until livers appeared translucent (Figure 4). Blanching of livers was interpreted as decellularization, as already reported.

Perfusion of the livers with detergents under oscillating pressure conditions (+P) resulted in a more homogenous decellularization compared with livers that were perfused without oscillating pressure conditions (–P) (Figure 3A). Perfusing the livers via the hepatic artery (A) appeared to further improve the decellularization homogeneity compared with livers perfused via the portal vein (PV). Thus, perfusion via the hepatic artery under oscillating pressure conditions (A + P) resulted in the most homogeneous and complete decellularization, while preserving the micro-anatomical structure of the livers (Figure 4). These results were reproducible and were observed regularly (data not shown).

3.2. Histological evaluation

Depending on the evaluated histological stain (see the Materials and Methods section), livers of experimental group, PV – P, were decellularized from 50% to 90%, resulting in an average decellularization rate of approximately 60%, as evaluated by visualization. In comparison livers of experimental group, A – P were completely decellularized without residual cells. Livers of the PV + P group were decellularized from 40% to 90% (average approximately 80%). Livers of the A + P group showed no cell residues in any of the stains evaluated (Figure 5; some data not shown). The reticular fibre network of decellularized liver matrices was intact, regardless of the experimental group. Furthermore, the remaining connective tissue harboured vascular structures. Collagen was visualized by Gömöri staining (Figure 5B). Sirius red staining revealed remaining parenchymal tissue (in yellow) in livers perfused via the portal vein, while in livers decellularized via the hepatic artery only collagen fibres (red) could be shown (Figure 5C). Remaining collagen IV could be shown in all experimental groups by immunohistochemistry (Figure 5D). Laminin was also shown by immunohistochemistry in all experimental groups, although more laminin was observed in groups perfused via the portal vein around remaining cell clusters (Figure 5E). Fibronectin was shown by immunohistochemistry in decellularized livers of all experimental groups (Figure 5F).

3.3. Biochemical analyses

Analysis of the DNA content revealed that all of the decellularization procedures markedly reduced the DNA content per dry weight compared with native livers (native liver vs.: PV – P, $p = 0.2408$; vs. PV + P, $p = 0.0152$; vs. A – P, $p = 0.0735$; vs. A + P, $p < 0.0001$) (Figure 6), although decellularized liver matrices significantly lost weight during the decellularization process (PV – P 783 ± 256.7 mg; PV + P 504.2 ± 87.42 mg; A – P 470.8 ± 229.2 mg; A + P 229.2 ± 4.167 mg; native 3646 ± 487.8 mg). The amount of residual DNA was lower in matrices that were decellularized under oscillating pressure compared with those that were decellularized without pressure changes (PV – P 3439 ± 1648 vs. PV + P 1576 ± 379, ns; A – P 2504 ± 1685 vs. A + P 723 ± 119, ns). These differences were not statistically significant in the Dunn's multiple comparison analysis (PV – P vs. PV + P, $p = 0.9999$; A – P vs. A + P, $p = 0.4885$) but showed clear trends and significant test results when analysed with the non-parametric Mann–Whitney-U test: (PV – P vs. PV + P, $p = 0{,}0649$; A – P vs. A + P, $p = 0.0022$). Furthermore, less residual DNA was observed in the liver matrices that were decellularized via the hepatic artery (A – P 2504 ± 1685 ng DNA/mg ECM; A + P 723 ± 119 ng DNA/mg ECM) compared with matrices that were decellularized via the portal vein (PV – P 3439 ± 1648 ng DNA/mg ECM; PV + P 1576 ± 379 ng DNA/mg ECM), although the differences were not statistically significant (PV – P vs. A – P, ns; PV + P vs. A + P, ns). The livers that were perfused via the hepatic artery under oscillating pressure conditions showed the lowest amounts of remaining DNA.

The glycosaminoglycan content in decellularized liver matrices was lower in three out of four experimental groups when compared with native livers (native vs. PV – P, $p = 0.0886$; native vs. PV + P, $p = 0.0229$; native vs. A – P, $p < 0.0001$, Figure 7). Whereas a generally higher

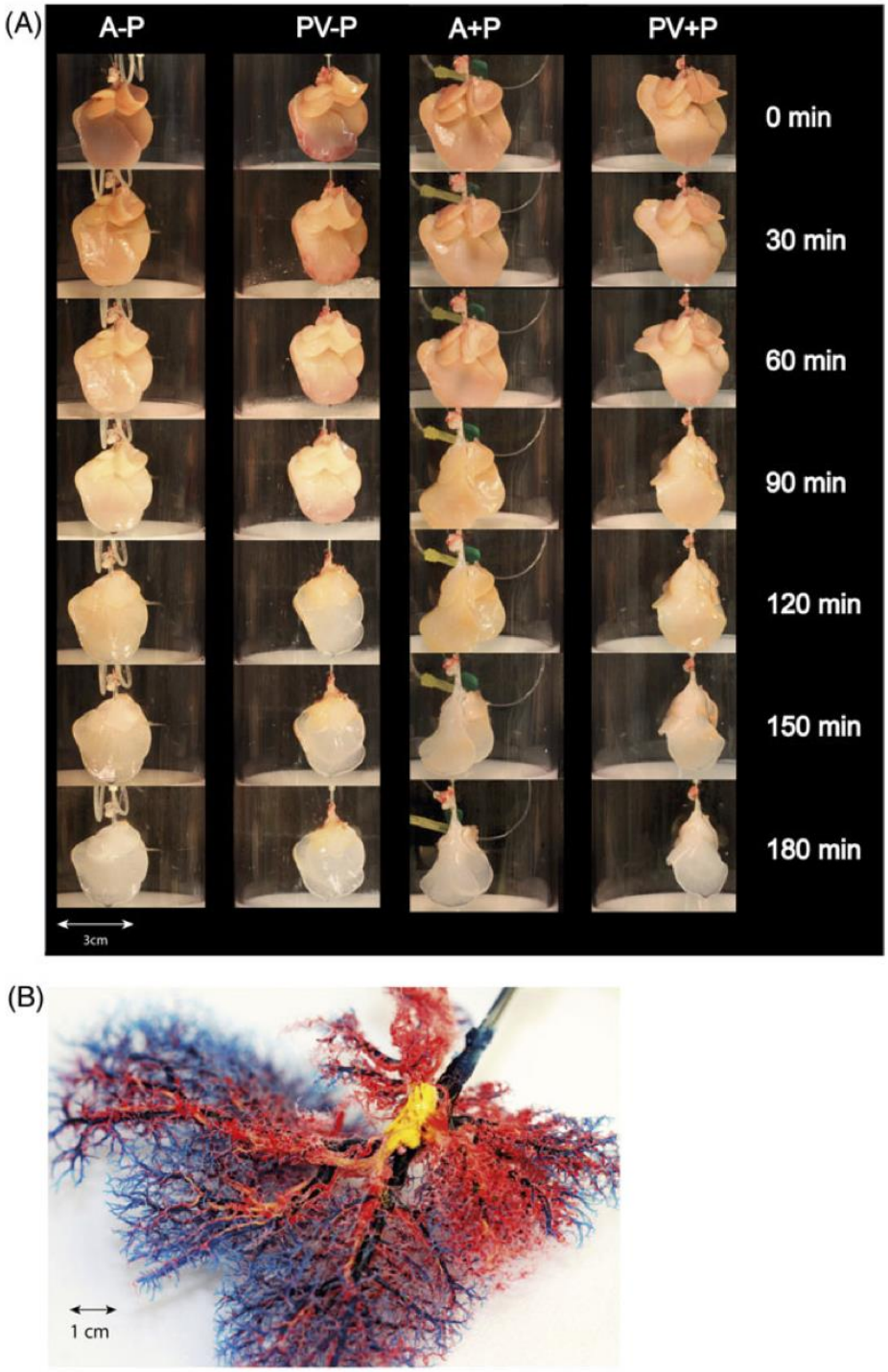

Figure 3. (A) Time-course of rat liver decellularization: A + P, liver that was perfused via the hepatic artery and under oscillating pressure conditions; PV + P, liver that was perfused via the portal vein and under oscillating pressure conditions; A-P, liver that was perfused via the hepatic artery and without oscillating pressure conditions; PV-P, liver that was perfused via the portal vein and without oscillating pressure conditions. (B) Corrosion cast of a decellularized liver matrix (A + P): blue, portal vein; red, hepatic artery; yellow, biliary tract; protein frameworks of all structures are intact after decellularization. [Colour figure can be viewed at wileyonlinelibrary.com]

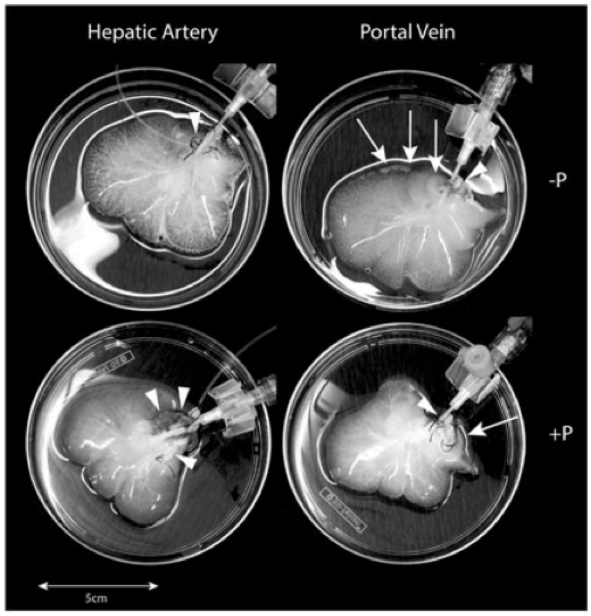

Figure 4. Decellularized, cannulated rat livers directly after processing. Livers were perfused via the hepatic artery (left) or via the portal vein (right). Either no oscillating pressure was applied (upper row, –P) or decellularization was performed under oscillating pressure conditions (below, +P). Remaining cells (clusters) within decellularized liver matrices are indicated by white arrows. Non-decellularized extrahepatic tissue (i.e. diaphragm, vena cava inferior, etc.) is indicated with white arrowheads

trend of GAGs was observed in the A + P group (PV – P 7.97 ± 3.00 mg/g; PV + P 8.26 ± 7.95 mg/g; A – P 1.85 ± 1.54 mg/g; A + P 15.27 ± 4.52 mg/g; vs. Native 83.48 ± 26.61 mg/g). Significant differences were found between the experimental groups A-P and A + P ($p = 0.0229$). The measured hepatocyte growth factor (HGF) content per mg ECM dry weight tended to be higher in the experimental groups than in native livers (PV-P: 2.30 pg/g ± 1.03 pg/g; PV + P: 2.43 pg/g ± 1.01 pg/g; A-P: 1.24 pg/g ± 1.04 pg/g; A + P: 1.63 pg/g ± 0.70; Native: 0.41 pg/g ± 0.24 pg/g), but showed significant differences only between livers that were decellularized via the portal vein and native livers (Group PV-P vs. Native: $p = 0.0090$; Group PV + P vs. Native: $p = 0.0043$) (Figure 8).

3.4. Corrosion casts

Corrosion casts of decellularized liver matrices of group A + P showed an intact (micro)structure for the portal vein, hepatic artery and biliary system (Figure 3B).

4. Discussion

Recent reports on liver decellularization and recellularization provide evidence that the perfusion of alkaline detergents and/or enzymatic solutions via the portal vein is feasible to obtain a three-dimensional non-immunogenic biomatrix, that supports and improves survival and functionality of liver and/or progenitor cells (Sellaro *et al.*, 2010; Badylak *et al.*, 2011; Zhou *et al.*, 2011; Wang *et al.*, 2013). To enhance engraftment, migration and proliferation as well as to prevent dedifferentiation and loss of function of hepatocytes used for the repopulation of decellularized scaffolds, an adequate composition of micro-environmental conditions of the ECM is essential (Jarvelainen *et al.*, 2009).

As all known agents for liver decellularization cause alteration and damage to the ECM, a 'gentler' decellularization method may provide optimal support for cellular repopulation (Crapo *et al.*, 2011). On the other hand, ineffective decellularization leading to cellular and antigenic remnants within the ECM of allogenic or xenogenic origin could cause deleterious immunogenic effects (i.e. rejection) after implantation *in vivo* (Badylak *et al.*, 2012). Thus, finding an optimal compromise between cellular removal and preservation of the ECM composition (i.e. invasiveness of decellularization) should be addressed in further investigations to provide standardized decellularization protocols for livers from different species.

However, although some reports on rat liver perfusion decellularization have been published (Shupe *et al.*, 2010; Uygun *et al.*, 2010; Bao *et al.*, 2011; Baptista *et al.*, 2011; De Kock *et al.*, 2011; Pan *et al.*, 2013), the inconsistency of published protocols (regarding duration of the procedure and perfusion rate) further indicates the need to optimize and standardize the technique. This study appears to be the first report on a rat liver perfusion device enabling decellularization (1) by selective perfusion via the hepatic artery and/or the portal vein and (2) optionally under oscillating pressure conditions.

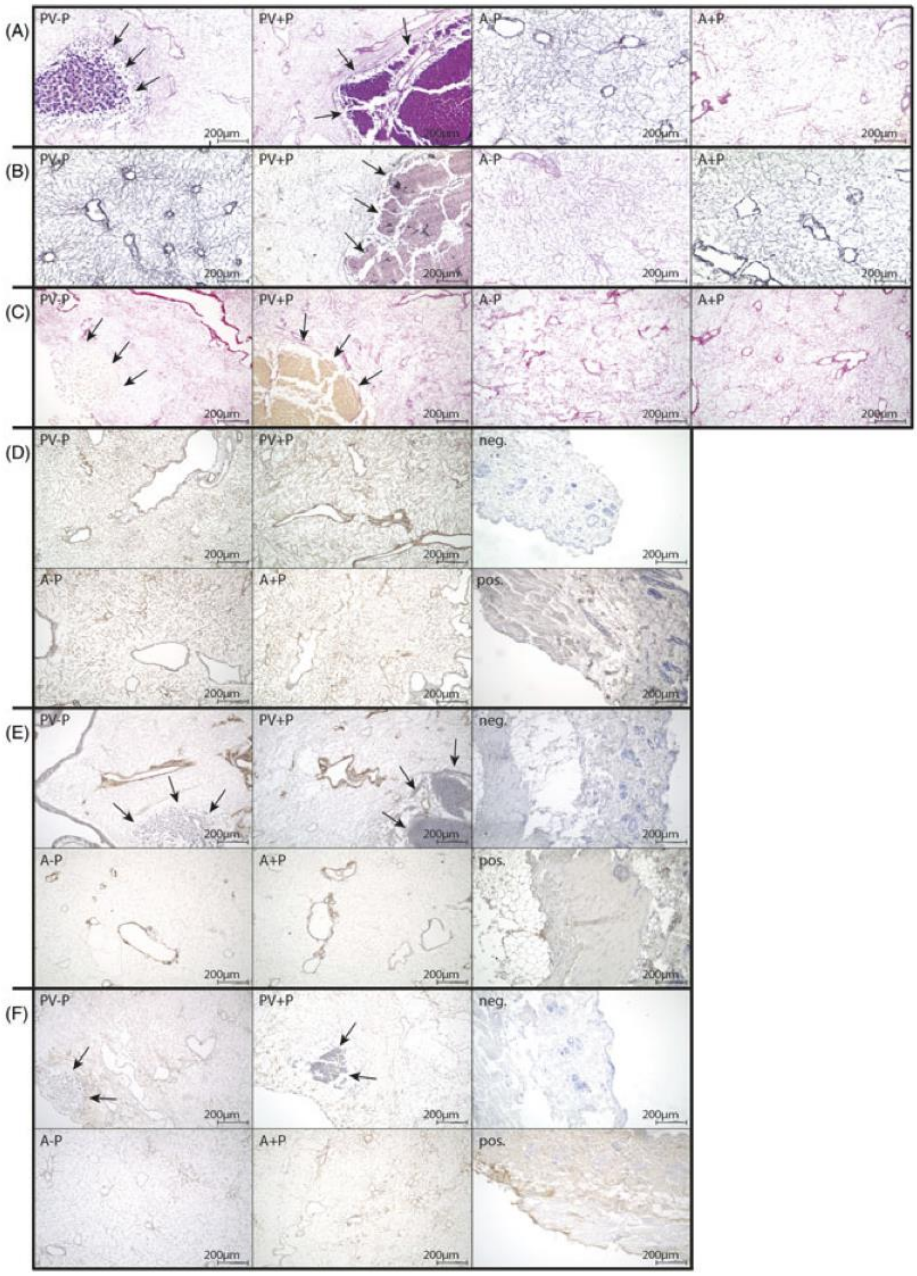

Figure 5. Histological staining of decellularized liver matrices (DLMs). PV – P, portal venous perfusion without oscillating pressure conditions; PV + P, portal venous perfusion with oscillating pressure conditions; A – P, arterial perfusion without oscillating pressure conditions; A + P, arterial perfusion with oscillating pressure conditions (see Table 1); neg., negative control (rat skin); pos., positive control (rat skin); black arrows, remaining cell clusters. (A) Haematoxylin and eosin (original magnification × 100): the extracellular matrix (ECM) is conserved during decellularization. Livers perfused via the portal vein show remaining cells. (B) Gömöri staining (original magnification × 100): livers perfused via the portal vein show remaining cell clusters. The ECM is conserved during decellularization. (C) Sirius Red staining: parenchymal tissue residues appear yellow and are only visible in slices of DLMs decellularized via the portal vein. Connective tissue fibres appear red and are detectable in DLMs of all experimental groups. (D) Immunohistochemical staining of Collagen IV (original magnification × 100): collagen IV is detectable in slices of DLMs of all experimental groups. (E) Immunohistochemical staining of Laminin (original magnification × 100): laminin was visualized in slices of DLMs of all groups, although livers perfused via the portal vein showed more remaining laminin in areas of remaining cell clusters. (F) Immunohistochemical staining of fibronectin (original magnification × 100): fibronectin was shown in slices of DLMs of all experimental groups within the remaining protein network. [Colour figure can be viewed at wileyonlinelibrary.com]

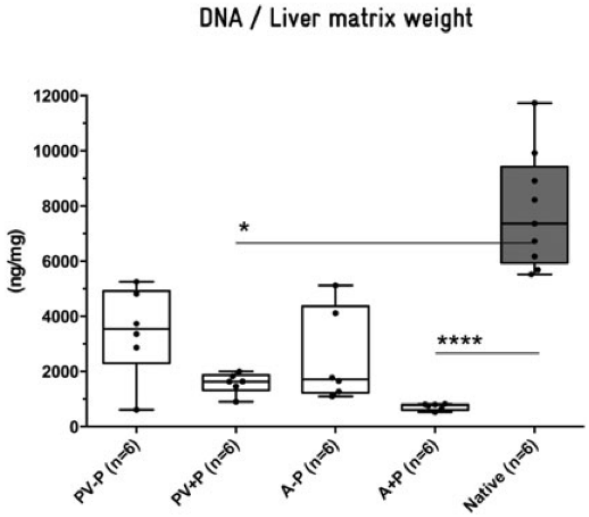

Figure 6. DNA content per mg of decellularized liver matrices (DLMs) after decellularization with different protocols. Decellularization markedly reduced the DNA content in liver weight in all experimental groups, although only in livers perfused with oscillating pressure conditions (+P) were these differences were significant

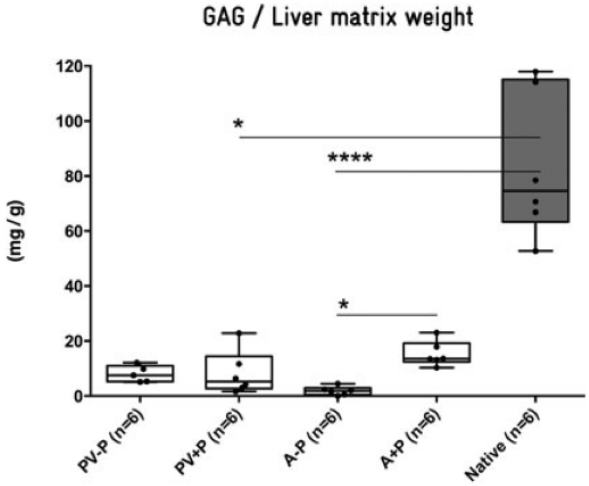

Figure 7. Content of glycosaminoglycans (GAGs) per g of decellularized liver matrices (DLMs) in different experimental groups. The GAG content declined in DLMs of all experimental groups compared with native livers, although these differences were only significant for livers of the PV + P and (A – P) group. The remaining GAG content was significantly higher in livers perfused via the hepatic artery with the application of oscillating pressure conditions (A + P) compared with those perfused without oscillating pressure conditions (A – P)

Such pressure conditions mimic intra-abdominal conditions during respiration which lead to improved microperfusion within liver tissue. *In situ* the liver is 'hung' under the copula of the diaphragm and directly affected by its movement: during expiration the portovenous flow is increased, while during inspiration the liver is squeezed (comparable to a sponge) to optimize the outflow of hepatic blood into the hepatic veins. Interestingly, in previous perfusion studies oscillating pressure conditions have already been shown to improve the outcomes of extracorporeally perfused livers in a porcine transplant model (Neuhaus, 1982; Schon *et al*., 2001).

In the present study, livers perfused under oscillating pressure conditions showed a bleaching that was more homogeneous than livers perfused without oscillating pressure. Although it has not been discussed in existing literature, the homogeneity of perfusion seems to be an important factor. If the decellularization of an organ is not homogeneous, areas of remaining cells within the organ can be removed by, for example (1) extending the

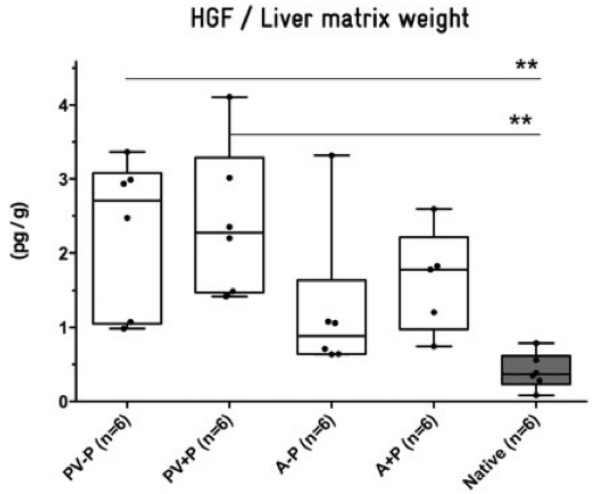

Figure 8. Remaining content of hepatocyte growth factor per g of decellularized liver matrices (DLMs). Compared with native livers the content of hepatocyte growth factor (HGF) (per g liver matrix) appeared to be significantly higher in livers perfused via the portal vein. Livers perfused via the hepatic vein also showed a higher HGF content, although differences were not statistically significant

perfusion duration or (2) increasing the perfusion rate (or pressure). Thus, livers of the PV – P group that were not completely decellularized at the end of the 3-h protocol could be completely decellularized by extending the perfusion with SDS for at least 30 min or more (data not shown). However, extending the duration or increasing the perfusion rate, increases the invasiveness of the methodology because well-perfused areas within the organ have to resist more of the altering detergents, to remove remaining cells within less perfused areas. Thus, by optimizing the homogeneity of perfusion decellularization the invasiveness of the methodology can be reduced.

These macroscopic findings were approved by the biochemical characterization of the DLMs. Livers of the pressure groups (+P) showed a smaller content of remaining DNA per weight compared with their counterparts without pressure (Figure 6), although DLMs of the pressure groups were lighter. Although the content of glycosaminoglycans did not differ significantly when comparing the routes of perfusion (portal vein vs. hepatic artery), a significantly higher GAG content was observed in the A + P group compared with the A – P group (Figure 7), showing at least slightly less alteration of the ECM composition in this group. The HGF concentration was measured to demonstrate that important factors for cellular survival and differentiation are conserved during the decellularization procedure. Interestingly, the amounts of HGF seemed to be higher in the DLMs than in native liver tissue (Figure 8), which appears contradictory. One possible explanation is that the weight and the composition of the DLM changed because of a significant removal of cellular protein mass, as already stated by Baptista *et al* (2011), who found higher collagen contents in DLMs than in native livers. In addition, perhaps in native liver HGF is predominantly in a soluble form while in decellularized liver it remains in an ECM-bound form.

In 2011, Badylak *et al.* introduced criteria to define decellularization as: (1) complete absence of visible nuclear material upon histological examination (haematoxylin and eosin and 4′-6-diamidino-2phenylindole (DAPI) stains); (2) less than 50 ng of dsDNA per mg ECM dry weight; and (3) remnant DNA molecules shorter than 200 bp (Crapo *et al.*, 2011). However, experimental evidence for the value of this definition in different (e.g. allogeneic, xenogeneic, blood-group incompatible, etc.) transplant settings still is rare (Zheng *et al.*, 2005; Nagata *et al.*, 2010; Mirmalek-Sani *et al.*, 2013; Park *et al.*, 2013). Although the main ECM molecules are highly conserved across species, it appears to be reasonable that varying tissues and organs from different species can cause different immunogenic reactions after *in vivo* implantation in varying host organisms (Badylak *et al.*, 2011). As already mentioned, an optimal decellularization method would be a compromise between removal (of antigenic material) and preservation (of non-immunogenic cell-supporting material) but, to date, no experimental data to define this optimal compromise is available. Thus, before different decellularization protocols and techniques can be qualitatively compared, species- and organ-specific standards have to be defined and approved by *in vivo* experiments.

5. Conclusion

Perfusion via the hepatic artery improves decellularization outcomes of rat livers compared with 'conventional' portal venous perfusion. Applying oscillating pressure conditions on extracorporeally perfused rat livers further enhances

microperfusion and thus the homogeneity of perfusion decellularization. Using this technique the invasiveness of applied methodology can be reduced, resulting in a gentle and quick (3 h) decellularization protocol for rat livers.

Conflict of interest

The authors have declared that there is no conflict of interest.

References

Adam R, Hoti E. 2009; Liver transplantation: the current situation. *Semin Liver Dis* **29**: 3–18.

Badylak SF, Taylor D, Uygun K. 2011; Whole-organ tissue engineering: decellularization and recellularization of three-dimensional matrix scaffolds. *Annu Rev Biomed Eng* **13**: 27–53.

Badylak SF, Weiss DJ, Caplan A *et al*. 2012; Engineered whole organs and complex tissues. *Lancet* **379**: 943–952.

Bahra M, Neuhaus P. 2011; Liver transplantation in the high meld era: a fair chance for everyone? *Langenbecks Arch Surg* **396**: 461–465.

Bao J, Shi Y, Sun H, *et al*. 2011; Construction of a portal implantable functional tissue-engineered liver using perfusion-decellularized matrix and hepatocytes in rats. *Cell Transplant* **20**: 753–766.

Baptista PM, Siddiqui MM, Lozier G, *et al*. 2011; The use of whole organ decellularization for the generation of a vascularized liver organoid. *Hepatology* **53**: 604–617.

Barakat O, Abbasi S, Rodriguez G, *et al*. 2012; Use of decellularized porcine liver for engineering humanized liver organ. *J Surg Res* **173**: e11–e25.

Bissell MJ, Aggeler J. 1987; Dynamic reciprocity: how do extracellular matrix and hormones direct gene expression? *Prog Clin Biol Res* **249**: 251–262.

Cortiella J, Niles J, Cantu A, *et al*. 2010; Influence of acellular natural lung matrix on murine embryonic stem cell differentiation and tissue formation. *Tissue Eng Part A* **16**: 2565–2580.

Crapo PM, Gilbert TW, Badylak SF. 2011; An overview of tissue and whole organ decellularization processes. *Biomaterials* **32**: 3233–3243.

De Kock J, Ceelen L, de Spiegelaere W, *et al*. 2011; Simple and quick method for whole-liver decellularization: a novel *in vitro* three-dimensional bioengineering tool? *Arch Toxicol* **85**: 607–612.

Farndale RW, Buttle DJ, Barrett AJ. 1986; Improved quantitation and discrimination of sulphated glycosaminoglycans by use of dimethylmethylene blue. *Biochim Biophys Acta* **883**(2): 173–177.

Fishman AP, Dickinson WR. 1988; Circulation of the Blood: Men and Ideas American Physiological Society Centennial Publications. Oxford University Press Inc.: New York.

Jarvelainen H, Sainio A, Koulu M, *et al*. 2009; Extracellular matrix molecules: potential targets in pharmacotherapy. *Pharmacol Rev* **61**: 198–223.

Ji R, Zhang N, You N, *et al*. 2012; The differentiation of mscs into functional hepatocyte-like cells in a liver biomatrix scaffold and their transplantation into liver-fibrotic mice. *Biomaterials* **33**: 8995–9008.

Kajbafzadeh A-M, Javan-Farazmand N, Monajemzadeh M, *et al*. 2013; Determining the optimal decellularization and sterilization protocol for preparing a tissue scaffold of a human-sized liver tissue. *Tissue Eng Part C Methods* **19**: 642–651.

Lechler RI, Sykes M, Thomson AW, *et al*. 2005; Organ transplantation – how much of the promise has been realized? *Nat Med* **11**: 605–613.

Mirmalek-Sani SH, Sullivan DC, Zimmerman C, *et al*. 2013; Immunogenicity of decellularized porcine liver for bioengineered hepatic tissue. *Am J Pathol* **183**(2): 558–565.

Nagata S, Hanayama R, Kawane K. 2010; Autoimmunity and the clearance of dead cells. *Cell* **140**: 619–630.

Neuhaus P. 1982; Extrakorporale Leberperfusion – Entwicklung und Erprobung eines neuen Modells. University Hospital of Hannover: Germany, 87–90.

Pan MX, Hu PY, Cheng Y, *et al*. 2013. An efficient method for decellularization of the rat liver. *J Formos Med Assoc*. doi: 10.1016/j.jfma.2013.05.003. [Epub ahead of print].

Park KM, Woo HM. 2012a; Porcine bioengineered scaffolds as new frontiers in regenerative medicine. *Transplant Proc* **44**: 1146–1150.

Park KM, Woo HM. 2012b; Systemic decellularization for multi-organ scaffolds in rats. *Transplant Proc* **44**: 1151–1154.

Park KM, Park SM, Yang SR, *et al*. 2013; Preparation of immunogen-reduced and biocompatible extracellular matrices from porcine liver. *J Biosci Bioeng* **115**: 207–215.

Ren H, Shi X, Tao L, *et al*. 2013; Evaluation of two decellularization methods in the development of a whole-organ decellularized rat liver scaffold. *Liver Int* **33**: 448–458.

Ross EA, Williams MJ, Hamazaki T, *et al*. 2009; Embryonic stem cells proliferate and differentiate when seeded into kidney scaffolds. *J Am Soc Nephrol* **20**: 2338–2347.

Schon MR, Kollmar O, Wolf S, *et al*. 2001; Liver transplantation after organ preservation with normothermic extracorporeal perfusion. *Ann Surg* **233**: 114–123.

Sellaro TL, Ranade A, Faulk DM, *et al*. 2010; Maintenance of human hepatocyte function in vitro by liver-derived extracellular matrix gels. *Tissue Eng Part A* **16**: 1075–1082.

Shirakigawa N, Ijima H, Takei T. 2012; Decellularized liver as a practical scaffold with a vascular network template for liver tissue engineering. *J Biosci Bioeng* **114**(5): 546–551.

Shupe T, Williams M, Brown A, *et al*. 2010; Method for the decellularization of intact rat liver. *Organogenesis* **6**: 134–136.

Soto-Gutierrez A, Zhang L, Medberry C, *et al*. 2011; A whole-organ regenerative medicine approach for liver replacement. *Tissue Eng Part C Methods* **17**: 677–686.

Stern MM, Myers RL, Hammam N, *et al*. 2009; The influence of extracellular matrix derived from skeletal muscle tissue on the proliferation and differentiation of myogenic progenitor cells *ex vivo*. *Biomaterials* **30**: 2393–2399.

Struecker B, Raschzok N, Sauer IM. 2013; Liver support strategies: cutting-edge technologies. *Nat Rev Gastroenterol Hepatol* **11**(3): 166–176.

Uygun BE, Soto-Gutierrez A, Yagi H, *et al*. 2010; Organ reengineering through development of a transplantable recellularized liver graft using decellularized liver matrix. *Nat Med* **16**: 814–820.

Wang X, Cui J, Zhang BQ, *et al*. 2013; Decellularized liver scaffolds effectively support the proliferation and differentiation of mouse fetal hepatic progenitors. *J Biomed Mater Res A* **102**(4): 1017–1025.

Wang Y, Cui CB, Yamauchi M, *et al*. 2011; Lineage restriction of human hepatic stem cells to mature fates is made efficient by tissue-specific biomatrix scaffolds. *Hepatology* **53**: 293–305.

Yagi H, Fukumitsu K, Fukuda K, *et al*. 2012; Human-scale whole-organ bioengineering for liver transplantation: a regenerative medicine approach. *Cell Transplant* **22**(2): 231–242.

Zheng MH, Chen J, Kirilak Y, *et al*. 2005; Porcine small intestine submucosa (SIS) is not an acellular collagenous matrix and contains porcine DNA: possible implications in human implantation. *J Biomed Mater Res B Appl Biomater* **73**: 61–67.

Zhou P, Lessa N, Estrada DC, *et al*. 2011; Decellularized liver matrix as a carrier for the transplantation of human fetal and primary hepatocytes in mice. *Liver Transpl* **17**: 418–427.

11. Lebenslauf

Mein Lebenslauf wird aus datenschutzrechtlichen Gründen in der elektronischen Version meiner Arbeit nicht veröffentlicht.

12. Publikationsliste

	Erstautorin	*Impact Factor*
1	*Evolution of graft morphology and function after recellularization of decellularized rat livers* **Butter A**, Aliyev K, Hillebrandt KH, Raschzok N, Kluge M, Seiffert N, Tang P, Napierala H, Ashraf MIM, Reutzel-Selke A, Andreou A, Pratschke J, Sauer IM, Struecker B J Tissue Eng Regen Med. 2018 Feb;12(2): e807-e816	*3,989*

	Co-Autorin	*Impact Factor*
1	*Porcine liver decellularization under oscillating pressure conditions: a technical refinement to improve the homogeneity of the decellularization process* Struecker B, Hillebrandt KH, Voitl R, **Butter A**, Schmuck RB, Reutzel-Selke A, Geisel D, Joehrens K, Pickerodt PA, Raschzok N, Puhl G, Neuhaus P, Pratschke J, Sauer IM. Tissue Eng Part C Methods. 2015; 21(3): 303-313	*4,25*
2	*Improved rat liver decellularization by arterial perfusion under oscillating pressure conditions* Struecker B, **Butter A**, Hillebrandt K, Polenz D, Reutzel-Selke A, Tang P, Lippert S, Leder A, Rohn S, Geisel D, Denecke T, Aliyev K, Jöhrens K, Raschzok N, Neuhaus P, Pratschke J, Sauer IM. J Tissue Eng Regen Med. 2014 Sep 4. doi: 10.1002/term.1948.	*5,19*
3	*Micron-sized iron oxide-containing particles for microRNA-targeted manipulation and MRI-based tracking of transplanted cells* Leder A, Raschzok N, Schmidt C, Arabacioglu D, **Butter A**, Kolano S, de Sousa Lisboa LS, Werner W, Polenz D, Reutzel-Selke A, Pratschke J, Sauer IM. Biomaterials. 2015; 51:129-137	*8,38*

4	*Procedure for Decellularization of Rat Livers in an Oscillating-pressure Perfusion Device* Hillebrandt K, Polenz D, Butter A, Tang P, Reutzel-Selke A, Andreou A, Napierala H, Raschzok N, Pratschke J, Sauer IM, Struecker B. J Vis Exp. 2015 Aug 10;(102):e53029	*1,11*
5	*Implantation of a Tissue-Engineered Neo-Bile Duct in Domestic Pigs* Struecker B, Hillebrandt KH, Raschzok N, Jöhrens K, **Butter A**, Tang P, Andreou A, Napierala H, Reutzel-Selke A, Denecke T, Pratschke J, Sauer IM. Eur Surg Res 2016;56:61-75	*1,15*

13. Danksagung

An dieser Stelle möchte ich mich bei allen bedanken, die mich in der Zeit meiner Promotion unterstützt haben.

Besonders danke ich Prof. Dr. med. Igor M. Sauer dafür, dass er mich in meinem Arbeiten immer unterstützt und vor allem inspiriert hat. Er ermöglichte mit an diesem überaus spannenden wissenschaftlichen Projekt zu arbeiten, daran zu wachsen und neue Methoden zu etablieren sowie meine Fähigkeiten durch die Hospitation in Boston, Massachusetts zu erweitern. Zudem gab er mir die Möglichkeit die Ergebnisse der gemeinsamen Projekte auf nationalen und internationalen Kongressen vorzustellen.

Zudem danke ich Univ. Prof. Dr. med. J. Pratschke für die Möglichkeit an der Chirurgischen Klinik promoviert zu werden sowie für die Bereitstellung der Labore und technischen Geräte.

Dr. med. Benjamin Strücker möchte ich ebenfalls in hohem Maße für die großartige Zusammenarbeit und Betreuung danken. Er ist derjenige, der mich immer wieder angetrieben hat, in dem Projekt weiterzumachen und mir die operationstechnischen Fähigkeiten beibrachte, die für dieses Projekt so wichtig waren.

Zudem danke ich PD Dr. med. Nathanael J. Raschzok für die ebenfalls sehr gute Betreuung und Motivation während der gesamten Zeit meines wissenschaftlichen Arbeitens.

Ich danke Khalid Aliyev sehr, dass er mir bei der Durchführung der Versuche immer sehr zuverlässig half.

Dr. Karl H. Hillebrandt danke ich besonders für die ebenfalls zuverlässige und sorgfältige Bearbeitung der histologischen Gewebeproben sowie für seine wertvolle Mitarbeit in diesem Projekt.

Besonderen Dank schulde ich Steffen Lippert und Peter Tang, die ich als Wissenschaftler sehr schätze, und ohne die die Auswertung meiner Doktorarbeit wohl kaum möglich gewesen wäre.

Weiterhin danke ich Anja Selke für die geduldige Hilfe bei der statistischen Auswertung der Daten. Weiteren Dank schulde ich Annekatrin Leder und Dietrich Polenz.

Abschließend möchte ich meinen Eltern, Uwe und Heike Butter, sowie meinem Bruder Michael Butter, danken, dass sie mich stets uneingeschränkt unterstützt haben und ich meine Ideen aber auch Zweifel stets mit ihnen teilen konnte.